BÁRBARA CAMPOLINA CARVALHO SILVA

Hiperparatireoidismo primário – novas perspectivas sobre qualidade óssea através da avaliação por tomografia computadorizada quantitativa periférica de alta resolução e escore de osso trabecular

Faculdade de Medicina
Universidade Federal de Minas Gerais
Belo Horizonte – Minas Gerais – Brasil
2012

BÁRBARA CAMPOLINA CARVALHO SILVA

Hiperparatireoidismo primário – novas perspectivas sobre qualidade óssea através da avaliação por tomografia computadorizada quantitativa periférica de alta resolução e escore de osso trabecular

Tese apresentada como requisito parcial para obtenção do título de Doutor no Programa de Pós-Graduação em Medicina Molecular da Faculdade de Medicina da Universidade Federal de Minas Gerais

.

Orientadora: Profa. Maria Marta Sarquis Soares

Co-Orientador: Prof. John P. Bilezikian

Faculdade de Medicina

Universidade Federal de Minas Gerais

Belo Horizonte – Minas Gerais – Brasil

2012

UNIVERSIDADE FEDERAL DE MINAS GERAIS

Reitor

Clélio Campolina Diniz

Pró-Reitor da Pós-graduação

Ricardo Santiago Gomez

Pró-Reitor de Pesquisa

Renato de Lima Santos

FACULDADE DE MEDICINA

Diretor

Francisco José Penna

Vice-Diretor

Tarcizo Afonso Nunes

Coordenador do Centro de Pós-graduação

Manoel Otávio da Costa Rocha

COLEGIADO DO CURSO DE MEDICINA MOLECULAR

Luiz Armando Cunha De Marco (Coordenador)

Débora Marques de Miranda (Subcoordenadora)

Carolina Cavaliéri Gomes

Marco Aurélio Romano Silva

Maria Marta Sarquis Soares

Vitor Bortolo de Rezende (discente, titular)

Luiz Alexandre V. Magno (discente, suplente)

Para minha preciosa família:

Meu marido Gustavo, pelo amor, companheirismo, paciência e ajuda incondicional. Por ter dividido esse sonho comigo e me ajudado a torná-lo real. Sem você eu não teria conseguido. Te amo.

Ao meu amado filho Mateus, pelo sorriso gostoso e abraço confortante, que me enchem a vida de sentido.

Aos meus queridos irmãos Clarissa e Lucas, companheiros de vida e de jogo, pelo amor, apoio e torcida constantes.

Aos meus amados pais, Rogério e Marília, meus primeiros e maiores exemplos de amor, respeito e dedicação. Obrigada pelo apoio e confiança. Começamos esse projeto juntos há alguns anos e, hoje, dedico-o a vocês.

AGRADECIMENTOS

Ao Prof. Luiz Armando De Marco pela confiança, presença, conselhos em momentos críticos e incentivo na realização desse projeto.

À Prof. Marta Sarquis, minha querida orientadora de mestrado e doutorado, pela amizade, paciência, confiança, incentivo e por despertar meu interesse por doenças osteometabólicas, pesquisa e ensino.

Ao Prof. John P. Bilezikian, meu orientador, por ter me acolhido na Universidade de Columbia e me confiado esse importante projeto. Pela ajuda fundamental na elaboração dos artigos e pelos ensinamentos sobre osteometabolismo, pesquisa clínica e elaboração de textos científicos. Sobretudo, pelo exemplo profissional e de vida, que me influenciaram como médica e como pessoa.

À Prof. Stavroula Kousteni por ter me acolhido com tanto carinho em seu laboratório e me ensinado sobre pesquisa básica, elaboração de projetos e apresentação em público. De nossa convivência, levo seu exemplo de luta, determinação, e a convicção de que podemos melhorar sempre.

À Julia Udesky, pela ajuda imprescindível e eficiente no recrutamento de pacientes e coleta de dados.

Ao Don McMahon e Amy (Chiyuan Zhang) pela ajuda na análise estatística dos dados, pelas longas e produtivas discussões sobre interpretação dos resultados, e por me ajudarem a entender um pouco mais sobre estatística.

À Dr[a] Stephanie Boutroy pela ajuda na revisão dos artigos, no entendimento sobre HRpQCT e, principalmente, por ter me apresentado e me incentivado a utilizar o escore de osso trabecular.

Ao Dr. Didier Hans pela colaboração na análise do escore de osso trabecular.

Ao Dr. Edward Guo, chefe do Laboratório de Bioengenharia Óssea do Departamento de Engenharia Biomédica da Universidade Columbia, e aos engenheiros Bin Zhao e Ji Wang pela análise de elementos finitos e ITS das imagens de HRpQCT.

Ao Dr. Serge Cremers e Elzbieta Dworakowski, pela realização das dosagens de PTH.

Ao "International Endocrine Scholars Program", uma parceria entre a Sociedade Brasileira de Endocrinologia e Metabologia e a Endocrine Society, e em especial à Dra Valéria Guimarães, ex-coordenadora do programa, por ter proporcionado meu contato incial com Dr Bilezikian, e o desenvolvimento desse projeto na Universidade de Columbia.

Ao CNPq, Conselho Nacional de Desenvolvimento Científico e Tecnológico, pelo apoio no programa de doutorado.

À equipe de endocrinologia do Hospital Felício Rocho pela fundamental ajuda na minha formação.

À equipe de endocrinologia da Santa Casa de Belo Horizonte por ter me admitido no ambulatório de Doenças Osteometabólicas, possibilitando aumento da minha vivência clínica nesta área.

RESUMO

Introdução: O hiperparatireoidismo primário (PHPT) apresenta-se, nos dias atuais, como uma doença assintomática ou oligossintomática, diagnosticado pelo achado fortuito de hipercalcemia. Nesta forma da doença, densitometria óssea revela diminuição de densidade mineral óssea areal (aBMD) em sítio cortical (rádio 33%), enquanto aBMD na coluna lombar, composta quase exclusivamente por osso trabecular, é usualmente normal. Estudos por microtomografia computadorizada (μCT) e histomorfometria de biópsia óssea de crista ilíaca confirmam preservação de osso trabecular. Esses achados contradizem o risco aumentado de fraturas vertebrais e não vertebrais no PHPT assintomático. Tecnologias emergentes, como a tomografia computadorizada quantitativa periférica de alta resolução (HRpQCT) e escore de osso trabecular (TBS) podem gerar informações adicionais sobre a microarquitetura e qualidade óssea em pacientes com PHPT. Além disso, análise de trabécula individual (ITS) e análise de elementos finitos (FEA) das imagens de HRpQCT fornecem dados detalhados da microestrutura trabecular e rigidez óssea, que se relacionam à competência biomecânica do esqueleto e risco de fratura.

Objetivos: Avaliar os compartimentos cortical e trabecular por HRpQCT e FEA, e o compartimento trabecular através da técnica de ITS em mulheres na pós-menopausa com PHPT, comparando-as com controles saudáveis. Correlacionar TBS com medidas por HRpQCT no PHPT.

Pacientes e métodos: 51 mulheres na pós menopausa portadoras de PHPT e 120 controles saudáveis foram avaliados por HRpQCT, ITS e FEA. TBS foi estimado em subgrupo de 22 mulheres com PHPT.

Resultados: aBMD da coluna lombar avaliada por densitometria óssea foi similar em pacientes e controles. No entanto, resultados da HRpQCT revelaram redução importante da densidade volumétrica total, cortical e trabecular em indivíduos com PHPT. Não apenas redução da espessura cortical, mas também maior espaçamento entre as trabéculas e distribuição trabecular heterogênea foram observadas no rádio e na tíbia de pacientes com PHPT. No rádio, observou-se ainda redução da espessura e número trabecular. Alterações trabeculares foram mais evidentes no rádio do que na tíbia. ITS revelou, em ambos sítios ósseos, redução das trabéculas em placa, com consequente redução da razão placa-haste. Diminuição da densidade de junções entre placas e entre hastes e placas foram observadas no rádio e tíbia. No rádio, houve também diminuição da densidade de

junções entre hastes. Essas anormalidades trabeculares e corticais resultaram em diminuição da rigidez do osso inteiro e trabecular. TBS correlacionou-se com índices determinados pela HRpQCT no rádio, com exceção de espessura trabecular (Tb.Th) e rigidez trabecular. Na tíbia, correlações foram observadas entre TBS e densidades volumétricas, espessura cortical, volume ósseo trabecular e rigidez de osso inteiro. Neste sítio ósseo, correlação de TBS com todas as medidas de microarquitetura trabecular, exceto Tb.Th, foi observada após ajuste para peso corporal.

Conclusão: Anormalidades da densidade e microarquitetura esquelética são universais no PHPT, não se limitando ao compartimento cortical, explicando o achado de redução da rigidez óssea total e trabecular e, possivelmente, risco aumentado de fratura no PHPT. Uma vez que HRpQCT não é um exame amplamente disponível em nosso meio, o achado de correlação significativa entre TBS e HRpQCT indica que o TBS poderia tornar-se útil na avaliação clínica desses pacientes.

Descritores: hiperparatireoidismo primário, paratormônio, tomografia computadorizada quantitativa periférica de alta resolução (HRpQCT), escore de osso trabecular (TBS), análise de trabécula individual (ITS), análise de elementos finitos (FEA).

ABSTRACT

Introduction: Primary hyperparathyroidism (PHPT) is predominantly an asymptomatic disease, diagnosed by the fortuitous finding of hypercalcemia. Typically, in this milder form of the disease, areal bone mineral density (aBMD) by DXA is reduced at the 1/3 radius, a site of predominantly cortical bone, while the lumbar spine, a site of predominantly cancellous bone, is generally well preserved. Histomorphometric and micro-computed tomography (μCT) analyses of iliac crest bone biopsies have confirmed these DXA results in PHPT by showing reduced cortical elements whereas the trabecular compartment appears to be relatively well preserved. These findings, however, are inconsistent with numerous epidemiological reports showing an increased in fracture risk at both vertebral and non-vertebral sites in PHPT. Emerging technologies, such as high-resolution peripheral quantitative computed tomography (HRpQCT), and trabecular bone score (TBS) may provide additional insight into microstructural features and bone quality in PHPT. Moreover, individual trabecula segmentation (ITS) and finite element analysis (FEA) of HRpQCT images offer even more detailed information about trabecular bone and bone stiffness, estimating the biomechanical competence of bone, and fracture risk in PHPT

Aims: To evaluate both cortical and trabecular compartments by HRpQCT and FEA, and the trabecular compartment by ITS analysis, in postmenopausal women with PHPT, as compared to healthy controls. To correlate TBS with HRpQCT measurements in PHPT.

Patients and Methods: HRpQCT, ITS and FE analyses were performed in 51 postmenopausal women with PHPT and 120 controls. TBS was assessed in a subgroup of 22 women with PHPT.

Results: aBMD at the lumbar spine by DXA was similar in cases and controls. However, women with PHPT showed, at both sites, decreased volumetric densities at trabecular and cortical compartments, thinner cortices, and more widely spaced and heterogeneously distributed trabeculae. At the radius, trabeculae were thinner and fewer in PHPT. The radius was affected to a greater extent in the trabecular compartment than the tibia. ITS analyses revealed, at both sites, that plate-like trabeculae were depleted, with a resultant reduction in the plate/rod ratio. Microarchitectural abnormalities were evident by decreased plate-rod and plate-plate junctions at the radius and tibia, and rod-rod junctions at the radius. These trabecular and cortical abnormalities resulted in decreased whole bone stiffness and trabecular stiffness. TBS was correlated with all HRpQCT and

mechanical measurements except for trabecular thickness (Tb.Th), and trabecular stiffness at the radius. At the tibia, correlations were observed between TBS and volumetric densities, cortical thickness, trabecular bone volume, and whole bone stiffness. All indices of trabecular microarchitecture, except Tb.Th, correlated with TBS after adjusting for body weight.

Conclusion: These results provide evidence that in PHPT, reduced volumetric densities and microstructural abnormalities are pervasive and not limited to the cortical compartment. These abnormalities seen by HRpQCT are likely to reflect reduced bone strength and may help to account for increased global fracture risk in PHPT. With significant correlations of TBS with mechanical and microstructural indices by HRpQCT, a method that is not generally available, TBS could become a helpful clinical tool in the assessment of trabecular microstructure in PHPT.

Key words: primary hyperparathyroidism, parathyroid hormone, high-resolution peripheral quantitative computed tomography (HRpQCT), trabecular bone score (TBS), individual trabecular segmentation (ITS), finite element analysis (μFEA).

LISTA DE ILUSTRAÇÕES

INTRODUÇÃO:

ARTIGO 1:

ARTIGO 2:

LISTA DE TABELAS

LISTA DE ABREVIATURAS

$1,25(OH)_2D$	1,25 di-hidroxi-vitamina D
25OHD	25 hidroxi-vitamina D
aBMD	densidade mineral óssea areal (do inglês, *areal bone mineral density*)
aBV/TV	fração do volume ósseo orientado em sentido axial (do inglês, *axial bone volume fraction*)
BMI	índice de massa corporal (do inglês, *body mass index*)
BV/TV	volume ósseo (do inglês, *bone volume*)
Conn.D	densidade da conectividade trabecular (do inglês, *conectivity density*)
Ct.Th	espessura cortical (do inglês, *cortical thickness*)
Ct.vBMD	densidade mineral óssea volumétrica cortical (do inglês, *cortical volumetric bone mineral density)*
Ctload distal	porcentagem de carga suportada pelo compartimento cortical na superfície distal (do inglês, *cortical load at distal surface*)
Ctload proximal	porcentagem de carga suportada pelo compartimento cortical na superfície proximal (do inglês, *cortical load at proximal surface*)
DXA	medida da absorção de raio-X de dupla energia (do inglês, *dual energy X-ray absortiometry*)
FEA	análise de elementos finitos (do inglês, *finite element analysis*)
HPT-JT	síndrome hiperparatireoidismo-tumor de mandíbula (do inglês, *hyperparathyroidism-jaw tumor syndrome*)
HRpQCT	tomografia computadorizada quantitativa periférica de alta resolução (do inglês, *high resolution peripheric quantitative computadorized tomography*)
ITS	Análise de trabécula individual (do inglês, *individual trabecula segmentation*)
MEN-1	neoplasia endócrina múltipla tipo 1 (do inglês, *multiple endocrine neoplasia type 1*)
MEN-2a	neoplasia endócrina múltipla tipo 2a (do inglês, *multiple endocrine neoplasia type 2a*)
P-P Junc.D	densidade de junções entre placas (do inglês, *plate-plate junction density)*
P-R Junc.D	densidade de junções entre placas e hastes (do inglês, *plate-rod junction density*)
Razão P-R	Razão placa-haste (do inglês, *plate-rod ratio*)

pBV/TV	Fração de volume ósseo em placas (do inglês, *plate bone volume fraction*)
PHPT	hiperparatireoidismo primário (do inglês, *primary hyperparathyroidism*)
pQCT	tomografia computadorizada quantitativa periférica (do inglês, *peripheric quantitative computadorized tomography*)
pTb.N	número de trabéculas em placas (do inglês, *trabecular plate number*)
pTb.S	área de superfície média das trabéculas em placa (do inglês, *mean trabecular plate surface area*)
pTb.Th	espessura média de trabéculas em placas (do inglês, *mean trabecular plate thickness*)
PTH	paratormônio
R-R Junc.D	densidade de junções entre hastes (do inglês, *rod-rod junction density*)
rBV/TV	Fração de volume ósseo em hastes (do inglês, *rod bone volume fraction*)
rTb. ℓ	comprimento médio das trabéculas em haste (do inglês, *mean trabecular rod length*)
rTb.N	número de trabéculas em hastes (do inglês, *trabecular rod number*)
rTb.Th	espessura média de trabéculas em hastes (do inglês, *mean trabecular rod thickness*)
Tb.N	número de trabéculas (do inglês, *trabecular number*)
Tb.Sp	Separação trabecular (do inglês, *trabecular separaration*)
Tb.Sp.SD	desvio padrão da separação trabecular ou distribuição trabecular (do inglês, *trabecular separation standard deviation* ou *trabecular distribution*)
Tb.Th	espessura trabecular (do inglês, *trabecular thichness*)
Tb.vBMD	densidade mineral óssea volumétrica trabecular (do inglês, *trabecular volumetric bone mineral density*)
TBS	escore de osso trabecular (do inglês, *trabecular bone score*)
vBMD	densidade mineral óssea volumétrica (do inglês, *volumetric bone mineral density*)
µCT	microtomografia computadorizada (do inglês, *micro-computed tomography*)

SUMÁRIO

7- ANEXOS

1- INTRODUÇÃO:

1.1- Hiperparatireoidismo Primário:

Hiperparatireoidismo primário (PHPT) é uma doença endócrina comum causada por disfunção de uma ou mais glândulas paratireoides, resultando, tipicamente, em hipercalcemia e níveis elevados ou inapropriadamente normais de paratormônio (PTH) (BRINGHURST *et al.*, 2008). Constitui a causa mais comum de hipercalcemia em pacientes ambulatoriais. As mulheres são mais afetadas que os homens, em uma relação de 3:1. O pico de incidência da doença é a sexta década de vida, sendo raramente encontrada em indivíduos menores de 15 anos de idade (VIEIRA, 2007; BRINGHURST *et al.*, 2008).

O excesso de PTH leva a maior reabsorção renal de cálcio, fosfatúria, aumento da síntese de 1,25 diidroxi-vitamina D [1,25$(OH)_2$D] e aumento da reabsorção óssea, perpetuando a hipercalcemia. Os resultados dessas ações evidenciam-se nas manifestações bioquímicas da doença, que além de hipercalcemia, cursa com hipofosfatemia, ou, mais comumente, fósforo sérico no limite inferior da normalidade, redução dos níveis séricos de 25 hidroxi-vitamina D (25OHD) e aumento dos níveis circulantes de 1,25$(OH)_2$D (HOLICK, 2007; BILEZIKIAN, 2012). Calciúria de 24 horas é normal ou aumentada, devido ao aumento da carga filtrada de cálcio. Marcadores de remodelação óssea são tipicamente elevados, indicando aumento da reabsorção e formação ósseas (BILEZIKIAN, 2012).

1.1.1- Etiologia e patogênese:

O PHPT é causado, em 80% dos casos, por adenoma de uma das glândulas paratireoides. Múltiplos adenomas são encontrados em 2 a 4% dos pacientes, e algumas vezes, esses tumores benignos localizam-se em regiões anatômicas que não as lojas paratireoidianas. Adenomas ectópicos são encontrados, mais comumente, dentro da glândula tireoide, mediastino superior ou timo (BILEZIKIAN *et al.*, 2012). Em aproximadamente 15% dos pacientes, o PHPT é causado por hiperplasia das 4 glândulas paratireoides e, muito raramente, em menos de 1% dos casos, câncer de paratireoide é a causa do PHPT (BRINGHURST *et al.*, 2008). Nesses casos, a doença tende a apresentar-se de forma

mais grave, com níveis calcêmicos muito elevados e sintomas evidentes (MARCOCCI *et al.*, 2008).

Na grande maioria dos casos, o PHPT é esporádico e causado por mutação no DNA das células principais da paratireoide, ocasionando sua expansão clonal, com consequente formação do adenoma (ARNOLD *et al.*, 1988). Mutações somáticas ativadoras do oncogene *Cyclin D1,* ou inativadoras do gene supressor de tumor *MEN1* foram descritas em pacientes portadores de adenoma da paratireoide (ARNOLD *et al.*, 2002). A origem do PHPT esporádico causado por hiperplasia das paratireoides é desconhecida, mas acredita-se que estímulos extra-paratireoidianos ou anormalidades genéticas presentes nas quatro glândulas contribuam para a proliferação celular anormal observada nessa condição (BRINGHURST *et al.*, 2008). Diferente do adenoma, a hiperplasia resulta de uma expansão policlonal das células principais da paratireoide (ARNOLD *et al.*, 1988). Em casos esporádicos de carcinoma de paratireoide, mutações somáticas foram identificadas nos genes *HRPT2, Cyclin D1, Rb, p53 e BRCA2* (MARCOCCI *et al.*, 2008).

As formas hereditárias de PHPT são raras, mas seu conhecimento é de fundamental importância, uma vez que requerem manejo diferenciado (SARQUIS *et al.*, 2008). As principais formas familiares de PHPT são as síndromes de neoplasia endócrina múltipla tipo 1 (MEN-1) e 2a (MEN-2a) e a síndrome hiperparatireoidismo-tumor de mandíbula (HPT-JT), associadas a mutações germinativas nos genes *MEN1, RET e HRPT2*, respectivamente (BRANDI *et al.*, 2001). Além do PHPT, presente em quase 100% dos portadores de MEN-1, tumores hipofisários e de ilhotas pancreáticas caracterizam essa síndrome. Na MEN-2a, caracterizada por carcinoma medular de tireoide e feocromocitoma, PHPT é evidente em apenas 5 a 20% dos pacientes. As duas condições manifestam-se em indivíduos mais jovens e, quando presente, o PHPT é mais frequentemente causado por hiperplasia (MARX *et al.*, 2002). Na síndrome HPT-JT, tumores fibrosos da mandíbula associam-se ao quadro de PHPT, sendo o carcinoma de paratireoide mais incidente nessa entidade (MARX *et al.*, 2002). Finalmente, o hiperparatireoidismo familiar isolado, outra forma hereditária de PHPT, não se acompanha de manifestações clínicas ou marcadores genéticos definidos (SIMONDS *et al.*, 2002).

1.1.2- Apresentação clínica do PHPT – forma clássica

Manifestações clínicas do PHPT resultam de sinais e sintomas relacionados à hipercalcemia (fraqueza muscular, depressão, apatia, poliúria, desidratação, constipação intestinal, coma), aumento da excreção renal de cálcio (nefrocalcinose, nefrolitíase, insuficiência renal) e/ou aumento da reabsorção óssea (osteíte fibrosa cística e fraturas por fragilidade) (VIEIRA, 2007; BRINGHURST *et al.*, 2008).

Os primeiros relatos de PHPT retratam uma condição de alta morbi-mortalidade (WILSON *et al.*, 1964). Sintomas neuro-psiquiátricos incluíam cefaleia, depressão, confusão mental, letargia e coma. Em 1949, Patten e colegas descreveram síndrome neuromuscular própria do PHPT, caracterizada por fraqueza muscular simétrica periférica, distúrbio da marcha, atrofia muscular, hiperreflexia generalizada e fasciculações da língua (PATTEN *et al.*, 1974). Sintomas gastro-intestinais como anorexia, náusea, vômitos e constipação eram observados com frequência. Além disso, pancreatite aguda e úlceras pépticas foram descritas em associação com a doença (KEATING, 1961). Poliúria e polidipsia graves, algumas vezes diagnosticadas como diabetes insipidus, foram também relatadas (COPE, 1966). Redução da função renal, nefrocalcinose e nefrolitíase eram evidentes. Antes de 1965, nefrolitíase era observada em até 80% dos pacientes com PHPT (KEATING, 1961; WILSON *et al.*, 1964). Nessa época, o diagnóstico de PHPT envolvia testes metabólicos complexos, uma vez que a dosagem sérica de PTH tornou-se disponível anos depois, em 1963 (BERSON *et al.*, 1963).

O envolvimento esquelético característico do PHPT, osteíte fibrosa cística, foi reportado pela primeira vez em 1891, por von Recklinghausen. No entanto, o reconhecimento de disfunção das paratireoides como causa da doença óssea deu-se mais tarde, em 1925, quando Mandl observou, em paciente jovem do sexo masculino, remissão das lesões ósseas após remoção cirúrgica de tumor da paratireoide (ALBRIGHT, 1948). Em 1926, Albright, Aub e Bauer estudaram o primeiro paciente diagnosticado com PHPT nos EUA, cujo adenoma de paratireoide, localizado na região torácica, foi removido após 6 explorações cirúrgicas mal sucedidas (ALBRIGHT, 1948). Antes da localização do adenoma, o paciente foi tratado clinicamente com dieta rica em cálcio, o que, apesar de aumentar seus níveis calcêmicos, contribuiu significativamente para melhora de sua doença óssea (POTTS, 2005). Nas décadas subsequentes, osteíte fibrosa cística foi

observada em vários pacientes com PHPT (KEATING, 1961; WILSON *et al.*, 1964; COPE, 1966; MALLETTE *et al.*, 1974). Achados característicos dessa condição são: 1- desmineralização óssea generalizada; 2- reabsorção subperióstea, mais evidente em falanges e região distal das clavículas; 3- aspecto em "sal e pimenta" à radiografia de crânio; 4- cistos ósseos, normalmente múltiplos, mais frequentes em metacarpos, ossos longos, pélvis e crânio; 5- osteoclastomas ou tumores marrons, que são tumores compostos por múltiplos osteoclastos e células estromais, encontrados mais frequentemente em ossos longos, costelas e mandíbula; e 6: fraturas patológicas. Clinicamente, pacientes acometidos por osteíte fibrosa cística podem apresentar dor óssea, cifose torácica, redução de estatura e colapso lateral da costela ou pélvis (BRINGHURST *et al.*, 2008).

1.1.3- Apresentação clínica do PHPT nos dias atuais

Após a década de 70, a instituição de dosagens de cálcio em exames de rotina mudou consideravelmente a forma de apresentação do PHPT em países desenvolvidos. Nos dias atuais, o PHPT é uma doença sobretudo assintomática, sendo descoberta pelo achado fortuito de hipercalcemia (SILVERBERG *et al.*, 1999; ADAMI *et al.*, 2002; BILEZIKIAN *et al.*, 2005; RUBIN *et al.*, 2008). No Brasil, a frequência de pacientes sintomáticos ainda é considerável, constituindo cerca de 40 a 50% dos casos (KULAK *et al.*, 1998; OHE *et al.*, 2005; BANDEIRA *et al.*, 2006). Estudo brasileiro mais recente envolvendo 91 pacientes portadores de PHPT evidenciou nefrolitíase e fratura por fragilidade em 52 e 4% dos casos, respectivamente (NEVES *et al.*, 2012). No entanto, observa-se, também em nosso meio, redução da frequência de doença sintomática nos últimos anos (OHE *et al.*, 2005).

A forma assintomática ou oligossintomática de PHPT apresenta-se, com frequência, com hipercalcemia leve e, portanto, sintomas sistêmicos decorrentes de elevação da calcemia estão, tipicamente, ausentes. Da mesma forma, nefrolitíase é reportada em apenas 10 a 25% dos casos (MOLLERUP *et al.*, 2002; RUBIN *et al.*, 2008). Sintomas neuropsiquiátricos como fraqueza, esquecimento, cansaço fácil, depressão e ansiedade, podem estar presentes mesmo nas formas leves de PHPT, podendo ou não melhorar com o tratamento cirúrgico da doença (PASIEKA *et al.*, 2002; QUIROS *et al.*, 2003; BOLLERSLEV *et al.*, 2007; WALKER *et al.*, 2009). Sintomas cardiovasculares como

hipertensão arterial, hipertrofia de ventrículo esquerdo, espessamento da camada médio-intimal da artéria carótida, calcificação miocárdica e valvular também foram reportados em vários estudos, mas não confirmados por outros (SILVERBERG *et al.*, 2009; WALKER *et al.*, 2010; CARRELLI *et al.*, 2012; IWATA *et al.*, 2012). Da mesma forma, a melhora desses parâmetros não é regra após paratireoidectomia, e portanto, a importância desses achados no PHPT assintomático requer investigação adicional (SILVERBERG *et al.*, 2009).

O achado de osteíte fibrosa cística em pacientes com PHPT é raro nos dias atuais. Em pacientes com PHPT assintomático, o acometimento esquelético é notado sobretudo pelo achado de osteoporose. No entanto, diferente de outras causas secundárias de osteoporose, o padrão de redução da densidade mineral óssea areal (aBMD) por medida da absorção de raio-X de dupla energia (DXA) é compatível com perda óssea cortical e preservação óssea trabecular. Esse conceito fundamenta-se na observação de que há propensão para maior redução da aBMD em rádio 33%, sítio ósseo composto predominantemente por osso cortical. Por outro lado, aBMD em coluna lombar, sítio ósseo essencialmente trabecular, tende a ser preservada quando comparada a indivíduos controle da mesma idade (SILVERBERG *et al.*, 1989; RUBIN *et al.*, 2008) (Figura 1). Confirmando esses achados densitométricos, histomorfometria de biópsia de crista ilíaca revela deterioração do compartimento cortical e preservação do compartimento trabecular em homens e mulheres na pré e pós menopausa portadores de PHPT. Quando comparados a controles da mesma idade e sexo, pacientes com PHPT possuem espessura cortical reduzida. No entanto, apresentam volume ósseo trabecular (BV/TV), número de trabéculas (Tb.N) e densidade da conectividade trabecular (Conn.D) maiores ou similares ao grupo controle (PARISIEN *et al.*, 1990; CHRISTIANSEN *et al.*, 1992; PARISIEN *et al.*, 1992; PARISIEN *et al.*, 1995). Em pacientes com PHPT, separação trabecular (Tb.Sp) é menor (PARISIEN *et al.*, 1990) e espessura trabecular (Tb.Th) é menor ou similar a controles normais (PARISIEN *et al.*, 1990; CHRISTIANSEN *et al.*, 1992). Da mesma forma, análise de biópsia de crista ilíaca por microtomografia computadorizada (μCT) confirmou que, quando comparadas a mulheres sadias na pós menopausa, mulheres na pós menopausa com PHPT apresentam BV/TV e Conn.D aumentados, e Tb.Sp diminuída (DEMPSTER *et al.*, 2007). Mulheres na pré-menopausa com PHPT possuem BV/TV semelhante a mulheres sadias de mesmo estado menopausal (Figura 2).

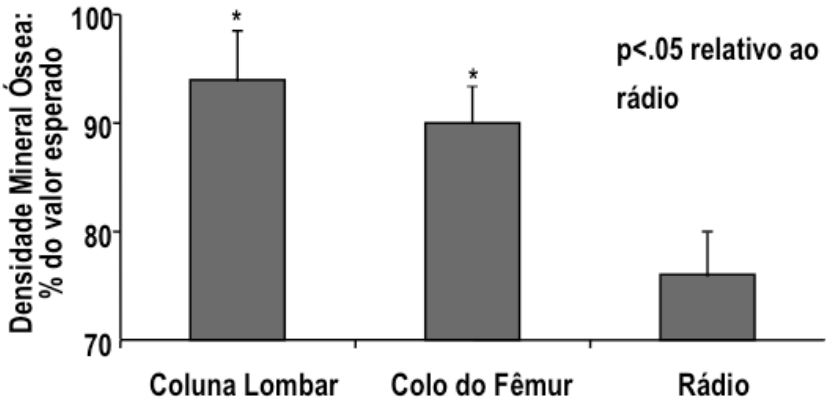

Figura 1: Padrão densitométrico típico do hiperparatireoidismo primário nos dias atuais. Densidade mineral óssea areal da coluna lombar, colo do fêmur e rádio apresentada em comparação a valores esperados para controles normais.
Adaptado de (SILVERBERG *et al.*, 1989)

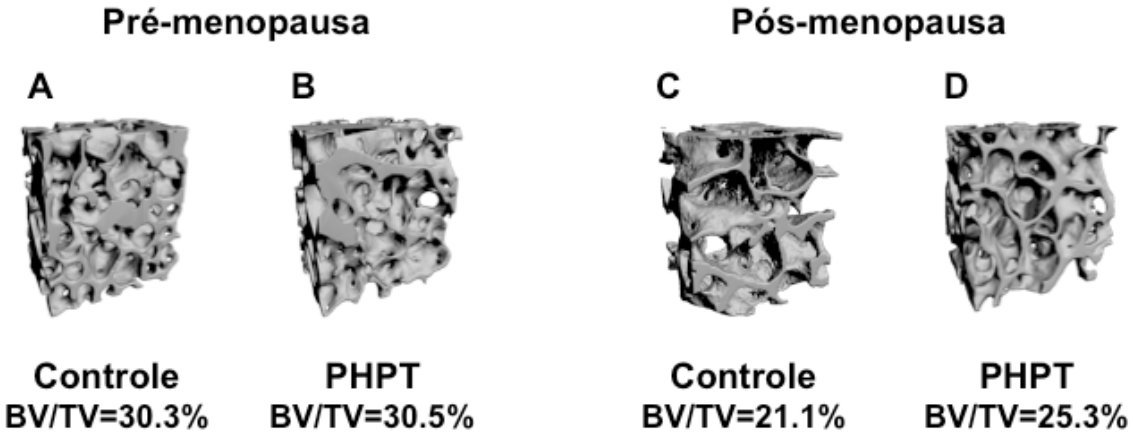

Figura 2: Microarquitetura em mulheres saudáveis e com PHPT. Reconstruções em 3D de imagens de microtomografia computadorizada de osso trabecular em mulheres com PHPT na pré e pós-menopausa (B e D) e controles sadios (A e C).
Adaptado de (DEMPSTER *et al.*, 2007).

1.1.4- Risco de fratura no PHPT

Apesar do padrão densitométrico típico do PHPT, com redução preferencial da aBMD em sítio cortical, confirmada por achados inequívocos de preservação de microarquitetura e volume trabecular em biópsias de crista ilíaca, numerosos estudos identificaram risco aumentado de fratura vertebral e não vertebral em pacientes com PHPT

(KOCHERSBERGER *et al.*, 1987; KHOSLA *et al.*, 1999; VESTERGAARD and MOSEKILDE, 2003; VIGNALI *et al.*, 2009; YU *et al.*, 2010). Pacientes avaliados nesses estudos eram, em sua maioria, portadores da forma assintomática da doença, e o número de indivíduos avaliados variou de 150 a 1.700. Risco global de fratura, assim como risco de fratura vertebral, pélvica, em costela e rádio foram maiores em pacientes com PHPT do que em indivíduos controles. Fratura de fêmur foi marginalmente mais incidente em indivíduos com PHPT (KHOSLA *et al.*, 1999). Análise prospectiva avaliando quase 2.000 pacientes com PHPT evidenciou aumento do risco de fratura de fêmur apenas em um subgrupo de homens submetidos a paratireoidectomia para tratamento da doença, mas não em toda a população do estudo (LARSSON *et al.*, 1993). Finalmente, risco de fratura vertebral foi semelhante em pacientes com PHPT assintomático e controles históricos (WILSON *et al.*, 1988). Apesar de alguns achados divergentes, grande maioria dos relatos aponta para risco aumentado de fraturas em PHPT e, portanto, reavaliação do conceito estabelecido de preservação do osso trabecular nessa entidade faz-se necessária.

Métodos de imagem não invasivos que permitam a avaliação individualizada dos compartimentos trabecular e cortical poderiam trazer informações adicionais e ser mais pertinentes à discussão do risco de fratura no PHPT assintomático. De fato, estudos de pacientes com PHPT por tomografia computadorizada quantitativa periférica (pQCT), avaliando tanto o rádio (CHEN *et al.*, 2003), quanto a tíbia (CHAROPOULOS *et al.*, 2006), evidenciam efeitos negativos do PTH em ambos os compartimentos esqueléticos. Esta tecnologia permite, através da avaliação de sítios periféricos com resolução de 500 a 590µm, a diferenciação dos compartimentos cortical e trabecular, além de avaliar a geometria óssea. Mais recentemente, estudo por tomografia computadorizada quantitativa periférica de alta resolução (HRpQCT), revelou perda óssea tanto cortical quanto trabecular em rádio distal em mulheres com PHPT (HANSEN *et al.*, 2010). Este estudo, no entanto, envolveu apenas 26 pacientes com PHPT e, as alterações em osso trabecular não foram confirmadas na tíbia. Além do mais, não se estudou se as alterações estruturais encontradas afetariam a competência biomecânica do osso. Portanto, estudos adicionais para avalição esquelética de pacientes com PHPT, utilizando técnicas de imagem não invasivas, que permitam análise do esqueleto trabecular com mais acurácia, poderiam trazer informações adicionais a respeito da qualidade óssea nessa doença, ampliando nosso conhecimento acerca do risco de fratura em pacientes com PHPT.

1.2- Tomografia Computadorizada Quantitativa periférica de Alta Resolução (HRpQCT):

HRpQCT é um método não invasivo que permite a avaliação *in vivo* da geometria, densidade mineral óssea volumétrica (vBMD) e microarquitetura dos compartimentos cortical e trabecular (BURGHARDT *et al.*, 2011). A utilização da HRpQCT para avaliação esquelética no PHPT é particularmente atraente, uma vez que acredita-se que o PTH exerça ações diferentes nos compartimentos cortical e trabecular. Além de avaliar geometria, vBMD e microarquitetura, métodos adicionais de avaliação têm sido aplicados a imagens de HRpQCT para avaliação mais detalhada da estrutura trabecular e da competência biomecânica do esqueleto.

HRpQCT foi desenvolvida para o estudo *in vivo* da extremidade distal do rádio e da tíbia com resolução suficiente (tamanho de voxel= 82 μm) para fornecer informações acerca da microestrutura trabecular e cortical, disponíveis anteriormente apenas através de estudos histomorfométricos de biópsia óssea. Além de ser um método de alta resolução, HRpQCT tem a vantagem de oferecer uma dose de radiação ionizante baixa (radiação efetiva de 1 a 3 mSv), não expondo órgãos internos aos efeitos nocivos da radiação (DAMILAKIS *et al.*, 2010). No entanto, a HRpQCT é uma técnica de alto custo e, portanto, poucos centros médicos no mundo têm acesso a essa tecnologia. Apesar de avaliar o rádio distal, área comumente sujeita a fratura osteoporótica (Fratura de Colles), HRpQCT não avalia sítios ósseos centrais como fêmur e coluna lombar, importantes alvos de fratura por fragilidade.

O instrumento utilizado para a realização do exame é fornecido atualmente por um único fabricante (XtremeCT; Scanco Medical AG, Brüttisellen, Suíça). Para a realização do exame, uma primeira imagem da região de interesse é adquirida em posição ântero-posterior e uma linha de referência é traçada na região distal do rádio e da tíbia. Uma série de 110 imagens paralelas sequenciais são então adquiridas, sendo a primeira obtida a 9,5 mm proximal à linha de referência do rádio e 22,5 mm proximal à linha de referência da tíbia. As imagens são reconstruídas, fornecendo uma imagem em 3 dimensões com 9 mm de comprimento (BOUTROY *et al.*, 2005; KHOSLA *et al.*, 2006).

Análise da imagem reconstruída se dá a partir de um protocolo padrão fornecido pelo fabricante. Os parâmetros fornecidos por essa análise-padrão e utilizados nesse trabalho

são: área total, que equivale à área de secção transversal; densidade mineral óssea volumétrica total (Total vBMD), cortical (Ct.vBMD) e trabecular (Tb.vBMD); espessura cortical (Ct.Th); volume ósseo trabecular (BV/TV); número trabecular (Tb.N); espessura trabecular (Tb.Th); separação trabecular (Tb.Sp) e desvio padrão da separação trabecular (Tb.Sp.SD). Essas variáveis são calculadas diretamente, ou a partir do cálculo das variáveis estimadas de forma direta.[1]

Apesar de apresentar correlação modesta com a histomorfometria quando diferentes regiões ósseas são avaliadas (COHEN A., *et al.*, 2010), medidas de microarquitetura avaliados por HRpQCT correlacionam-se significativamente com resultados de histomorfometria ou μCT avaliados em mesmas regiões ósseas (MACNEIL and BOYD, 2007; BOUTROY *et al.*, 2011). Estudos clínicos iniciais para avaliação do método demonstraram que a HRpQCT é capaz de detectar diferenças na microestrutura óssea entre homens e mulheres, bem como alterações relacionadas ao envelhecimento ou a outras causas de perda óssea (BOUTROY *et al.*, 2005; KHOSLA *et al.*, 2006). Mais recentemente, vários estudos confirmaram que medidas de densidade mineral óssea volumétrica e microarquitetura óssea por HRpQCT distinguem indivíduos com história de fraturas vertebrais e não vertebrais de controles normais, independentemente de aBMD em rádio ultra-distal ou fêmur total (SORNAY-RENDU *et al.*, 2007; VICO *et al.*, 2008; STEIN *et al.*, 2010; STEIN *et al.*, 2011; STEIN *et al.*, 2012).

[1]As seguintes variáveis são calculadas de modo direto: área total, Total vBMD, Ct.vBMD, Tb.VBMD, Ct.Th e Tb.N. O cálculo do BV/TV é derivado de Tb.vBMD, assumindo que um osso totalmente mineralizado tem densidade de 1.200 mg de hidroxiapatita por centímetro cúbico (BV/TV (%)= 100 X (Tb.vBMD/1.200). Uma vez que a HRpQCT tem resolução suficiente para medir a distância entre as trabéculas, a medida do Tb.N é determinada diretamente medindo o inverso do distância média entre as trabéculas. Por outro lado, a espessura média das trabéculas, entre 100 e 150μm, limita sua visualização, uma vez que cada trabécula ocupa 1 a 2 voxels. Dessa forma seu cálculo é derivado de BV/TV e Tb.N: Tb.Th= (BV/TV)/ Tb.N. O cálculo da Tb.Sp é feito de maneira semelhante (Tb.Sp=(1−BV/TV)/Tb.N).

1.2.1- Análise de trabécula individual (ITS)

Análise de trabécula individual (ITS) é uma nova técnica de análise do compartimento trabecular em imagens de alta resolução. A técnica foi desenvolvida por Liu e Guo (LIU *et al.*, 2008) e inicialmente aplicada a imagens de μCT obtidas de amostras ósseas de colo de fêmur, tíbia proximal e vértebras lombares. Mais recentemente, ITS foi validada para análise de imagens de HRpQCT (LIU *et al.*, 2011a).

A estrutura do osso trabecular é constituída por uma rede interconectada de hastes e placas. A técnica de ITS consiste em identificar cada trabécula óssea, classificando-a como haste ou placa, e analisando sua orientação dentro do compartimento trabecular, ou seja, se cada haste ou placa se dispõe de maneira transversal, longitudinal ou oblíqua em relação ao eixo ósseo axial (LIU *et al.*, 2008). À partir da caracterização de cada elemento trabecular é possível estimar a fração do volume ósseo trabecular representada por placas e hastes (pBV/TV e rBV/TV, respectivamente) e a razão entre essas duas medidas (razão P-R). Da mesma forma, determina-se o número e espessura de cada tipo trabecular - número de placas e hastes (pTb.N e rTb.N) e espessura média de placas e hastes (pTb.Th e rTb.Th). O comprimento médio das trabéculas em haste (rTb. ℓ) e a área de superfície média das trabéculas em placa (pTb.S) são também considerados. Além disso, a conectividade trabecular é calculada de acordo com a morfologia de cada placa, estimando-se a densidade de junções entre placas (P-P Junc.D), entre hastes (R-R Junc.D) ou entre placas e hastes (P-R Junc.D). Por último, como a orientação trabecular também é avaliada pelo método, é possível calcular a fração do volume trabecular orientado no sentido axial (aBV/TV) (Figura 3).

Em sua descrição inicial em estudo *ex vivo*, os resultados de ITS foram correlacionados com análise padrão por μCT e com parâmetros biomecânicos estimados por análise de elementos finitos (FEA) de imagens de μCT. Resultados desses estudos indicam que trabéculas em placa são as determinantes primárias da resistência óssea e que o aumento da razão P-R está associado a maior rigidez[2] óssea. Além disso, dentre todas as variáveis estudadas, aBV/TV teve a melhor correlação com as medidas de competência mecânica óssea (LIU *et al.*, 2008).

[2] do inglês, *stiffness*.

Em estudos clínicos, ITS derivada de imagens de HRpQCT revelou que mulheres na pré menopausa com osteoporose idiopática apresentam redução preferencial de trabéculas em placas, além de redução de aBV/TV (LIU *et al.*, 2010). Além disso, ITS demonstrou diferenças-chave entre o esqueleto de mulheres caucasianas e chinesa-americanas, explicando o achado de risco reduzido de fratura em mulheres chinesas, apesar de medidas semelhantes de aBMD (LIU *et al.*, 2011b). Finalmente, estudo avaliando fratura por fragilidade em mulheres na pós menopausa revelou que ITS foi capaz de distinguir mulheres com história de fratura de controles saudáveis. Nesse estudo, fratura osteoporótica vertebral e não vertebral foi associada a osso trabecular constituído principalmente por hastes e redução de placas, além de redução de aBV/TV e da conectividade trabecular (LIU *et al.*, 2012).

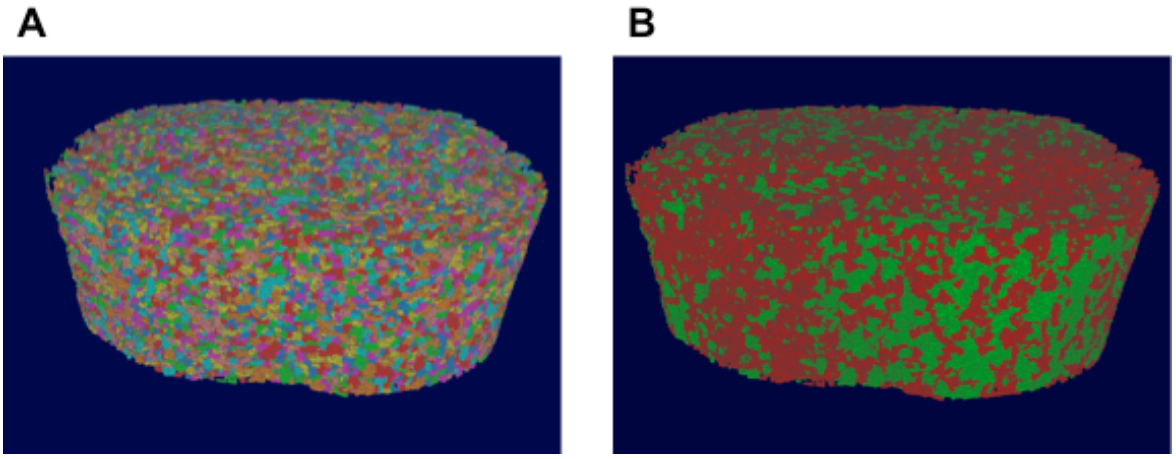

Figura 3: Imagens de osso trabecular segmentado em trabéculas individuais
(A) Diferentes cores foram usadas para visualização de trabéculas individualmente; (B) Representação de trabéculas em placa (verde) e em haste (vermelho). Imagens de tíbia distal obtidas de mulher saudável na pós menopausa
Imagens cordialmente cedidas por Dr. Edward Guo e Bin Zhou

1.2.2- Análise de elementos finitos (FEA):

Além de fornecer dados acerca da densidade volumétrica e estrutura esquelética, HRpQCT tem o potencial de estimar a competência biomecânica do osso. Através da FEA de imagens de HRpQCT, determina-se rigidez óssea, parâmetro fortemente correlacionado com resistência óssea e risco de fratura (BOUTROY *et al.*, 2008).

Competência biomecânica do osso refere-se à sua capacidade de sustentar certa carga sem sofrer fratura, e rigidez é a capacidade do material em resistir à deformação, quando uma força lhe é aplicada. Rigidez óssea, calculada através de FEA de imagens em 3 dimensões de HRpQCT, apresenta forte correlação com resistência óssea medida por ensaios de compressão mecânica (PISTOIA *et al.*, 2002; MACNEIL and BOYD, 2008). Além disso, estudos envolvendo mulheres na pós menopausa ou homens idosos confirmam que a rigidez óssea estimada por FEA de imagens de HRpQCT é significativamente menor em indivíduos com história de fratura por fragilidade do que em controles sem história de fratura (BOUTROY *et al.*, 2008; STEIN *et al.*, 2010; VILAYPHIOU *et al.*, 2010; STEIN *et al.*, 2011; VILAYPHIOU *et al.*, 2011).

FEA estima rigidez do osso inteiro, quando os compartimentos cortical e trabecular são avaliados, e rigidez trabecular, quando apenas este compartimento é considerado para análise. Outras variáveis calculadas por esse método de análise e reportadas nesse trabalho são a porcentagem de carga suportada pelo compartimento cortical nas superfícies distal e proximal do volume de interesse (Ctload distal e Ctload proximal). Estas medidas levam em conta a integridade do compartimento trabecular, uma vez que refletem a porcentagem de carga que **não** pode ser sustentada pelo osso trabecular e portanto é transferida para o osso cortical. Ou seja, quanto maior o déficit estrutural do compartimento trabecular, maior será a porcentagem de carga suportada pelo compartimento cortical.

Apesar da HRpQCT ser capaz de fornecer informações fundamentais para avaliação da qualidade óssea no PHPT, esse é um exame de alto custo e difícil acesso. Dessa forma, seria de suma importância a avaliação de métodos acessíveis na prática clínica para avaliação mais acurada do compartimento trabecular em pacientes com PHPT.

1.3- Escore de Osso Trabecular (TBS):

TBS é um novo método de avaliação de imagem desenvolvido para estimar a microarquitetura trabecular (POTHUAUD *et al.*, 2008). Qualquer imagem de radiografia óssea pode ser utilizada para avaliação do TBS, mas sua principal vantagem clínica baseia-se na possibilidade de poder ser calculado a partir de imagens de densitometria óssea. Isso possibilita que o TBS seja estimado como complementação da avaliação de

aBMD, ou em exames de densitometria realizados previamente, sem necessidade de aquisição de novas imagens. O cálculo de TBS foi incialmente desenvolvido a partir de imagens de densitometria óssea da coluna lombar (HANS *et al.*, 2011a) e, portanto, estudos clínicos que avaliam a aplicabilidade do método baseiam-se em TBS da coluna lombar. TBS calculado a partir de imagens do fêmur está em desenvolvimento, mas ainda não disponível para fins de pesquisa clínica.

No primeiro estudo a descrever a técnica, TBS foi calculado a partir de imagens de μCT em 2 dimensões (imagens de μCT projetadas em um plano) e correlacionado com medidas diretas de microarquitetura trabecular por μCT (POTHUAUD *et al.*, 2008). Os resultados demonstraram correlação significativa entre TBS (medida indireta de microestrutura trabecular) e BV/TV, Tb.N, Conn.D e Tb.Sp (medidas diretas por μCT). Esse estudo utilizou peças ósseas humanas de vértebras torácicas baixas e lombares, colo de fêmur e rádio, e as correlações foram estimadas no mesmo sítio ósseo. Em um segundo passo para validação do método, TBS foi derivado de imagens de densitometria óssea de vértebras lombares de cadáveres humanos (HANS *et al.*, 2011a). TBS assim calculado mostrou, novamente, correlação significativa com as mesmas medidas de microestrutura trabecular por μCT descritas anteriormente. aBMD foi avaliada nas mesmas amostras ósseas e correlacionada com TBS. Não houve correlação significativa entre aBMD e TBS, indicando que os dois métodos, apesar de calculados a partir da mesma imagem, traduzem características diferentes do osso. Confirmando essa teoria, algumas amostras ósseas revelaram ter diferentes cálculos de TBS (e diferentes estruturas ósseas por μCT) a despeito de densidades ósseas similares (HANS *et al.*, 2011a).

TBS é calculado por software próprio (TBS iNsight Software, MedImaps, França), que pode ser instalado no computador que gerencia o aparelho de densitometria óssea ou em computador não conectado àquele aparelho. Em ambos os casos, arquivos não processados contendo as imagens de coluna lombar são utilizados para análise do TBS. TBS é expresso em valores sem unidade de medida e seu cálculo se dá a partir de variograma da imagem bidimensional do osso trabecular. A fórmula considera as diferenças entre os vários tons de cinza em pixels da imagem. A quantidade de pixels com diferentes tons de cinza e o quão diferente os tons são entre si têm importância no cálculo. O valor final de TBS dá-se pelo cálculo da inclinação da curva do variograma em um diagrama log-log. Dessa forma, uma imagem com vários tons de cinza, mas com

pequena diferença entre os tons, resulta em valores maiores de TBS (microarquitetura normal). Imagem com número menor de cinzas, mas com grande variação entre os tons, gera valores baixos de TBS (microarquitetura deteriorada) (HANS *et al.*, 2011a). TBS é avaliado na mesma região de interesse usada para o cálculo da aBMD e o valor representa a média dos valores encontrados de L1 a L4 (Figura 4).

Em estudos clínicos envolvendo mulheres na pós menopausa, TBS em coluna lombar foi associado a risco de fraturas vertebrais e não vertebrais, estimando seu risco independentemente dos valores de aBMD (POTHUAUD *et al.*, 2009; RABIER *et al.*, 2010; WINZENRIETH *et al.*, 2010; DEL RIO *et al.*, 2012). Além disso, a combinação de TBS com aBMD em coluna lombar aumentou a predição do risco de fratura em comparação a cada um dos testes isoladamente. Esses achados foram confirmados pelo Estudo de Manitoba, que avaliou mais de 29.000 mulheres na pós-menopausa no Canadá (HANS *et al.*, 2011b). Recentemente, Boutroy *et al* mostraram que além de estimar fraturas osteoporóticas tão bem quanto aBMD de coluna lombar, TBS foi capaz de identificar um subgrupo de mulheres não-osteoporóticas com alto risco de fratura (BOUTROY *et al.*, 2012).

Apesar de não haver consenso acerca de valores de TBS considerados alterados, alguns autores estudaram o valor de 1,20 como possível limite inferior da normalidade (LAMY *et al.*, 2012; POPP *et al.*, 2012; VASIC *et al.*, 2012). Esses estudos foram publicados em forma de resumos em anais de congressos, e avaliaram apenas mulheres na pós menopausa. Os resultados demonstram que o achado de T-score ≤ -2,5 por DXA em qualquer sítio ósseo *ou* TBS < 1,20 em coluna lombar, identificou uma proporção significativamente maior de mulheres com história de fraturas por fragilidade que o achado isolado de T-score ≤ -2,5. De forma similar, em mulheres não osteoporóticas com TBS < 1,209, a incidência de fraturas por fragilidade foi significativamente maior que no grupo com valores de TBS acima desse limite (BOUTROY *et al.*, 2012). Quando as mulheres participantes do Estudo de Manitoba foram estratificadas em tercis de acordo com valores de TBS, os valores encontrados como limite entre os 3 grupos foram 1,20 e 1,35 (comunicação pessoal). Nesse estudo, o tercil de mulheres com menores valores TBS tiveram maior risco de fratura osteoporótica do que as mulheres do terço médio ou superior (HANS *et al.*, 2011b). Baseado nesses estudos, os seguintes pontos de corte

foram sugeridos para classificação de TBS em mulheres na pós menopausa: TBS≤1,20= microarquitetura degradada; TBS entre 1,20 e 1,35= microarquitetura parcialmente degradada; TBS ≥1,35= microarquitetura normal.

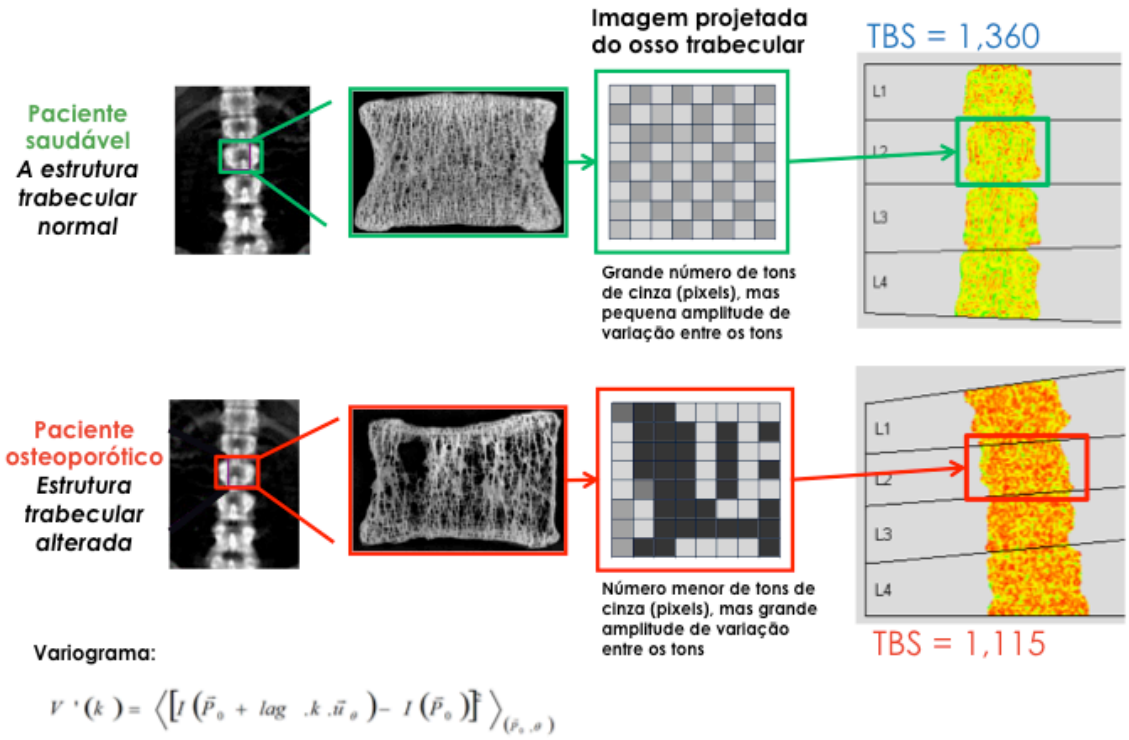

Figura 4: Princípios do escore de osso trabecular

Adaptado de (POTHUAUD *et al.*, 2008; HANS *et al.*, 2011a)

TBS= Escore de osso trabecular

Figura cordialmente cedida por Dr. Didier Hans

O presente estudo consiste na avaliação óssea através de HRpQCT e TBS de mulheres na pós menopausa com diagnóstico estabelecido de PHPT. Além das medidas usuais fornecidas pela técnica de HRpQCT, ITS e FEA foram realizadas para avaliação mais detalhada do compartimento ósseo trabecular e da competência biomecânica do esqueleto. Os resultados foram comparados aos de 120 mulheres saudáveis da mesma faixa-etária e estado pós menopausal. TBS foi estimado em um subgrupo de mulheres com PHPT e correlacionado com medidas por HRpQCT.

2- OBJETIVOS:

2.1- Artigo 1:

Determinar, através de HRpQCT, geometria óssea, densidade volumétrica e índices microestruturais dos compartimentos cortical e trabecular em mulheres na pós-menopausa com PHPT, comparando-as com um grupo controle.

Investigar a competência biomecânica do osso através de FEA de imagens de HRpQCT e, pela primeira vez em pacientes com PHPT, analisar as imagens de HRpQCT através da técnica de ITS para avaliação mais detalhada do compartimento ósseo trabecular nessa doença.

2.2- Artigo 2:

Avaliar a correlação entre TBS e medidas por HRpQCT em pacientes com PHPT.

3- RESULTADOS:

3.1- Artigo 1:

Primary Hyperparathyroidism is Associated with Abnormal Cortical and Trabecular Microstructure and Reduced Bone Stiffness in Postmenopausal Women

Artigo aceito para publicação no "*Journal of Bone and Mineral Research*" em 26 de novembro de 2012.

Primary Hyperparathyroidism is Associated with Abnormal Cortical and Trabecular Microstructure and Reduced Bone Stiffness in Postmenopausal Women

Emily M Stein[1]*, Barbara C Silva[1,3]*, Stephanie Boutroy[1], Bin Zhou[2], Ji Wang[2], Julia Udesky[1], Chiyuan Zhang[1], Donald J McMahon[1], Megan Romano[1], Elzbieta Dworakowski[1], Aline G. Costa[1], Natalie Cusano[1], Dinaz Irani[1], Serge Cremers[1], Elizabeth Shane[1], X Edward Guo[2], John P Bilezikian[1#]

**** These authors contributed equally to this work***

1- Metabolic Bone Diseases Unit, Division of Endocrinology, Department of Medicine, College of Physicians and Surgeons, Columbia University, New York, NY, USA

2- Bone Bioengineering Laboratory, Department of Biomedical Engineering, Columbia University, New York, NY, USA

3- College of Medicine of Federal University of Minas Gerais, Belo Horizonte, Brazil

Correspondence to:
John P. Bilezikian. M.D.
College of Physicians and Surgeons
630 W, 168th Street, New York, NY 10032, USA
Phone: 212.305.6257
Fax: 212.305.6486
e-mail: jpb2@columbia.edu

Abstract:

Typically, in the milder form of primary hyperparathyroidism (PHPT), seen in most countries now, bone density by DXA and detailed analyses of iliac crest bone biopsies by histomorphometry and μCT show detrimental effects in cortical bone, whereas the trabecular site (lumbar spine by DXA) and the trabecular compartment (by bone biopsy) appear to be relatively well preserved. Despite these findings, fracture risk at both vertebral and non-vertebral sites is increased in PHPT. Emerging technologies, such as high-resolution peripheral quantitative computed tomography (HRpQCT), may provide additional insight into microstructural features at sites such as the forearm and tibia that have heretofore not been easily accessible. Using HRpQCT, we determined cortical and trabecular microstructure at the radius and tibia in 51 postmenopausal women with PHPT and 120 controls. Individual trabecula segmentation (ITS) and micro finite element (μFE) analyses of the HRpQCT images were also performed to further understand how the abnormalities seen by HRpQCT might translate into effects on bone strength. Women with PHPT showed, at both sites, decreased volumetric densities at trabecular and cortical compartments, thinner cortices, and more widely spaced and heterogeneously distributed trabeculae. At the radius, trabeculae were thinner and fewer in PHPT. The radius was affected to a greater extent in the trabecular compartment than the tibia. ITS analyses revealed, at both sites, that plate-like trabeculae were depleted, with a resultant reduction in the plate/rod ratio. Microarchitectural abnormalities were evident by decreased plate-rod and plate-plate junctions at the radius and tibia, and rod-rod junctions at the radius. These trabecular and cortical abnormalities resulted in decreased whole bone stiffness and trabecular stiffness. These results provide evidence that in PHPT, microstructural abnormalities are pervasive and not limited to the cortical compartment. They may help to account for increased global fracture risk in PHPT.

Key words: Primary hyperparathyroidism, high-resolution peripheral quantitative computed tomography, individual trabecula segmentation, finite element analysis, fracture risk.

Introduction

Primary hyperparathyroidism (PHPT), a common endocrine disorder, is characterized primarily by hypercalcemia and elevated levels of parathyroid hormone (PTH). Although the disease harbors a potential for extensive destruction of the skeleton, and commonly presented in this way during the first several decades of its description (1), asymptomatic PHPT has become the predominant form of the disease since the 1970s (2-4). Typically, in this milder form of PHPT, bone density by dual energy X-ray absorptiometry (DXA) is reduced with a proclivity for greatest reduction at the 1/3 radius, a site of cortical bone. By DXA, the lumbar spine, a site comprised predominantly of cancellous bone, tends to be preserved and similar to age-matched control subjects (5). Histomorphometric and micro-computed tomography (μCT) analyses of iliac crest bone biopsies have confirmed these DXA results by specific measurements of cortical and trabecular compartments. Cortical width is reduced and cortical porosity is increased. Trabecular bone volume is above average while trabecular number, connectivity and separation are preserved (6-10). However, these results are not consistent with evidence from many different studies demonstrating increased fracture risk at both vertebral and non-vertebral sites in PHPT (11-14). While the fracture data are still incomplete, the likelihood of overall increased fracture risk would argue, on the one hand, that DXA is not accurately depicting microstructure of bone due to its limited resolving power, and on the other hand, that the bone biopsy data from the iliac crest, in which the microstructure of bone is easily depicted, is not representative of load-bearing sites or other sites that are predisposed to fracture. Occasional reports of reduced trabecular bone density in PHPT (15, 16) argue that trabecular bone, clearly a potential target in severe disease, might also be affected in more mild disease and that more highly resolved technologies that can be applied to sites of loaded and unloaded bone would be revealing.

High resolution, noninvasive imaging methods, enabling *in vivo* assessment of cortical and trabecular bone microarchitecture and biomechanical competence, could provide additional insight into compartment-specific (trabecular *vs* cortical) effects of PTH in PHPT and be more pertinent to the clinical discussion of fracture risk in PHPT. To this end, High Resolution peripheral Quantitative Computed Tomography (HRpQCT), a non-invasive technique has sufficient resolution (voxel size, 82 μm) to quantitate trabecular and cortical microstructure that previously could be assessed only in bone biopsy samples. Moreover, HRpQCT has been developed to visualize the microstructure of the

distal radius, an unloaded site, and the distal tibia, a loaded site. Strong correlations between microarchitecture assessed by HRpQCT and histomorphometry or μCT at the same bony regions have been demonstrated (17, 18). This technology further distinguishes subjects who have sustained vertebral and non-vertebral fractures from normal controls (19-23), and detects changes in bone microstructure related to aging or other causes of bone loss (24-26). Recently, Hansen *et al* observed, by HRpQCT, altered trabecular and cortical structure at the radius in PHPT, and improvement in volumetric density and bone microarchitecture following parathyroidectomy (27, 28). This report supports the idea that if sites more relevant to fracture risk in PHPT are measured with highly resolved technologies, abnormalities in trabecular bone can be observed.

In addition to assessing microstructure, HRpQCT images can be used to measure mechanical competence of bone by microstructural finite-element analysis (μFEA) (29). Recent advances have demonstrated that individual trabecula segmentation (ITS)-based morphologic analysis of HRpQCT images can provide even more specific information about trabecular bone microarchitecture. ITS resolves the HRpQCT image into individual trabeculae, characterizing trabecular elements as either plates or rods. Plate-like trabeculae are the primary determinants of bone strength; a higher plate/rod ratio is associated with greater strength (30, 31). μFE and ITS analyses of HRpQCT images distinguish among individuals with and without osteoporosis and fragility fractures, independent of DXA measurements (23, 32-35). ITS analyses of HRpQCT images have also demonstrated key differences between the Caucasian American and Chinese American skeleton, helping to account for reduced fracture risk in Chinese women despite similar bone mineral densities (36).

In this study, we have utilized HRpQCT to determine microstructural indices of cortical and trabecular compartments at the radius and tibia in 51 postmenopausal women with PHPT and 120 normal controls. We have also utilized μFE and, for the first time, ITS analyses of HRpQCT images to assess trabecular morphology and bone compartment-specific mechanical competence in PHPT. The results of this study provide new insights into bone quality in postmenopausal women with PHPT.

Patients and Methods

Study Subjects:

51 postmenopausal community-dwelling women, with well-characterized PHPT (elevated serum calcium and abnormal PTH levels) were recruited from Columbia University Medical Center (CUMC) in New York. The 120 control individuals were healthy postmenopausal women selected independently of their areal bone mineral density by DXA, also recruited from CUMC by advertisement, self or physician referral. All control subjects had normal serum calcium levels and no history of PHPT or low trauma fracture. Exclusion criteria included significant use of glucocorticoids within the past 2 years, history of Cushing's syndrome, uncontrolled thyroid disease, malabsorption syndrome, significant liver disease, creatinine clearance < 30 mL/min, and any chronic disorders of mineral metabolism such as Paget's disease or osteogenesis imperfecta. Use of bisphosphonates, raloxifene, and hormone replacement therapy (HRT) were not an exclusionary criterion. Women were considered postmenopausal if they had not had a menstrual period for over 1 year.

The study was approved by the Institutional Review Board of Columbia University Medical Center, and all subjects gave written informed consent.

Dual-energy X-ray absorptiometry (DXA):

Areal bone mineral density (aBMD) was measured at the lumbar spine (L1–L4), total hip, femoral neck, and nondominant forearm [ultradistal (UD radius) and one-third radius (1/3 radius)] by DXA (Hologic 4500A; Hologic Inc., Bedford, MA, USA). Short term, *in vivo* precision error was 0.5% for L1–L4, 1.5% for total hip and femoral neck, and 1% for the forearm.

HRpQCT:

The nondominant distal radius and tibia were measured using the HRpQCT system (Xtreme CT; Scanco Medical AG, Brüttisellen, Switzerland) at CUMC. This device uses a 2D detector array and a 0.08-mm point-focus X-ray tube enabling the simultaneous acquisition of a stack of a parallel CT slices with a nominal resolution (voxel size) of 82μm. The following settings were used: effective energy of 60kVp, x-ray tube current of 900μA, and image matrix size of 1,536 x 1,536.

An antero-posterior scout view was used to define the measurement region. A reference line was manually placed at the end plate of the radius and tibia. A stack of 110 parallel CT slices was acquired (distal to proximal), with the first slice being 9.5 mm proximal to the reference line at the radius and 22.5 mm proximal to the reference line at the tibia. At each skeletal site, a 3D image of approximately 9 mm in the axial direction was obtained. Attenuation data were converted to equivalent hydroxyapatite (HA) densities. For quality control, the manufacturer phantom was scanned daily.

Image analysis has been described and validated (17, 24, 25, 37). Briefly, the entire volume of interest is automatically separated into cortical and trabecular regions by using a threshold-based algorithm. Mean cortical thickness (Ct.Th) is defined as the mean cortical volume divided by the outer bone surface. Cortical and trabecular bone densities (Ct.vBDM and Tb.vBMD) are defined as the average bone density within the cortical or trabecular volume of interest, respectively. Trabecular bone volume (BV/TV) is derived from Tb.vBMD assuming that fully mineralized bone has the density of 1,200 mg hydroxyapatite (HA) per cubic centimeter (BV/TV (%)=100x (Tb.vBMD/1,200). Since the nominal spatial resolution of the XtremeCT (82 μm) is in the range of trabecular dimensions, visualization of individual trabeculae is limited. Therefore, measurements of trabecular microstructure are assessed using a thickness-independent algorithm. To this end, trabecular elements are identified by a mid-axis transformation method and the distance between them is assessed by the distance-transform method. Trabecular number (Tb.N) is taken as the inverse of the mean spacing of the mid-axes. Trabecular thickness (Tb.Th) and trabecular separation (Tb.Sp) are then derived from BV/TV and Tb.N using standard methods of histomorphometry, *i.e.*, Tb.Th=(BV/TV)/Tb.N and Tb.Sp=(1−BV/TV)/Tb.N. Distance transformation techniques also enable the calculation of intra-individual distribution of separation (Tb.Sp.SD), quantified by the SD of the separation, a parameter reflecting the heterogeneity of the trabecular network.

ITS-based morphological analyses of HRpQCT images:

The trabecular bone compartment was manually extracted from the cortex of each HRpQCT image of the distal radius and distal tibia. All trabecular bone images were then subjected to ITS-based morphological analyses. A complete volumetric decomposition technique was applied to segment the trabecular network into individual plates and rods (30). Briefly, digital topological analysis (DTA)-based skeletonization is performed to

transform the trabecular bone image into a schematic comprised of surfaces and curves skeleton. The topology (*i.e*, connectivity, tunnels, and cavities), as well as the rod and plate morphology of the trabecular microarchitecture, are preserved. Each skeletal voxel is uniquely classified as either a surface (plate) or a curve (rod) type. Using an iterative reconstruction method, each bone voxel of the original image is classified as belonging to either type of trabecula. ITS parameters of scale evaluate plate and rod bone volume fraction (pBV/TV and rBV/TV), plate and rod number density (pTb.N and rTb.N, 1/mm), plate and rod thickness (pTb.Th and rTb.Th, mm), plate surface area (pTb.S, mm^2), and rod length (rTb.ℓ, mm). Plate-to-rod ratio (P-R ratio) was defined as plate bone volume divided by rod bone volume. Trabecular network connectivity is characterized by plate–plate, plate–rod, and rod–rod junction density (P-P, P-R, and R-R Junc.D, $1/mm^3$), calculated as the total junctions between trabecular plates and rods normalized by the bulk volume. Lastly, the orientation of trabecular bone network is characterized by axial bone volume fraction (aBV/TV), defined as axially aligned bone volume divided by the bulk volume.

µFEA of HRpQCT images:

Whole bone and trabecular HRpQCT images of the radius and tibia were converted into micro finite element models. µFEA was then performed to estimate whole bone and trabecular stiffness. For each µFE model, a uniaxial compression test was performed with displacement equivalent to 1% apparent strain to calculate stiffness. Bone tissue was assumed to have an isotropic linear material property with Young's modulus 15 GPa and Poisson's ratio 0.3. Whole bone stiffness, defined as reaction force divided by the applied displacement, characterizes the mechanical competence of both cortical and trabecular compartments and is closely related to whole bone strength (38). Similarly, trabecular bone stiffness characterizes the mechanical competence of the trabecular bone compartment. Percent load carried by the cortical compartment at the distal and proximal surface of bone segments was also calculated.

Biochemical analysis

Blood samples were drawn in a fasting state. Serum total calcium and albumin were analyzed using standard methods (Quest Diagnostics, Madison, NJ, USA). Calcium values were corrected for low albumin (albumin < 4 g/dL). In patients with PHPT, intact PTH was measured by immunoradiometric assay (Scantibodies, Santee, CA, USA) in the

Bone Marker Laboratory of the Metabolic Bone Diseases Program at CUMC. The normal range was 14 to 66 pg/mL, and the precision inter- and intra-assay coefficients were below 7% and 5%, respectively.

Statistical Analysis:

Descriptive statistics and group comparisons are expressed as mean ± SEM. Differences in continuous variables between cases and controls were assessed by Student's t-test. Dichotomous variables were compared using the chi-square test. Comparisons of percent difference in HRpQCT, ITS and mechanical measurements between cases and controls at the radius and tibia were calculated and then assessed by Student's t-test for paired samples. Since serum PTH levels and BMI did not follow a normal distribution, the Spearman correlation test was used to estimate their correlation with HRpQCT indices. Finally, comparisons of correlations between groups and between sites were examined by Fisher's Z transformation (39). All statistical tests were performed at the two-sided 0.05-level of significance. Statistical analysis was performed using SAS, version 9.2 (SAS Institute, Inc., Cary, NC, USA).

Results

Baseline clinical, biochemical and densitometric data of the 51 postmenopausal women with PHPT and 120 controls are described in Table 1. Case and control subjects did not differ on the basis of age, body weight, height, BMI, years since menopause, and current use of HRT and raloxifene. Bisphosphonate use was significantly greater among patients. As expected, serum calcium levels were higher in the PHPT group. The majority of PHPT patients (77%) were asymptomatic. Only 12 subjects had nephrolithiasis (n=6) and/or fragility fracture (n=8).

aBMD by DXA:

aBMD was significantly lower in PHPT subjects than in controls at the total hip, femoral neck, and UD radius. Mean aBMD by DXA was similar in PHPT and controls at the lumbar spine and 1/3 radius (Table 1). In the PHPT group, the lumbar spine and total hip T-scores were higher than the T-scores at the femoral neck and both radial sites (Table 1).

HRpQCT standard analysis:

As shown in Table 2 and representative 3D images of the radius in Figure 1, PHPT was associated with reduced volumetric densities (vBMD), and altered cortical and trabecular microarchitecture as assessed by HRpQCT.

At the radius and tibia, total bone area was not significantly different from control subjects. Total vBMD was significantly lower in PHPT at the radius (-19%) and tibia (-13%). Ct.vBMD and Ct.Th. were 6% and 18% lower at the radius, and 7% and 15% lower at the tibia in PHPT *vs* control subjects ($p<.001$ for all). Significant reductions of Tb.vBMD at the radius (-23%) and tibia (-11%) were also observed in PHPT ($p<0.01$). At the radius, trabecular microarchitectural indices in PHPT were different from controls ($p< 0.05$) with lower Tb.N (-13%), Tb.Th (-12%) and increased Tb.Sp (+32%). At the tibia, there were no significant differences in Tb.N and Tb.Th between the two groups, but Tb.Sp was higher in PHPT subjects (+16%) (Table 2 and Figure 2).

As shown in Figure 2, compared to tibial measurements, the percentage differences between cases and controls were more pronounced at the radius for total vBMD ($p=0.006$), Tb.vBMD ($p=0.0004$), and Tb.N ($p=0.02$).

ITS-analysis of HRpQCT images:

ITS analysis of the trabecular compartment revealed key microstructural differences at the radius, and, to a lesser extent, at the tibia in PHPT (Table 3 and Figure 3).

At the radius, plate and rod bone volume fraction (pBV/TV, rBV/TV), plate and rod trabecular number (pTb.N, rTb.N), and plate-rod ratio (P-R ratio) were 31%, 13%, 11%, 5% and 22% lower in PHPT *vs.* controls, respectively ($p<0.01$). At the tibia, pBV/TV, pTb.N and P-R ratio were 20%, 5% and 19% lower in PHPT patients, respectively ($p<0.01$), whereas no significant differences for tibial rBV/TV and rTb.N were found.

The axial bone volume fraction (aBV/TV) was significantly reduced at the radius (-25%), and at the tibia (-16%) in PHPT *vs* controls. At the radius, rod-to-rod, plate-to-rod and plate-to-plate junction densities (R-R, P-R, and P-P JuncD) were significantly lower in PHPT at 13%, 26%, and 30%, respectively. Similarly, there was a significant decrease in P-R (-9%), and P-P JuncD (-15%) at the tibia in patients with PHPT.

The percentage-differences between cases and controls were again more pronounced at the radius as compared to the tibia for virtually all ITS parameters (Figure 3).

µFEA of HRpQCT images:

The differences in volumetric density, cortical and trabecular microstructure were associated with significant changes in bone mechanical properties (Table 3 and Figure 3). Trabecular stiffness was 46% and 18% lower in the PHPT than in the control group at the radius and tibia, respectively. Whole bone stiffness was reduced by 22% at the radius, and 10% at the tibia. At the radius, the percentage of load carried by the cortical compartment was greater in PHPT, at both distal and proximal surfaces, at the radius (Figure 3). The increased percentage of load carried by the cortical compartment observed in PHPT may be explained by the abnormal trabecular microstructure, resulting in a shift in load distribution to the cortical compartment at the radius. At the tibia, since the trabecular abnormalities, although present, were not as great as at the radius, shift in load bearing to the cortical compartment did not differ statistically between groups.

As shown in Figure 3, percentage differences between cases and controls were greater at the radius than at the tibia for trabecular and whole bone stiffness, and for the percentage of load carried by the cortical compartment at the distal surface.

Analysis of the subgroup not on bisphosphonate therapy:

Since the use of bisphosphonate was significantly greater among PHPT patients, we verified whether or not bisphosphonate use would change our outcomes. The comparison between cases and controls not currently on bisphosphonate therapy shows reduced volumetric densities, deterioration of microarchitecture by standard HRpQCT and ITS, and decreased bone strength in PHPT patients (data not shown). These results are similar to the ones observed when the whole group was analyzed, indicating that bisphosphonate use did not influence any of the outcome measures.

Relationships between PTH and BMI with Cortical and Trabecular indices:

Among subjects with PHPT, serum PTH levels were inversely correlated with total vBMD, Tb.vBMD, and Tb.Th at the radius (r=-0.300, -0.326, -0.407, respectively; $p<0.05$ for all). At the tibia, significant negative correlations were found between serum PTH and total vBMD (r=-0.354), Ct.vBMD (r=-0.352), and Ct.Th (r=-0.350) (Figure 4). Similarly, at the radius, serum PTH levels correlated inversely and significantly with all ITS and mechanical parameters, except for rTb.N, pTb.S and R-R JuncD. At the tibia, whole bone stiffness, pBV/TV, aBV/TV, pTb.N, rTb.Th, P-P and P-R Junc.D were inversely correlated with serum PTH ($p<0.05$). In contrast, serum PTH did not show significant correlations with aBMD by DXA at any site (data not shown). Serum calcium was also not correlated with aBMD, vBMD, microstructural parameters or bone stiffness (data not shown).

To evaluate the influence of mechanical loading on trabecular and cortical bone compartments, we examined the relationships between BMI with HRpQCT-derived parameters at the tibia, a load bearing bone, in cases and controls and at the radius, a non-load bearing bone. At the tibia, cortical parameters were positively correlated with BMI in control subjects, whereas in the PHPT group, the correlation between Ct.vBMD and Ct.Th with BMI was not significant. Conversely, correlation coefficients between BMI and HRpQCT for trabecular indices such as Tb vBMD, Tb.N, and Tb.Sp were greater in PHPT (Table 4). The correlation coefficient between BMI and Tb.N at the tibia was significantly higher in the PHPT group ($p=0.02$ for comparison of correlations). The comparison of these correlations between cases and controls at the radial site did not show such major differences. Correlation coefficients between BMI and cortical HRpQCT indices, in comparison to the radial site, were greater at the tibia in the control

group (Table 4). In PHPT, these correlations showed greater dependence upon BMI at the tibia than at the radius with regard to the following indices: Tb.N, Tb.Sp, Tb.Sp.SD, and Tb.vBMD (Table 4).

Discussion

The results of this study signal a major change in analytical approaches to bone strength in PHPT. Previously, DXA and histomorphometric analyses of the iliac crest bone biopsy gave important information but each was limited in either its resolving power (DXA) or in the fact that the iliac crest is not clearly representative of bones at risk in this disease for fracture. With HRpQCT, questions relevant to fracture risk in PHPT can be analyzed with regard to skeletal microstructure and, further, with ITS, a novel approach that allows for specific assignments of microarchitecture based on topological orientation and type of trabeculae. In addition, compartmental analyses of cortical and trabecular bone at a loaded (tibia) or unloaded (radius) site provide new insights into how in PHPT, a disorder of chronic PTH excess, compromised structural integrity is not limited to the cortical skeleton.

At the radius, by HRpQCT, women with PHPT have lower total, cortical, and trabecular densities along with a thinner cortex. Trabecular microarchitecture is affected with fewer, thinner, more widely and heterogeneously distributed trabeculae. At the tibia, these changes are not as widespread but reductions in vBMDs and cortical thickness are evident, along with more widely and heterogeneously distributed trabeculae. In contrast to the radius, no abnormalities at the tibia were appreciated in trabecular number or trabecular thickness.

The catabolic effects of PTH on both cortical and trabecular bone compartments reported here have been observed by peripheral quantitative computed tomography (pQCT) in PHPT (15, 40). While qualitatively similar to our observations, the resolution of pQCT is poor relative to HRpQCT (voxel size: 500-590 μm *vs* 82 μm) and thus does not permit a detailed compartmental analysis of cortical and trabecular bone. Applying HRpQCT, Hansen *et al.* (27) recently did show changes at the radius in 26 pre and postmenopausal women with PHPT. These investigators, however, were not able to appreciate significant differences at the tibia, perhaps because of the small number of subjects in their study (only 23 postmenopausal women) and less dramatic changes at the tibial site.

This report provides further insights, not explored previously, into trabecular microstructure at the individual trabecula level by ITS analysis of the HRpQCT images. ITS analysis, developed by Guo and his associates, has been validated for assessing

trabecular microarchitecture by significant concordance with μCT (41). In PHPT, we found that plate-like trabeculae are depleted, and that the P-R ratio is reduced. This topological disturbance in microstructure leads to a trabecular network that is abnormal in plate-rod and plate-plate junctions at the radius and tibia, and rod-rod junctions at the radius. With relatively more rods than plates in the trabecular network, μFE analysis indicates that bone strength is compromised in terms of whole bone and trabecular stiffness. While both radial and tibial sites are compromised, greater deficits are seen in the distal radius. Such distortions lead to a significant increase in the load carried by the cortical compartment in the radius. These changes highlight another insight gleaned from this report, namely that with abnormal cortical structure in PHPT, the load carried by this compartment is disproportionately distributed from the trabecular compartment because it too is compromised.

Based upon these findings, the pattern of bone loss in PHPT shown in many studies by DXA needs to be reexamined. The discordant observations of preserved lumbar spine aBMD by DXA and trabecular microstructure abnormalities by HRpQCT could be explained by the DXA technology. As a 2D measure, DXA is influenced by bone size. The increased cross sectional area in patients with PHPT observed by us an others (40, 42-44), which might be a compensatory mechanism or a direct effect of PTH, could have accounted for the apparent preserved aBMD at the lumbar spine. Thus, the preservation of lumbar spine bone density by DXA in PHPT illustrates the uncertainty of this technology if geometric or microstructural abnormalities are present. Even the microstructural data by histomorphometric analysis of iliac crest bone biopsies in PHPT needs to be reexamined in light of these new data. By histomorphometry of bone biopsies from iliac crest, trabecular bone in postmenopausal women with PHPT is preserved as documented by no abnormalities in trabecular number, connectivity, or separation (5-8, 10, 45). In fact, μCT analysis of bone biopsy specimens showed that trabecular bone volume in postmenopausal women with PHPT is increased (9). It is becoming increasing clear, however, that the iliac crest might not be an ideally representative site of the peripheral skeleton. In fact, Cohen *et al* (46) have found modest or no correlations between microarchitecture parameters as assessed by HRpQCT of radius and tibia and histomorphometry and μCT of iliac crest biopsies. Since previous studies have shown strong correlations between microarchitecture assessed by HRpQCT and histomorphometry or μCT *at the same bony regions* (17, 18), site-to-site differences are

likely to contribute to the weak correlations observed in the study of Cohen et al (46).

Even at peripheral sites, such as the radius and tibia, there are differences to be observed. The differences may well be due to the extent to which a site is loaded (tibia) or unloaded (radius). Deficits in skeletal microstructure were less pronounced at the tibia in other studies (19, 23), perhaps due to positive effects of mechanical loading at this site. We observed greater effects of loading on the cortical bone in normal postmenopausal women than in PHPT patients, as observed by higher correlation coefficients between BMI and cortical indices at the tibia in controls. In PHPT, the effect of loading was also compartment-specific with the trabecular bone affected to a greater extent than cortical bone. In fact, cortical parameters at the tibia were not significantly correlated with BMI, whereas the correlation coefficients between BMI and trabecular measurements were greater in PHPT than in controls. Further supporting the idea that mechanical loading ameliorates catabolic actions of PTH on trabecular bone, we showed that trabecular bone was much more profoundly affected at the distal radius than at the tibia, whereas cortical bone was equally affected at the radius and tibia in PHPT. In addition, correlations between PTH and HRpQCT-derived trabecular indices were significant at the radius but not at the tibia, indicating that the negative effects of PTH are blunted at the load-bearing tibial site. These data suggest that mechanical loading does not prevent cortical loss in PHPT, but it may help to counteract the deleterious effects of PTH on trabecular bone. These results provide a framework for understanding that the osteoanabolic action of PTH is not seen in PHPT, a state of chronic PTH excess, but rather is limited to the intermittent administration of the hormone when used as a therapeutic for osteoporosis.

These observations have implications for assessment of fracture risk in PHPT. The HRpQCT analysis that we have conducted suggests that there is a biomechanical basis for increased fracture risk in this disease. While studies of fracture risk in PHPT are by no means definitive, the cumulative experience suggests that both the central (trabecular) and peripheral (cortical) skeleton are at risk. If HRpQCT analyses correlate with fracture risk, then the clinical observations of fracture risk in PHPT and the detailed microstructural observations of this study are consistent. In fact, previous studies have correlated HRpQCT-based abnormalities in skeletal microstructure with fracture risk in postmenopausal women (19-23, 34, 35). Similarly, reductions in plate and rod BV/TV, plate and rod trabecular number, less axially aligned trabecular network, and reduced

connectivity between plate-plate, and plate-rod like trabeculae by ITS-analysis of HRpQCT scans, all of which have been demonstrated in this study, have been described in postmenopausal women with fragility fractures (32). In several of these studies, deterioration of skeletal microstructure could distinguish between women with and without fractures even after adjusting for aBMD or T-score by DXA (19, 23, 32). Moreover, in the study by Pistoia *et al* (47), the correlation between bone strength (mechanically measured) and failure load predicted by 3DpQCT-based μFEA was stronger than its correlation with aBMD assessed by DXA. Our subjects with PHPT have similar deficiencies in skeletal microstructure and stiffness to those observed in postmenopausal women with fractures. Thus, the data provide a biomechanical mechanism to account for increased fracture risk in PHPT.

This study has some limitations. Only postmenopausal women were studied so that it is not known whether the results are applicable to men or premenopausal women with PHPT. Our study was not designed to assess differences between patients with or without fractures within the PHPT group. It remains to be seen whether these abnormalities will be appreciated to a greater extent among those who have sustained a fracture. The cross-sectional design prevented us from investigating whether or not the microstructural abnormalities at cortical and tibial sites as measured by HRpQCT will worsen over time in patients with PHPT and, if so, whether there are predictive features to this expectation. We have not yet studied subjects after parathyroidectomy in comparison to these preoperative, baseline data. HRpQCT is an analytical device that measures only peripheral sites, and, thus, it is possible that our findings will not reflect central sites such as the lumbar spine. This is unlikely in view of the recent study by Liu *et al* (48) in which volumetric density, bone microstructure and mechanical properties of peripheral sites as determined by HRpQCT correlated significantly with mechanical competence of the spine and hip.

Despite these limitations, our study has important strengths. The analytical power of HRpQCT applied to sites of great relevance to fracture risk is noteworthy. The added analytical power of ITS with μFEA provides another dimension not previously examined in this disease. The data provide greater understanding of biomechanical compromise in PHPT, helping to resolve a previous conundrum in which preserved trabecular bone by DXA or by histomorphometric studies of the iliac crest were not consistent with the

clinical observations of increased fracture risk in PHPT. Further studies are likely to provide even greater insights into microstructural features of bone in PHPT and permit greater understanding of fracture risk in this disease.

Disclosures:

The authors state that they have no conflicts of interest

Acknowledgments:

All authors met guidelines for authorship: Study design (JPB, DJM), Study conduct (EMS, BCS, JPB, JU, MR, NC, DI, AGC, ED, SC), Data analysis (BCS, CZ, DM, BZ, JW), Data interpretation (BCS, EMS, JPB, ES, NC, XEG, SB), Drafting the manuscript (BCS and JPB), Revising manuscript content (all authors), Approving final version of manuscript (all authors). Supported in part by the following NIH grants: DK32333, UL1 RR024156, K24 AR052665 (E. Shane), AR 055068, AR058004, AR051376, K23 DK 084337 (EM. Stein), K23 DK 095944 (N Cusano), and the Brazilian National Council of Technological and Scientific Development – CNPq (BC Silva).

Figures:

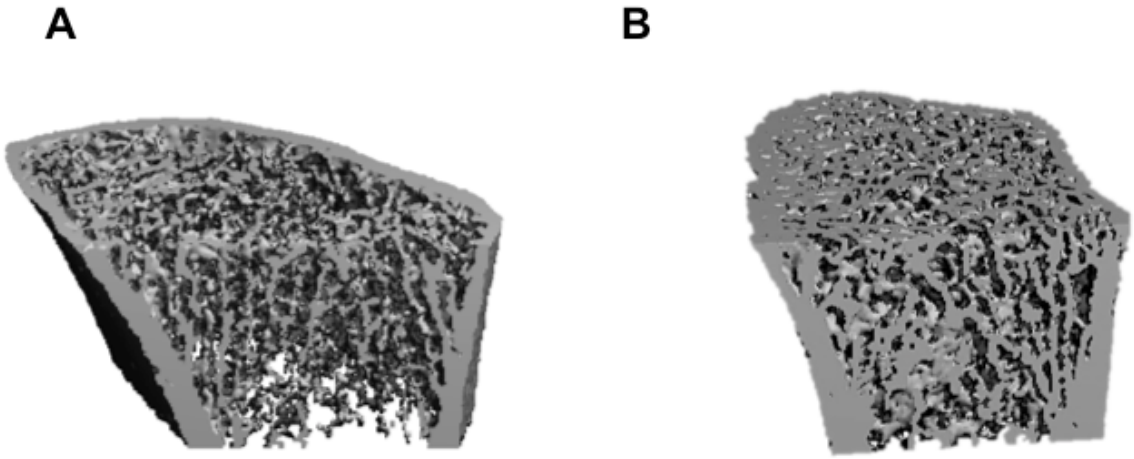

Figure 1: Representative HRpQCT images of the distal radius of PHPT (A) and control (B) subjects

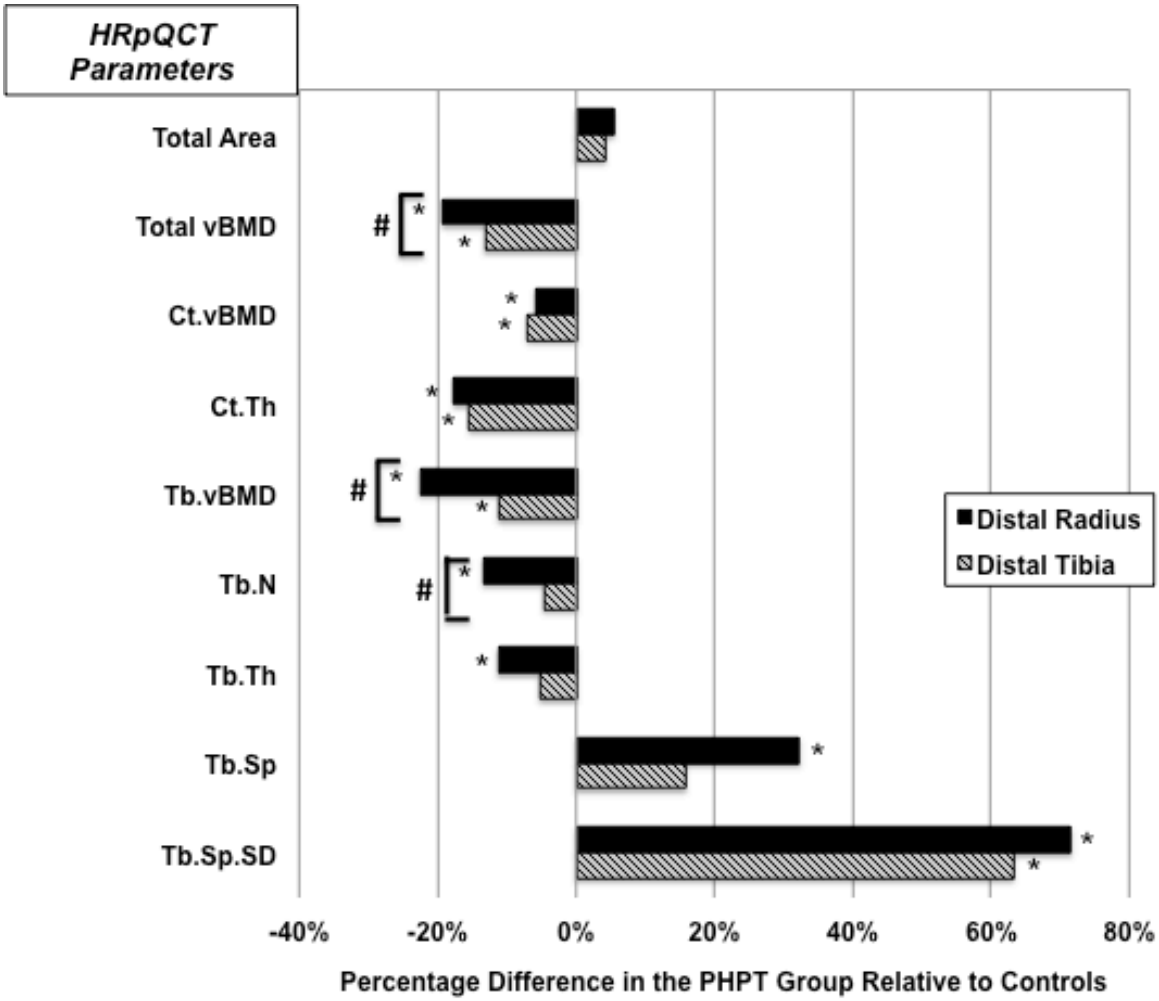

Figure 2: Comparison of HRpQCT results at the distal radius and tibia in PHPT and control groups

* Represent significant differences between groups ($p<0.05$)

Represent significant differences for comparisons of the percentage difference between radius and tibia ($p<0.05$)

Total vBMD= total volumetric bone mineral density; Ct.vBMD= cortical volumetric bone mineral density; Ct.Th= cortical thickness, Tb.vBMD= trabecular volumetric bone mineral density; Tb.N= trabecular number; Tb.Th= trabecular thickness; Tb.Sp= trabecular separation; Tb.Sp.SD= trabecular distribution

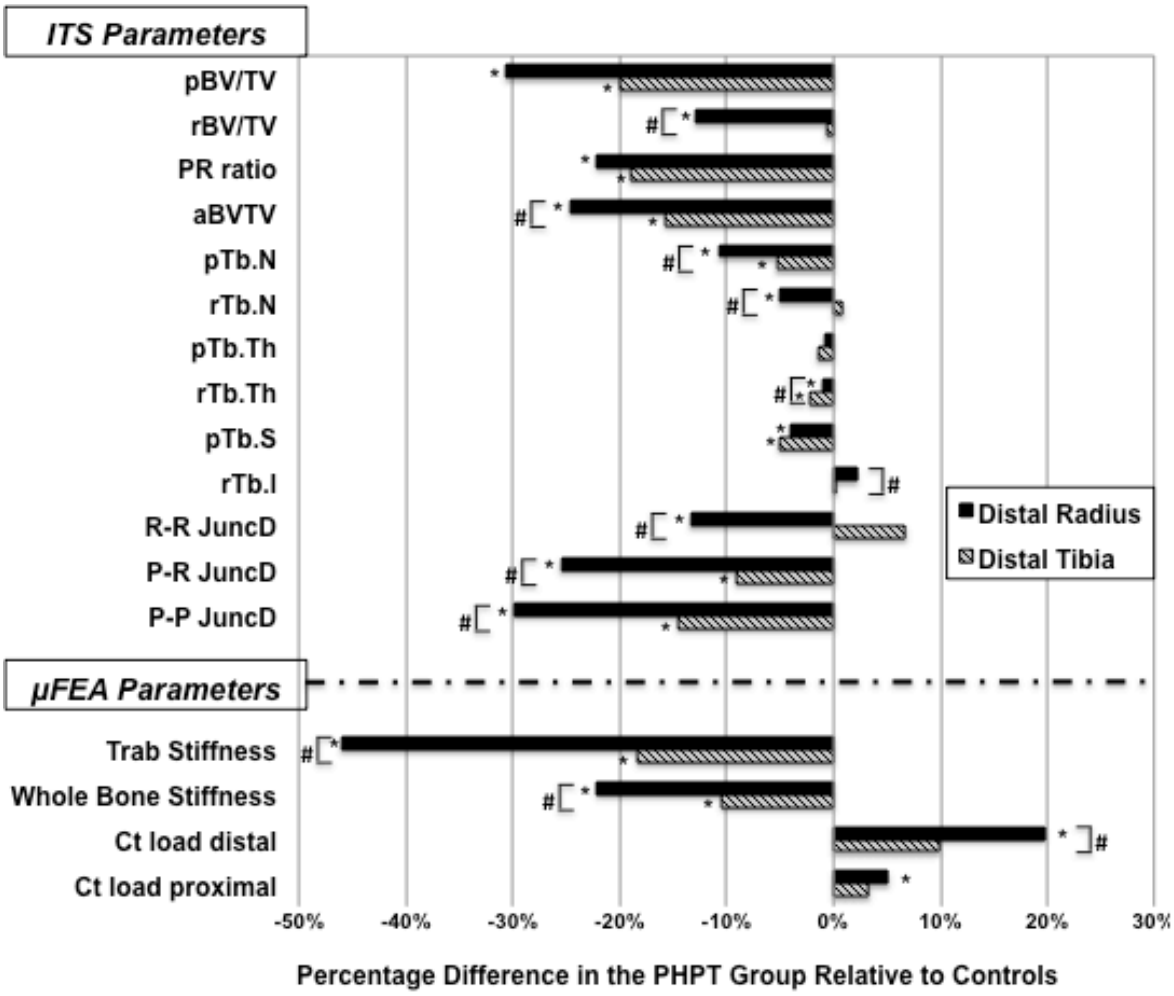

Figure 3: Comparison of the ITS and μFEA results at the distal radius and tibia in PHPT and control groups

* Represent significant differences between the groups ($p<0.05$)

Represent significant differences for comparisons of the percentage difference between radius and tibia ($p<0.05$)

pBV/TV= plate bone volume fraction; rBV/TV= rod bone volume fraction; P-R ratio= plate-to-rod ratio; aBV/TV= axial bone volume fraction; pTb.N= plate number density; rTb.N= rod number density; pTb.Th= plate thickness; rTb.Th= rod thickness; pTb.S= plate surface area; rTb.ℓ= rod length; R-R Junc.D= rod–rod junction density; P-R Junc.D= plate–rod junction density; P-P Junc.D= plate–plate junction density, Trab. Stiffness= trabecular stiffness; Stiffness= whole bone stiffness; Ctload distal= cortical load at distal surface; and Ctload proximal= cortical load at proximal surface

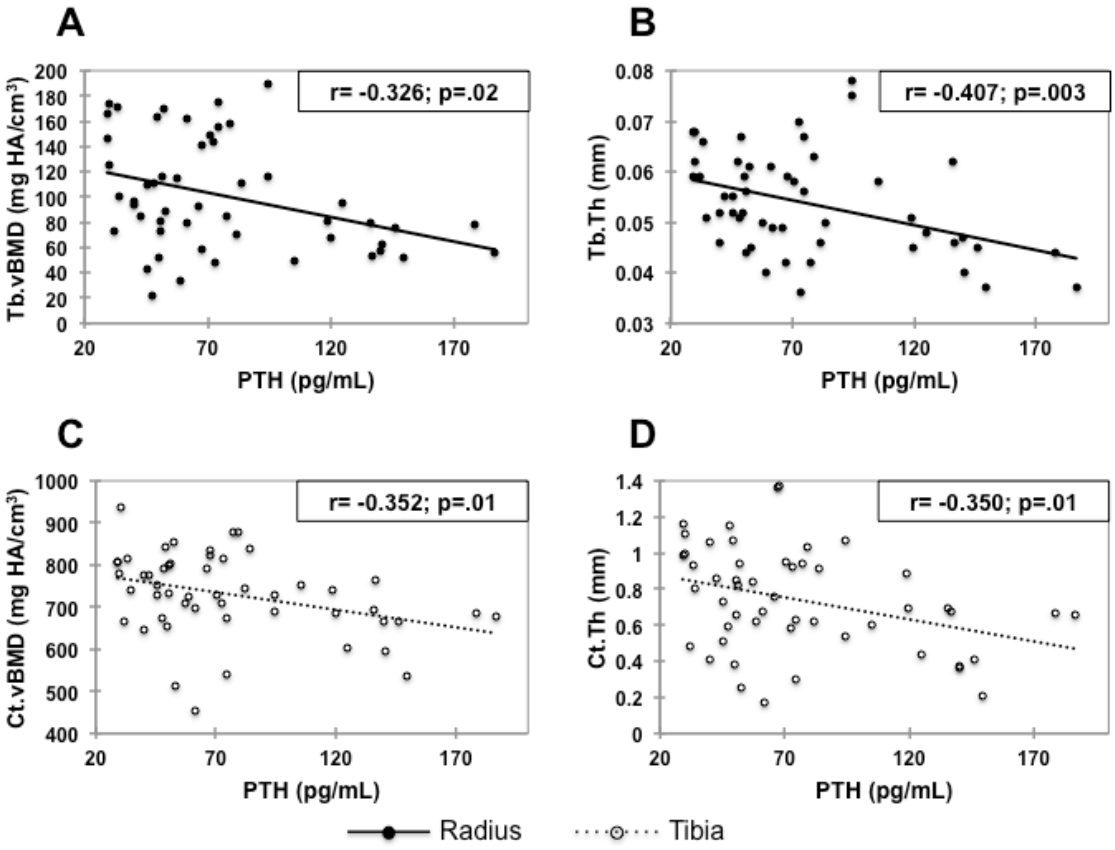

Figure 4: Correlations between PTH and Tb.vBMD (A) and Tb.Th (B) at the radius, and Ct.vBMD (C) and Ct.Th (D) at the tibia, in the PHPT group. Ct.vBMD and Ct.Th at the radius, and Tb.vBMD and Tb.Th at the tibia were not significantly correlated with PTH. PTH= parathyroid hormone; Tb.vBMD= trabecular volumetric bone mineral density; Tb.Th= trabecular thickness; Ct.vBMD= cortical volumetric bone mineral density; and Ct.Th= cortical thickness.

Table 1: Baseline clinical, biochemical and densitometric data of 51 PHPT and 120 control subjects:

Characteristics	PHPT (n=51)	Controls (n=120)	*p-value*
Age (years)	70 ± 1	68 ± 1	.20
Weight (kg)	67 ± 2	69	.37
Height (cm)	160 ± 1	160 ± 1	.94
BMI (kg/cm^2)	26.0 ± 0.9	26.8 ± 0.6	.42
Years since menopause	18 ± 2	19 ± 1	.86
Years since diagnosis	8.4 ± 1.1	NA	
Current medication use (%):			
Bisphosphonate	20	3	<.0001
HRT	10	6	.66
Raloxifene	6	4	.94
Serum total calcium (mg/dL)	10.6 ± 0.1	9.5 ± 0.0	<.0001
PTH (pg/mL)	76 ± 6	ND	
L1-L4 BMD (g/cm^2)	0.915 ± 0.024	0.931 ± 0.013	.56
T-score	-1.1 ± 0.2	-1.2 ± 0.1	.74
Total hip BMD (g/cm^2)	0.758 ± 0.019	0.812 ± 0.019	.015
T-score	-1.5 ± 0.2	-1.1 ± 0.1	.034
Femoral neck BMD (g/cm^2)	0.642 ± 0.017	0.668 ± 0.009	.03
T-score	-1.9 ± 0.2	-1.7 ± 0.1	.23
1/3 radius BMD (g/cm^2)	0.589 ± 0.014	0.610 ± 0.007	.16
T-score	-1.8 ± 0.2	-1.4 ± 0.1	.15
UD radius BMD (g/cm^2)	0.338 ± 0.011	0.379 ± 0.006	.0007
T-score	-1.8 ± 0.2	-1.2 ± 0.1	.0026

NA: not applicable; ND: no data

Table 2: Bone geometry, density and microarchitecture by HRpQCT in PHPT patients and controls:

	HRpQCT parameters	PHPT (n=51)	Control (n=120)	*p*-value
Radius	Total Area (cm^2)	236 ± 7	224 ± 4	.09
	Total vBMD ($mgHA/cm^3$)	241 ± 11	299 ± 7	<.0001
	Ct.vBMD ($mgHA/cm^3$)	801 ± 12	851 ± 7	.0001
	Ct.Th (mm)	0.595 ± 0.026	0.722 ± 0.017	<.0001
	Tb.vBMD ($mgHA/cm^3$)	101 ± 6	131 ± 4	<.0001
	Tb.N (1/mm)	1.53 ± 0.07	1.77 ± 0.03	.003
	Tb.Th (mm)	0.054 ± 0.001	0.061 ± 0.001	.0001
	Tb.Sp (mm)	0.711 ± 0.063	0.538 ± 0.02	.01
	Tb.Sp SD (mm)	0.465 ± 0.070	0.271 ± 0.021	.01
Tibia	Total Area (cm^2)	690 ± 16	662 ± 9	.13
	Total vBMD ($mgHA/cm^3$)	212 ± 8	245 ± 5	.0003
	Ct.vBMD ($mgHA/cm^3$)	730 ± 14	785 ± 6	.0005
	Ct.Th (mm)	0.739 ± 0.040	0.874 ± 0.025	.004
	Tb.vBMD ($mgHA/cm^3$)	130 ± 5	146 ± 3	.006
	Tb.N (1/mm)	1.65 ± 0.07	1.73 ± 0.03	.27
	Tb.Th (mm)	0.067 ± 0.002	0.071 ± 0.001	.13
	Tb.Sp (mm)	0.613 ± 0.042	0.529 ± 0.011	.06
	Tb.Sp SD (mm)	0.419 ± 0.069	0.257 ± 0.012	.02

Total vBMD= total volumetric bone mineral density; Ct.vBMD= cortical volumetric bone mineral density; Ct.Th= cortical thickness; Tb.vBMD= trabecular volumetric bone mineral density; Tb.N= trabecular number; Tb.Th= trabecular thickness; Tb.Sp= trabecular separation; Tb.Sp.SD= trabecular distribution

Table 3: ITS and mechanical parameters in PHPT patients and controls:

	ITS and mechanical parameters	PHPT (n=51)	Control (n=120)	*p*-value
Radius	pBV/TV (%)	4.8 ± 0.4	6.9 ± 0.3	.0003
	rBV/TV (%)	14.0 ± 0.6	16.1 ± 0.3	.0005
	P-R ratio	0.334 ± 0.021	0.429 ± 0.019	.0037
	aBV/TV (%)	6.1 ± 0.4	8.1 ± 0.2	<.0001
	pTb.N (1/mm)	1.158 ± 0.030	1.296 ± 0.020	.0002
	rTb.N (1/mm)	1.720 ± 0.029	1.811 ± 0.014	.0061
	pTb.Th (mm)	0.204 ± 0.002	0.206 ± 0.000	.3466
	rTb.Th (mm)	0.212 ± 0.000	0.214 ± 0.000	.0192
	pTb.S (mm^2)	0.135 ± 0.002	0.142 ± 0.003	.0441
	rTb.ℓ (mm^2)	0.710 ± 0.006	0.695 ± 0.008	.1717
	R-R Junc.D ($1/mm^3$)	2.451 ± 0.124	2.831 ± 0.066	.0042
	P-R Junc.D ($1/mm^3$)	2.207 ± 0.169	2.964 ± 0.109	.0003
	P-P Junc.D ($1/mm^3$)	0.966 ± 0.081	1.378 ± 0.057	.0001
	Trab Stiffness (N/mm)	5,585± 943	10,359 ± 734	.0003
	Stiffness (N/mm)	54,175 ± 2,845	69,567 ± 1,686	<.0001
	Ctload distal (%)	50.0 ± 1.5	41.8 ± 0.9	<.0001
	Ctload proximal (%)	95.3 ± 0.7	90.7 ± 0.6	<.0001
Tibia	pBV/TV (%)	9.1 ± 0.5	11.4 ± 0.4	.0006
	rBV/TV (%)	14.3 ± 0.6	14.4 ± 0.3	.8894
	P-R ratio	0.690 ± 0.046	0.852 ± 0.040	.0086
	aBV/TV (%)	9.5 ± 0.3	11.3 ± 0.3	.0001
	pTb.N (1/mm)	1.396 ± 0.022	1.475 ± 0.013	.0017
	rTb.N (1/mm)	1.762 ± 0.031	1.746 ± 0.016	.6189
	pTb.Th (mm)	0.216 ± 0.002	0.219 ± 0.001	.06
	rTb.Th (mm)	0.213 ± 0.001	0.218 ± 0.000	.003
	pTb.S (mm^2)	0.149 ± 0.003	0.157 ± 0.003	.0384
	rTb.ℓ (mm^2)	0.669 ± 0.004	0.668 ± 0.006	.8882
	R-R Junc.D ($1/mm^3$)	2.549 ± 0.151	2.388 ± 0.073	.338
	P-R Junc.D ($1/mm^3$)	3.132 ± .0147	3.446 ± 0.077	.0427
	P-P Junc.D ($1/mm^3$)	1.619 ± 0.072	1.894 ± 0.045	.0014
	Trab Stiffness (N/mm)	65,372 ± 4,248	80,078 ± 2,896	.0067
	Stiffness (N/mm)	184,204 ± 6,187	205,746 ± 4,061	.005
	Ctload distal (%)	30.2 ± 1.2	27.5 ± 0.8	.0649
	Ctload proximal (%)	72.4 ± 0.01.6	70.1 ± 0.8	.1058

pBV/TV= plate bone volume fraction; rBV/TV= rod bone volume fraction; P-R ratio= plate-to-rod ratio; aBV/TV= axial bone volume fraction; pTb.N= plate number density; rTb.N= rod number density; pTb.Th= plate thickness; rTb.Th= rod thickness; pTb.S= plate surface area; rTb.ℓ= rod length; R-R Junc.D= rod–rod junction density; P-R Junc.D= plate-rod junction density; P-P Junc.D= plate–plate junction density, Trab. Stiffness= trabecular stiffness; Stiffness= whole bone stiffness; Ctload distal= cortical load at distal surface; and Ctload proximal= cortical load at proximal surface

Table 4: Correlations (r values) between BMI and HRpQCT parameters at the radius and at the tibia in subjects with PHPT and controls:

HRpQCT parameters	BMI (kg/m^2)			
	Radial Comparisons		Tibial Comparisons	
	PHPT	Control	PHPT	Control
Total Area (cm^2)	0.031	0.053	0.205	0.079
Total vBMD ($mgHA/cm^3$)	0.249	0.299**	0.307*	0.340***
Ct.vBMD ($mgHA/cm^3$)	0.023	0.148	-0.039	0.211*
Ct.Th (mm)	0.210	0.289**	0.158	0.341***
Tb.vBMD ($mgHA/cm^3$)	0.312*	0.312**	0.396**	0.294**
Tb.N (1/mm)	0.287*	0.309**	0.533***	0.226*
Tb.Th (mm)	0.109	0.164	-0.156	0.189
Tb.Sp (mm)	-0.299*	-0.324**	-0.532***	-0.258*
Tb.Sp SD (mm)	-0.295*	-0.328**	-0.487***	-0.165

*p<.05 ; **p<.01 ; ***p< .001

References:

1. Cope O. The study of hyperparathyroidism at the Massachusetts General Hospital. N Engl J Med. 1966;274(21):1174-82. Epub 1966/05/26. doi: 10.1056/NEJM196605262742105. PubMed PMID: 5327350.

2. Rubin MR, Bilezikian JP, McMahon DJ, Jacobs T, Shane E, Siris E, et al. The natural history of primary hyperparathyroidism with or without parathyroid surgery after 15 years. J Clin Endocrinol Metab. 2008;93(9):3462-70. Epub 2008/06/12. doi: jc.2007-1215 [pii]
10.1210/jc.2007-1215. PubMed PMID: 18544625; PubMed Central PMCID: PMC2567863.

3. Silverberg SJ, Shane E, Jacobs TP, Siris E, Bilezikian JP. A 10-year prospective study of primary hyperparathyroidism with or without parathyroid surgery. N Engl J Med. 1999;341(17):1249-55. Epub 1999/10/21. doi: 10.1056/NEJM199910213411701. PubMed PMID: 10528034.

4. Bilezikian JP, Brandi ML, Rubin M, Silverberg SJ. Primary hyperparathyroidism: new concepts in clinical, densitometric and biochemical features. J Intern Med. 2005;257(1):6-17. Epub 2004/12/21. doi: JIM1422 [pii]
10.1111/j.1365-2796.2004.01422.x. PubMed PMID: 15606372.

5. Silverberg SJ, Shane E, de la Cruz L, Dempster DW, Feldman F, Seldin D, et al. Skeletal disease in primary hyperparathyroidism. Journal of bone and mineral research : the official journal of the American Society for Bone and Mineral Research. 1989;4(3):283-91. Epub 1989/06/01. doi: 10.1002/jbmr.5650040302. PubMed PMID: 2763869.

6. Parisien M, Cosman F, Mellish RW, Schnitzer M, Nieves J, Silverberg SJ, et al. Bone structure in postmenopausal hyperparathyroid, osteoporotic, and normal women. Journal of bone and mineral research : the official journal of the American Society for Bone and Mineral Research. 1995;10(9):1393-9. Epub 1995/09/01. doi: 10.1002/jbmr.5650100917. PubMed PMID: 7502712.

7. Parisien M, Mellish RW, Silverberg SJ, Shane E, Lindsay R, Bilezikian JP, et al. Maintenance of cancellous bone connectivity in primary hyperparathyroidism: trabecular strut analysis. Journal of bone and mineral research : the official journal of the American Society for Bone and Mineral Research. 1992;7(8):913-9. Epub 1992/08/01. doi: 10.1002/jbmr.5650070808. PubMed PMID: 1442205.

8. Parisien M, Silverberg SJ, Shane E, de la Cruz L, Lindsay R, Bilezikian JP, et al. The histomorphometry of bone in primary hyperparathyroidism: preservation of cancellous bone structure. J Clin Endocrinol Metab. 1990;70(4):930-8. Epub 1990/04/01. PubMed PMID: 2318948.

9. Dempster DW, Muller R, Zhou H, Kohler T, Shane E, Parisien M, et al. Preserved three-dimensional cancellous bone structure in mild primary hyperparathyroidism. Bone. 2007;41(1):19-24. Epub 2007/05/11. doi: S8756-3282(07)00339-0 [pii]
10.1016/j.bone.2007.03.020. PubMed PMID: 17490921; PubMed Central PMCID: PMC2721277.

10. Uchiyama T, Tanizawa T, Ito A, Endo N, Takahashi HE. Microstructure of the trabecula and cortex of iliac bone in primary hyperparathyroidism patients determined using histomorphometry and node-strut analysis. J Bone Miner Metab. 1999;17(4):283-8. Epub 1999/11/27. PubMed PMID: 10575593.

11. Khosla S, Melton LJ, 3rd, Wermers RA, Crowson CS, O'Fallon W, Riggs B. Primary hyperparathyroidism and the risk of fracture: a population-based study. Journal of bone and mineral research : the official journal of the American Society for Bone and Mineral Research. 1999;14(10):1700-7. Epub 1999/09/22. doi: jbm588 [pii]
10.1359/jbmr.1999.14.10.1700. PubMed PMID: 10491217.

12. Vignali E, Viccica G, Diacinti D, Cetani F, Cianferotti L, Ambrogini E, et al. Morphometric vertebral fractures in postmenopausal women with primary hyperparathyroidism. J Clin Endocrinol Metab. 2009;94(7):2306-12. Epub 2009/04/30. doi: jc.2008-2006 [pii]
10.1210/jc.2008-2006. PubMed PMID: 19401378.

13. Yu N, Donnan PT, Flynn RW, Murphy MJ, Smith D, Rudman A, et al. Increased mortality and morbidity in mild primary hyperparathyroid patients. The Parathyroid Epidemiology and Audit Research Study (PEARS). Clin Endocrinol (Oxf). 2010;73(1):30-4. Epub 2009/12/31. doi: CEN3766 [pii]
10.1111/j.1365-2265.2009.03766.x. PubMed PMID: 20039887.

14. Vestergaard P, Mosekilde L. Fractures in patients with primary hyperparathyroidism: nationwide follow-up study of 1201 patients. World journal of surgery. 2003;27(3):343-9. Epub 2003/02/28. doi: 10.1007/s00268-002-6589-9. PubMed PMID: 12607064.

15. Charopoulos I, Tournis S, Trovas G, Raptou P, Kaldrymides P, Skarandavos G, et al. Effect of primary hyperparathyroidism on volumetric bone mineral density and bone

geometry assessed by peripheral quantitative computed tomography in postmenopausal women. J Clin Endocrinol Metab. 2006;91(5):1748-53. Epub 2006/02/24. doi: 10.1210/jc.2005-2102. PubMed PMID: 16492695.

16. Silverberg SJ, Locker FG, Bilezikian JP. Vertebral osteopenia: a new indication for surgery in primary hyperparathyroidism. J Clin Endocrinol Metab. 1996;81(11):4007-12. Epub 1996/11/01. PubMed PMID: 8923852.

17. Boutroy S, Vilayphiou N, Roux JP, Delmas PD, Blain H, Chapurlat RD, et al. Comparison of 2D and 3D bone microarchitecture evaluation at the femoral neck, among postmenopausal women with hip fracture or hip osteoarthritis. Bone. 2011;49(5):1055-61. Epub 2011/08/23. doi: 10.1016/j.bone.2011.07.037. PubMed PMID: 21856461.

18. MacNeil JA, Boyd SK. Accuracy of high-resolution peripheral quantitative computed tomography for measurement of bone quality. Medical engineering & physics. 2007;29(10):1096-105. Epub 2007/01/19. doi: 10.1016/j.medengphy.2006.11.002. PubMed PMID: 17229586.

19. Sornay-Rendu E, Boutroy S, Munoz F, Delmas PD. Alterations of cortical and trabecular architecture are associated with fractures in postmenopausal women, partially independent of decreased BMD measured by DXA: the OFELY study. Journal of bone and mineral research : the official journal of the American Society for Bone and Mineral Research. 2007;22(3):425-33. Epub 2006/12/22. doi: 10.1359/jbmr.061206. PubMed PMID: 17181395.

20. Vico L, Zouch M, Amirouche A, Frere D, Laroche N, Koller B, et al. High-resolution pQCT analysis at the distal radius and tibia discriminates patients with recent wrist and femoral neck fractures. Journal of bone and mineral research : the official journal of the American Society for Bone and Mineral Research. 2008;23(11):1741-50. Epub 2008/07/31. doi: 10.1359/jbmr.080704. PubMed PMID: 18665795.

21. Stein EM, Liu XS, Nickolas TL, Cohen A, McMahon DJ, Zhou B, et al. Microarchitectural Abnormalities Are More Severe in Postmenopausal Women with Vertebral Compared to Nonvertebral Fractures. J Clin Endocrinol Metab. 2012. Epub 2012/07/24. doi: 10.1210/jc.2012-1968. PubMed PMID: 22821893.

22. Stein EM, Liu XS, Nickolas TL, Cohen A, Thomas V, McMahon DJ, et al. Abnormal microarchitecture and stiffness in postmenopausal women with ankle fractures. J Clin Endocrinol Metab. 2011;96(7):2041-8. Epub 2011/04/22. doi: 10.1210/jc.2011-0309. PubMed PMID: 21508142; PubMed Central PMCID: PMC3135193.

23. Stein EM, Liu XS, Nickolas TL, Cohen A, Thomas V, McMahon DJ, et al. Abnormal microarchitecture and reduced stiffness at the radius and tibia in postmenopausal women with fractures. Journal of bone and mineral research : the official journal of the American Society for Bone and Mineral Research. 2010;25(12):2572-81. Epub 2010/06/22. doi: 10.1002/jbmr.152. PubMed PMID: 20564238; PubMed Central PMCID: PMC3149820.

24. Boutroy S, Bouxsein ML, Munoz F, Delmas PD. In vivo assessment of trabecular bone microarchitecture by high-resolution peripheral quantitative computed tomography. J Clin Endocrinol Metab. 2005;90(12):6508-15. Epub 2005/09/29. doi: 10.1210/jc.2005-1258. PubMed PMID: 16189253.

25. Khosla S, Riggs BL, Atkinson EJ, Oberg AL, McDaniel LJ, Holets M, et al. Effects of sex and age on bone microstructure at the ultradistal radius: a population-based noninvasive in vivo assessment. Journal of bone and mineral research : the official journal of the American Society for Bone and Mineral Research. 2006;21(1):124-31. Epub 2005/12/16. doi: 10.1359/JBMR.050916. PubMed PMID: 16355281; PubMed Central PMCID: PMC1352156.

26. Bacchetta J, Boutroy S, Vilayphiou N, Juillard L, Guebre-Egziabher F, Rognant N, et al. Early impairment of trabecular microarchitecture assessed with HR-pQCT in patients with stage II-IV chronic kidney disease. Journal of bone and mineral research : the official journal of the American Society for Bone and Mineral Research. 2010;25(4):849-57. Epub 2009/09/25. doi: 10.1359/jbmr.090831. PubMed PMID: 19775204.

27. Hansen S, Beck Jensen JE, Rasmussen L, Hauge EM, Brixen K. Effects on bone geometry, density, and microarchitecture in the distal radius but not the tibia in women with primary hyperparathyroidism: A case-control study using HR-pQCT. Journal of bone and mineral research : the official journal of the American Society for Bone and Mineral Research. 2010;25(9):1941-7. Epub 2010/05/26. doi: 10.1002/jbmr.98. PubMed PMID: 20499376.

28. Hansen S, Hauge EM, Rasmussen L, Jensen JE, Brixen K. Parathyroidectomy improves bone geometry and microarchitecture in female patients with primary hyperparathyroidism. A 1-year prospective controlled study using high resolution peripheral quantitative computed tomography. Journal of bone and mineral research : the official journal of the American Society for Bone and Mineral Research. 2012. Epub 2012/01/10. doi: 10.1002/jbmr.1540. PubMed PMID: 22228118.

29. Liu XS, Zhang XH, Sekhon KK, Adams MF, McMahon DJ, Bilezikian JP, et al. High-resolution peripheral quantitative computed tomography can assess microstructural and mechanical properties of human distal tibial bone. Journal of bone and mineral research : the official journal of the American Society for Bone and Mineral Research. 2010;25(4):746-56. Epub 2009/09/25. doi: 10.1359/jbmr.090822. PubMed PMID: 19775199; PubMed Central PMCID: PMC3130204.

30. Liu XS, Sajda P, Saha PK, Wehrli FW, Bevill G, Keaveny TM, et al. Complete volumetric decomposition of individual trabecular plates and rods and its morphological correlations with anisotropic elastic moduli in human trabecular bone. Journal of bone and mineral research : the official journal of the American Society for Bone and Mineral Research. 2008;23(2):223-35. Epub 2007/10/03. doi: 10.1359/jbmr.071009. PubMed PMID: 17907921; PubMed Central PMCID: PMC2665696.

31. Liu XS, Bevill G, Keaveny TM, Sajda P, Guo XE. Micromechanical analyses of vertebral trabecular bone based on individual trabeculae segmentation of plates and rods. Journal of biomechanics. 2009;42(3):249-56. Epub 2008/12/23. doi: 10.1016/j.jbiomech.2008.10.035. PubMed PMID: 19101672; PubMed Central PMCID: PMC3381008.

32. Liu XS, Stein EM, Zhou B, Zhang CA, Nickolas TL, Cohen A, et al. Individual trabecula segmentation (ITS)-based morphological analyses and microfinite element analysis of HR-pQCT images discriminate postmenopausal fragility fractures independent of DXA measurements. Journal of bone and mineral research : the official journal of the American Society for Bone and Mineral Research. 2012;27(2):263-72. Epub 2011/11/11. doi: 10.1002/jbmr.562. PubMed PMID: 22072446; PubMed Central PMCID: PMC3290758.

33. Liu XS, Cohen A, Shane E, Stein E, Rogers H, Kokolus SL, et al. Individual trabeculae segmentation (ITS)-based morphological analysis of high-resolution peripheral quantitative computed tomography images detects abnormal trabecular plate and rod microarchitecture in premenopausal women with idiopathic osteoporosis. Journal of bone and mineral research : the official journal of the American Society for Bone and Mineral Research. 2010;25(7):1496-505. Epub 2010/03/05. doi: 10.1002/jbmr.50. PubMed PMID: 20200967; PubMed Central PMCID: PMC3131618.

34. Boutroy S, Van Rietbergen B, Sornay-Rendu E, Munoz F, Bouxsein ML, Delmas PD. Finite element analysis based on in vivo HR-pQCT images of the distal radius is associated with wrist fracture in postmenopausal women. Journal of bone and mineral

research : the official journal of the American Society for Bone and Mineral Research. 2008;23(3):392-9. Epub 2007/11/14. doi: 10.1359/jbmr.071108. PubMed PMID: 17997712.

35. Vilayphiou N, Boutroy S, Sornay-Rendu E, Van Rietbergen B, Munoz F, Delmas PD, et al. Finite element analysis performed on radius and tibia HR-pQCT images and fragility fractures at all sites in postmenopausal women. Bone. 2010;46(4):1030-7. Epub 2010/01/02. doi: 10.1016/j.bone.2009.12.015. PubMed PMID: 20044044.

36. Liu XS, Walker MD, McMahon DJ, Udesky J, Liu G, Bilezikian JP, et al. Better skeletal microstructure confers greater mechanical advantages in Chinese-American women versus white women. Journal of bone and mineral research : the official journal of the American Society for Bone and Mineral Research. 2011;26(8):1783-92. Epub 2011/02/26. doi: 10.1002/jbmr.378. PubMed PMID: 21351150.

37. Laib A, Hauselmann HJ, Ruegsegger P. In vivo high resolution 3D-QCT of the human forearm. Technology and health care : official journal of the European Society for Engineering and Medicine. 1998;6(5-6):329-37. Epub 1999/04/01. PubMed PMID: 10100936.

38. Macneil JA, Boyd SK. Bone strength at the distal radius can be estimated from high-resolution peripheral quantitative computed tomography and the finite element method. Bone. 2008;42(6):1203-13. Epub 2008/03/25. doi: 10.1016/j.bone.2008.01.017. PubMed PMID: 18358799.

39. Fisher RA. Statistical Methods for Research Workers. Fourteenth ed: Hafner Publishing Company; 1970.

40. Chen Q, Kaji H, Iu MF, Nomura R, Sowa H, Yamauchi M, et al. Effects of an excess and a deficiency of endogenous parathyroid hormone on volumetric bone mineral density and bone geometry determined by peripheral quantitative computed tomography in female subjects. J Clin Endocrinol Metab. 2003;88(10):4655-8. Epub 2003/10/15. PubMed PMID: 14557436.

41. Liu XS, Shane E, McMahon DJ, Guo XE. Individual trabecula segmentation (ITS)-based morphological analysis of microscale images of human tibial trabecular bone at limited spatial resolution. Journal of bone and mineral research : the official journal of the American Society for Bone and Mineral Research. 2011;26(9):2184-93. Epub 2011/05/11. doi: 10.1002/jbmr.420. PubMed PMID: 21557311.

42. Adami S, Braga V, Squaranti R, Rossini M, Gatti D, Zamberlan N. Bone measurements in asymptomatic primary hyperparathyroidism. Bone. 1998;22(5):565-70. Epub 1998/05/26. PubMed PMID: 9600793.

43. Bilezikian JP. Bone strength in primary hyperparathyroidism. Osteoporosis international : a journal established as result of cooperation between the European Foundation for Osteoporosis and the National Osteoporosis Foundation of the USA. 2003;14 Suppl 5:S113-5; discussion S5-7. Epub 2003/09/25. doi: 10.1007/s00198-003-1482-4. PubMed PMID: 14504715.

44. Parfitt AM. Parathyroid hormone and periosteal bone expansion. Journal of bone and mineral research : the official journal of the American Society for Bone and Mineral Research. 2002;17(10):1741-3. Epub 2002/10/09. doi: 10.1359/jbmr.2002.17.10.1741. PubMed PMID: 12369776.

45. Christiansen P, Steiniche T, Vesterby A, Mosekilde L, Hessov I, Melsen F. Primary hyperparathyroidism: iliac crest trabecular bone volume, structure, remodeling, and balance evaluated by histomorphometric methods. Bone. 1992;13(1):41-9. Epub 1992/01/01. PubMed PMID: 1581108.

46. Cohen A, Dempster DW, Muller R, Guo XE, Nickolas TL, Liu XS, et al. Assessment of trabecular and cortical architecture and mechanical competence of bone by high-resolution peripheral computed tomography: comparison with transiliac bone biopsy. Osteoporosis international : a journal established as result of cooperation between the European Foundation for Osteoporosis and the National Osteoporosis Foundation of the USA. 2010;21(2):263-73. Epub 2009/05/21. doi: 10.1007/s00198-009-0945-7. PubMed PMID: 19455271; PubMed Central PMCID: PMC2908272.

47. Pistoia W, van Rietbergen B, Lochmuller EM, Lill CA, Eckstein F, Ruegsegger P. Estimation of distal radius failure load with micro-finite element analysis models based on three-dimensional peripheral quantitative computed tomography images. Bone. 2002;30(6):842-8. Epub 2002/06/08. PubMed PMID: 12052451.

48. Liu XS, Cohen A, Shane E, Yin PT, Stein EM, Rogers H, et al. Bone density, geometry, microstructure, and stiffness: Relationships between peripheral and central skeletal sites assessed by DXA, HR-pQCT, and cQCT in premenopausal women. Journal of bone and mineral research : the official journal of the American Society for Bone and Mineral Research. 2010;25(10):2229-38. Epub 2010/05/26. doi: 10.1002/jbmr.111. PubMed PMID: 20499344; PubMed Central PMCID: PMC3128822.

3.2- Artigo 2:

Trabecular Bone Score – TBS – a novel method to evaluate bone microarchitecture in patients with Primary Hyperparathyroidism

Artigo submetido ao “The Journal of Clinical Endocrinology & Metabolism”.

Trabecular Bone Score – TBS – a novel method to evaluate bone microarchitecture in patients with Primary Hyperparathyroidism

Barbara C Silva[1,2], Stephanie Boutroy[1], Chiyuan Zhang[1], Donald J McMahon[1], Bin Zhou[3], Ji Wang[3], Julia Udesky[1], Serge Cremers[1], Marta S. Sarquis[2], X Edward Guo[3], Didier Hans[4], John P Bilezikian[1#]

1- *Metabolic Bone Diseases Unit, Division of Endocrinology, Department of Medicine, College of Physicians and Surgeons, Columbia University, New York, NY, USA*
2- *College of Medicine of Federal University of Minas Gerais, Belo Horizonte, Brazil*
3- *Bone Bioengineering Laboratory, Department of Biomedical Engineering, Columbia University, New York, NY, USA*
4- *Center of Bone diseases, Lausanne University Hospital, Lausanne, Switzerland*

Correspondence to:
John P. Bilezikian. M.D.
College of Physicians and Surgeons
630 W, 168th Street, New York, NY 10032, USA
Phone: 212.305.6257
Fax: 212.305.6486
e-mail: jpb2@columbia.edu

Abstract:

Introduction: Typically, in the milder form of primary hyperparathyroidism (PHPT), aBMD by DXA is reduced at the predominantly cortical 1/3 radius, while cancellous bone, represented by aBMD at the lumbar spine, is generally preserved. Recent studies utilizing High Resolution peripheral Quantitative Computed Tomography (HRpQCT) has shown, however, that both cortical and trabecular bone compartments are compromised in PHPT, which agrees with epidemiology evidence for increased overall fracture risk in this disease. Since DXA cannot direct measure trabecular bone, and HRpQCT is not widely available, we used trabecular bone score (TBS), a novel gray-level textural analysis that can be applied to spine DXA images, to estimate trabecular microarchitecture.

Aims: To assess TBS from spine DXA images in postmenopausal women with PHPT in relation to HRpQCT indices and bone stiffness.

Patients and Methods: 22 women (67 ± 2 yr.) with PHPT were studied. aBMD was assessed by DXA (QDR 4500A, Hologic), and site-matched spine TBS indices were derived from DXA images using TBS iNsight software (v1.9, Medimaps SA). By HRpQCT, distal radius and tibia analyses were performed, and bone stiffness at these sites was assessed by finite element analysis (FEA).

Results: TBS in PHPT is abnormal representing a partially degraded microstructure. The mean value was 1.24 ± 0.02 (definition of normal here). TBS was significantly correlated with all HRpQCT and mechanical measurements except for Tb.Th, and trabecular stiffness at the radius. At the tibia, significant correlations were observed between TBS and volumetric densities, Ct.Th, BV/TV and whole bone stiffness. All indices of trabecular microarchitecture, except Tb.Th, became significant after adjusting for body weight.

Conclusion: TBS showed significant correlations with biomechanical and microstructural indices by HRpQCT. TBS shows promise as a readily available measurement tool in the assessment of trabecular microstructure in PHPT.

Key words: Primary hyperparathyroidism, trabecular bone score, high-resolution peripheral quantitative computed tomography, finite element analysis, fracture risk.

Introduction

Primary hyperparathyroidism (PHPT) is a common endocrine disorder characterized by hypercalcemia and elevated or inappropriately normal levels of parathyroid hormone (PTH). With the advent of the multichannel autoanalyzer in the early 1970's, the clinical presentation of PHPT changed from symptomatic (1) to asymptomatic (2-4). While overt skeletal disease, formerly a common finding, is rarely seen now, bone mineral densitometry (aBMD) routinely detects evidence for skeletal involvement. The distal 1/3 radius, a site of cortical bone, is typically more involved than the lumbar spine, a site comprised predominantly of trabecular bone (5). These findings, however, are not consistent with recent observations utilizing technologies that have greater resolving power than DXA, such as High Resolution peripheral Quantitative Computed Tomography (HRpQCT) in which trabecular microarchitectural deficits are seen (6, 7). By HRpQCT, both trabecular and cortical compartments are abnormal at the radius and tibia in postmenopausal women with PHPT. These deficits are associated with reduced whole bone and trabecular stiffness by FEA (7). Hansen *et al.* (6) have also observed similar structural deficits at the distal radius in PHPT. These more recent findings by HRpQCT and FEA are consistent with epidemiological evidence of increased fracture risk at both vertebral and non-vertebral sites in PHPT (8-11). While HRpQCT has added a dimension of insight not previous appreciated with regard to trabecular bone in PHPT, HRpQCT is not widely available and, considering the cost of the instrumentation, is not likely to be.

Trabecular bone score (TBS) is a novel gray-level textural analysis that can be applied to DXA images to estimate trabecular microarchitecture (12). Using experimental variograms of 2D projection images, TBS differentiates between 3D bone structures that exhibit the same aBMD, but different trabecular microarchitecture (13). TBS analysis is readily available from the lumbar spine DXA image without the need for further imaging or expensive instrumentation. Studies in cadaveric bones have shown significant correlations between TBS and 3D trabecular microarchitecture measurements by micro-computed tomography (μCT) (12, 13). In clinical studies, TBS enhanced DXA's ability to predict fracture risk (14-19). Moreover, in a recent study involving over 29,000 postmenopausal women, TBS predicted osteoporotic fractures, independent of aBMD (19). Finally, Boutroy *et al.* (20) showed that TBS predicts osteoporotic fracture as well

as lumbar spine aBMD, and that TBS helped to define a subset of non-osteoporotic women at high risk for fracture.

The ability of TBS to estimate trabecular microarchitecture and predict fracture risk, along with its direct utilization from DXA images led us to investigate its potential utility in evaluating the trabecular skeleton in PHPT. To this end, we assessed TBS from spine DXA images in postmenopausal women with PHPT, and correlated it, for the first time, with HRpQCT measurements of volumetric bone density, skeletal microarchitecture, and bone stiffness. Our results indicate that TBS has the potential to provide additional data on trabecular bone quality in PHPT and that it can be readily applied without the need for expensive equipment.

Patients and Methods

Study Subjects:

22 postmenopausal women were recruited from Columbia University Medical Center (CUMC). Subjects were eligible for inclusion if they had well-characterized PHPT (elevated serum calcium and elevated or inappropriately normal PTH levels). Exclusion criteria included use of bisphosphonates or glucocorticoids within the past 2 years, history of Cushing's syndrome, uncontrolled thyroid disease, malabsorption syndrome, significant liver disease, creatinine clearance < 30 mL/min, and any chronic disorders of mineral metabolism such as Paget's disease or osteogenesis imperfecta. Women were considered postmenopausal if they had not had a menstrual period for over 1 year.

The study was approved by the Institutional Review Board of Columbia University Medical Center, and all subjects gave written informed consent.

Dual-energy X-ray absorptiometry (DXA):

aBMD by DXA was measured at the lumbar spine (L1–L4), total hip, femoral neck, and nondominant forearm [ultradistal (UD radius) and one-third radius (1/3 radius)] using Discovery A (Hologic Inc., Bedford, MA, USA) at CUMC. Bone density was expressed in T-score for comparisons of subjects with young-normal population.

Trabecular Bone Score (TBS):

Site-matched spine TBS parameters were extracted from the DXA image using TBS iNsight software (v1.9, Medimaps SA, France). TBS measurements were performed in the Bone Disease Unit at the University of Lausanne, Lausanne, Switzerland, using de-identified spine DXA files from scans obtained at CUMC. TBS was evaluated, by determining the variogram of the trabecular bone projected image, calculated as the sum of the squared gray-level differences between pixels at a specific distance. TBS was then calculated as the slope of the log-log transform of this variogram (13). TBS was assessed in the same regions of measurement as those used for the lumbar spine BMD. The mean value of the individual measurements for L1 to L4 represents the lumbar spine TBS.

To ensure comparability with previous TBS studies, calibration on the DXA machine at CUMC was performed using a TBS-specific phantom (MedImaps). From previous reports, based upon over 29 thousands female subjects, TBS≤1.2 is described as degraded

microarchitecture, TBS between 1.20 and 1.35 is partially degraded microarchitecture, and TBS≥1.35 is considered normal (18-23)

High Resolution peripheral Quantitative Computed Tomography (HRpQCT):

Volumetric bone mineral density (vBMD) and microarchitecture were measured at the nondominant distal radius and tibia using the HRpQCT system (Xtreme CT; Scanco Medical AG, Brüttisellen, Switzerland) at CUMC, as previously described (24)

Image analysis has been validated and detailed elsewhere (24-27). The following indices were evaluated at the distal radius and tibia: total area; total, cortical and trabecular volumetric bone densities (Total vBMD, Ct.vBDM and Tb.vBMD, respectively); cortical thickness (Ct.Th); trabecular bone volume (BV/TV); trabecular number (Tb.N); trabecular thickness (Tb.Th); trabecular separation (Tb.Sp); and standard deviation of trabecular separation (Tb.Sp. SD), a parameter reflecting the heterogeneity of the trabecular network.

Finite Element Analysis (FEA) of HRpQCT images:

FEA was performed to estimate whole bone and trabecular stiffness by converting whole bone and trabecular HRpQCT images into finite-element models. For each FE model, a uniaxial compression test was performed with displacement equivalent to 1% apparent strain to calculate stiffness. Bone tissue was assumed to have an isotropic linear material property with Young's modulus 15 GPa and Poisson's ratio 0.3. Whole bone stiffness was defined as reaction force divided by the applied displacement. It characterizes the mechanical competence of both cortical and trabecular compartments and it is closely related to whole bone strength (28). Similarly, trabecular bone stiffness characterizes the mechanical competence of the trabecular bone compartment.

Biochemical analysis

Serum total calcium and albumin were measured using standard methods (Quest Diagnostics, Madison, NJ, USA) and calcium values were corrected for low albumin (albumin < 4 g/dL). Intact PTH was measured by immunoradiometric assay (Scantibodies, Santee, CA, USA) in the Bone Marker Laboratory at CUMC. The normal range was 14 to 66 pg/mL, and the precision inter- and intra-assay coefficients were < 7% and 5%, respectively.

Statistical Analysis:

Descriptive statistics are expressed as mean ± SEM. Correlation of TBS with HRpQCT indices, mechanical parameters and DXA measurements was assessed by the Pearson correlation test. Since Tb.Sp and Tb.Sp SD did not follow a normal distribution, they were log-transformed and then correlated using Pearson Correlation. Correlations adjusted of weight were performed by partialing out weight. Linear regression analyses were applied to estimate the variability in HRpQCT and mechanical parameters when TBS, aBMD at the lumbar spine or the combination of both were used as the explanatory variables. All statistical tests were performed at the two-sided 0.05-level of significance. Statistical analysis was performed using SAS, version 9.2 (SAS Institute, Inc., Cary, NC, USA).

Results

Baseline characteristics of 22 postmenopausal women with PHPT are described in Table 1. The majority of PHPT patients (77%) were asymptomatic. Only 1 subject had a history of nephrolithiasis, while 4 had a history of fragility fracture.

TBS and aBMD by DXA:

Mean TBS, aBMD and T-scores by DXA are reported in Table 1. Although the prevalence of osteoporosis at any site was 50%, L1-L4 T-score by DXA was well above the WHO osteoporosis threshold (T-score ≤2.5) in the vast majority of subjects. Only 3 (14%) patients were classified as osteoporotic, 7 (32%) as osteopenic, whereas the remaining 12 (53%) subjects presented with normal L1-L4 T-scores by DXA.

In contrast, TBS at the lumbar spine showed degraded microarchitecture (TBS≤1.20) in 8 (36%) patients, partially degraded (TBS>1.20 and <1.35) in an additional 8 (36%), and normal values (TBS≥1.35) in only 6 (27%) subjects (Figure 1A and 1B). The mean TBS of the whole group was 1.24, representing a partially degraded microarchitecture.

Relationship between TBS and aBMD by DXA:

Correlations between TBS and aBMD at the lumbar spine (r=0.367), total hip (r=0.269), and femoral neck (r=0.350) were not significant, whereas significant correlations were found between TBS and aBMD at the 1/3 radius (r=0.427; p=0.047), and UD radius (r=0.450; p=0.036).

Relationship between TBS, HRpQCT and mechanical parameters:

As shown in Table 2, at the radius, TBS was significantly correlated with all HRpQCT and biomechanical measurements except total area, Tb.Th, and trabecular stiffness. Significant correlations remained after adjusting for body weight (Table 2 and Figure 2).

At the tibia, significant correlations were observed between TBS and volumetric densities, Ct.Th, BV/TV and whole bone stiffness. All indices of trabecular microarchitecture, except Tb.Th, became significant after adjusting for body weight (Table 2 and Figure 2).

Using linear regression analysis, TBS or L1-L4 aBMD alone explained 20 to 50% of variances in HRpQCT measurements of volumetric densities, Ct.Th, BV/TV and whole bone stiffness at the radius and tibia. TBS and aBMD together better predict the

variability in these HRpQCT indices and whole bone stiffness than either one alone (Table 3).

At the radius, TBS explained 25% and 20% of the variance in Tb.N and Tb.Sp, respectively, with a slight increase in the degree of variance explained by the combination of TBS with L1-L4 aBMD (Table 3). At the tibia, TBS was a poor predictor of the variances in HRpQCT measurements of trabecular microarchitecture.

Discussion

The results of this study show, for the first time, significant correlations between TBS and HRpQCT measurements of volumetric densities, skeletal microarchitecture and bone stiffness at the radius and tibia, in a group of postmenopausal women with PHPT. Previous HRpQCT studies have shown that not only cortical, but also trabecular bone, is compromised in PHPT, even in the mild form of this disease (6, 7). This technology, however, is not widely accessible, and a clinical tool to assess trabecular microarchitecture could be helpful in the evaluation of this disease. TBS, an indirect measurement of trabecular microarchitecture, is now an FDA-approved application to DXA and readily available. Significant correlations between TBS and HRpQCT indices demonstrated here indicate that it may serve as a valuable additional index in the assessment of skeletal microstructure in PHPT.

Significant correlations between TBS and 3D direct measurements of trabecular microstructure were previously observed in human cadaver bone specimens (vertebrae, femur and radius) (12, 13). The TBS pivotal study showed significant relationships between TBS evaluated from 2D projection images directly derived from 3D μCT reconstruction and direct 3D measurements of trabecular microarchitecture by μCT (12). Following this observation, TBS was derived from DXA images of lumbar vertebrae, and significant correlations between trabecular indices by μCT and TBS were confirmed (13). In agreement with these data, we observed a positive correlation of TBS with BV/TV and Tb.N, and a negative correlation with Tb.Sp and Tb.Sp. SD at the radius. Similar results were shown at the tibia after adjusting for body weight. TBS did not show a significant relationship with Tb.Th at the radius or tibia, even after adjusting for weight. In fact, unexpected inverse correlation between TBS and Tb.Th was previously found in an *ex vivo* study (13), and the reason for this observation is not clear.

Unadjusted correlations between TBS at the lumbar spine and trabecular indices of microstructure at the tibia were not significant. Although lumbar spine and tibia are both load-bearing sites, they are subjected to different loading forces, which might explain this observation. In fact, after adjusting for body weight, a surrogate for mechanical loading, correlations of TBS with Tb.N, Tb.Sp and Tb.Sp SD became significant at the tibia. Differences in the quality of trabecular bone can also be appreciated when HRpQCT findings are compared with histomorphometric and μCT analyses of iliac crest bone

biopsies in PHPT. While both cortical and trabecular bone are affected at peripheral sites by HRpQCT, histomorphometry and μCT studies of iliac crest biopsies show that trabecular bone volume, number, separation and connectivity are either preserved or increased in patients with PHPT (29-33). Cohen *et al.* (34) have also found modest or no correlations between microarchitecture parameters as assessed by HRpQCT of radius and tibia and histomorphometry and μCT of iliac crest biopsies. Since previous studies have shown strong correlations between microarchitecture assessed by HRpQCT and histomorphometry or μCT at the same bony regions (26, 35), site-to-site differences are likely to contribute to the weak correlations observed by Cohen *et al.* (34). The discrepant observations by histomorphometric analysis of bone biopsies vis a vis fracture incidence in this disease suggest that HRpQCT and now TBS might be more clinically pertinent to fracture risk in PHPT.

Despite the fact that TBS estimates trabecular microarchitecture, our results also revealed positive correlations of TBS with Ct.vBMD and Ct.Th at the radius and tibia. This is not surprising, since cortical and trabecular compartments are both affected in PHPT, leading to strong correlations between measurements of trabecular and cortical microarchitecture and density, even among HRpQCT indices (*e.g.* correlation between Tb.N and Ct.Th at the radius: r=0.667; p=0.001).

The results of this study also showed positive correlations between TBS and whole bone stiffness at the radius (r=0.442; p=0.04) and tibia (r=0.516; p=0.02) as measured by FEA of HRpQCT images. An *ex vivo* study on 16 human vertebrae confirmed the positive relationship between TBS and mechanically measured bone strength (36). Reduced bone stiffness assessed by FEA of HRpQCT images, as well as low TBS, have been associated with fragility fractures in postmenopausal women (14-16, 18-20, 37-39). Even though these studies did not involve patients with PHPT, our findings suggest that low TBS may be related with decreased bone stiffness, and consequently, fracture risk, also in PHPT.

Although we observed significant correlations between TBS and HRpQCT parameters of volumetric densities, skeletal microarchitecture and bone stiffness, it is important to note that, by linear regression analysis, variations in HRpQCT indices of trabecular microarchitecture and stiffness were better predicted by L1-L4 aBMD. The combination of TBS and L1-L4 aBMD was slightly better in predicting the variance of those HRpQCT

indices than either one alone. Moreover, TBS was a poor predictor of variances in HRpQCT measurements of trabecular microarchitecture at the tibia. Since these relationships are comparing TBS, an indirect measurement of trabecular microarchitecture at the lumbar spine, with measurements of cancellous microstructure at the radius and tibia (HRpQCT), it is possible that site-to-site differences in the trabecular compartment are, again, contributing to these observations. In fact, when TBS, aBMD and measurements of trabecular microstructure by μCT were assessed at the same bony region, correlations of aBMD and TBS with BV/TV, Tb.N, Tb.Sp and connectivity density were similar (13).

As reported previously (22, 40), we observed modest or no correlation between TBS and aBMD at all sites. Weak relationships of TBS with aBMD at the lumbar spine (r=0.33), femoral neck (r=0.27) and total hip (r=0.26) were also reported in The Manitoba Study (19). Similarly, recent studies evaluating the effect of anti-resorptives, and more specifically, zoledronic acid therapy on TBS confirmed weak or no correlation between treatment-changes in TBS and aBMD (40, 41). The poor correlation between TBS and aBMD at the lumbar spine, despite the fact that both evaluate the same region of bone, implies that these measurements are, at least, partial independent of each other. In contrast, Boutroy *et al.* (20) found significant correlations between TBS and L1-L4 aBMD ($r=0.58$; $p<0.001$) in 560 women from the OFELY cohort. There may be a tendency for higher correlations between these two indices when Hologic scanners are used (20, 42) as opposed to GE-Lunar DXA devices (19, 41). This observation, however, is not universal (18, 43), and the reason for these paradoxical findings is still unclear.

A TBS threshold of 1.200 has been used in numerous studies to identify patients at high risk of fracture. Results from these studies, which involved from 500 to 1,200 postmenopausal women, have shown that a significant greater number of subjects at high risk of fragility fracture are identified when a combination of either aBMD T-score ≤ 2.5 or TBS <1.200 are considered, as opposed to aBMD T-score ≤ 2.5 alone (18, 22, 23). Similarly, in the study of Boutroy *et al.* (26), non-osteoporotic women whose TBS values were below 1.209 (the first TBS quartile threshold) had a significant higher incidence of fragility fracture. Using cut off points previously reported as having the best sensitivity and specificity in regards to fracture, we showed that 36% of PHPT patients had a degraded microarchitecture (TBS$\leq$1.20), an additional 36% a partially degraded

microarchitecture (TBS>1.20 and <1.35) and 27% of them presented normal TBS values (TBS≥1.35). Accordingly, while 72% of PHPT patients showed degraded or partially degraded microarchitecture by TBS, only 46% of them were classified as osteopenic or osteoporotic by lumbar spine T-score. Similarly, patients with PHPT were found to have lower TBS values than healthy controls, despite similar lumbar spine aBMDs by DXA (42). Therefore, TBS may help to identify abnormalities in trabecular bone in PHPT even in patients with apparent preserved lumbar spine aBMD by DXA.

This study has some limitations. We studied a fairly small number of subjects, so that we could not evaluate the association between TBS and fracture risk in PHPT. Moreover, it remains to be seen whether these findings would be appreciated when a larger number of patients is studied. We did not include a healthy control group, since our main aim was to correlate TBS with HRpQCT-derived measurements of microarchitecture and biomechanical competence in PHPT. However, it would be helpful to compare TBS between PHPT and control subjects, as well as to verify if the significant correlations reported here are also present in healthy individuals. Only postmenopausal women were studied so that it is not known whether the results are applicable to men or premenopausal women with PHPT.

Despite these limitations, our study has important strengths. This is the first clinical study to report significant correlations between TBS and direct measurements of trabecular microstructure by HRpQCT. The positive relationship between TBS and bone stiffness assessed by FEA of HRpQCT images suggest that, in PHPT, low TBS may also indicate increased fracture risk. Moreover, our results demonstrate that TBS has the potential to identify PHPT subjects with abnormalities in trabecular bone not captured by lumbar spine aBMD. TBS has the major clinical advantage of being readily available from images of DXA, a test routinely performed in PHPT. With significant correlations between TBS and volumetric and microstructural indices, as well as biomechanical measurements by HRpQCT, a method that has greater resolving power but is not widely accessible, TBS could become a helpful clinical tool in the assessment of skeletal involvement in PHPT.

Disclosures:

Didier Hans is a co-owner of the TBS patent. The other authors state that they have no conflicts of interest.

Acknowledgments:

Supported in part by the following NIH grants: DK32333, and the Brazilian National Council of Technological and Scientific Development – CNPq (BC Silva).

Figures:

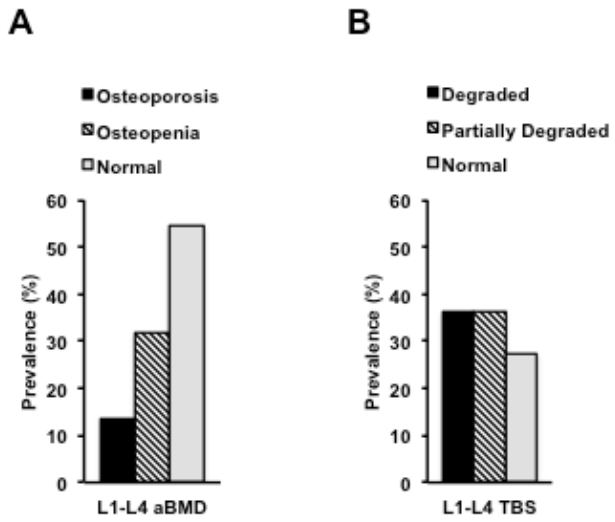

Figure 1: Comparison of aBMD by DXA and TBS. Prevalence of subjects with: (A) osteoporosis, osteopenia or normal aBMD at the lumbar spine by DXA; and (B) degraded microarchitecture (TBS<1.2), partially degraded microarchitecture (TBS>1.2 and <1.35), and normal TBS at the lumbar spine (TBS>1.35).

DXA= dual-energy X-ray absorptiometry; aBMD= areal bone mineral density; and TBS= trabecular bone score.

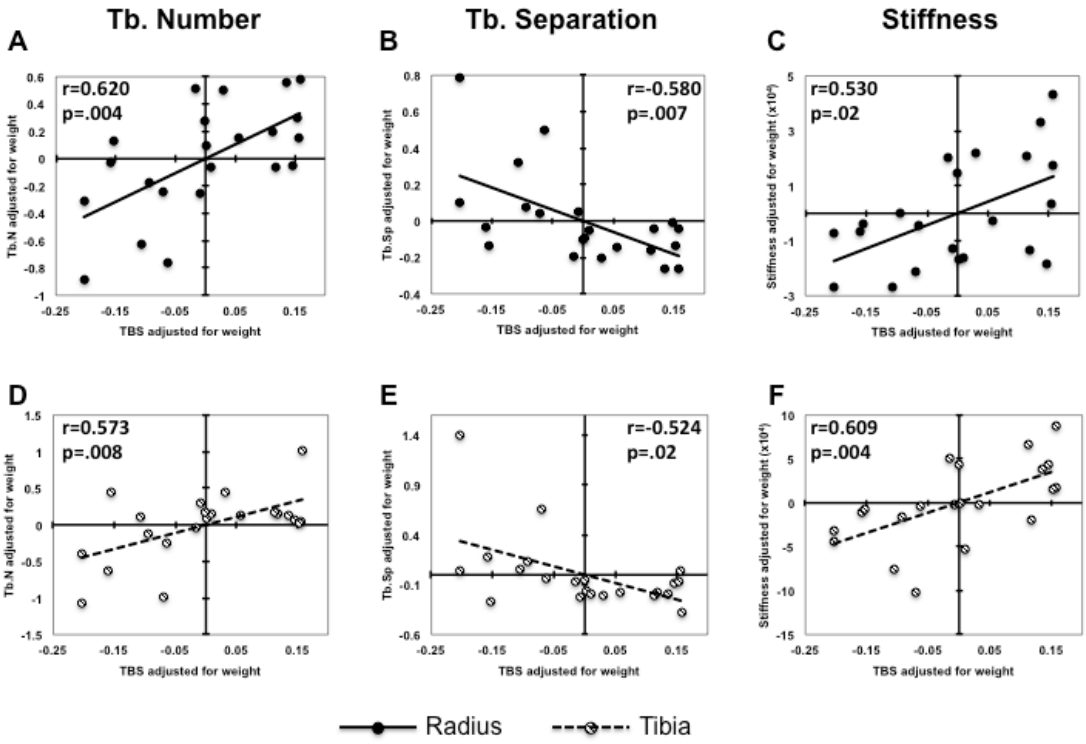

Figure 2: Correlations adjusted for body weight between TBS and trabecular number (A), trabecular separation (B), and stiffness (C) at the radius; and trabecular number (D), trabecular separation (E), and stiffness (F) at the tibia.

TBS= trabecular bone score; Tb.N= trabecular number; Tb.Sp= trabecular separation; Stiffness= whole bone stiffness

Table 1: Baseline characteristics of 22 subjects with PHPT:

Characteristics	PHPT (n=22)
Age (years)	67± 2
Weight (kg)	71 ± 4
Height (cm)	161.5 ± 1.9
BMI (kg/cm^2)	27.2 ± 1.5
Years since menopause	15 ± 2
Years since diagnosis	6 ± 1
Serum total calcium (mg/dL)	10.4 ± 0.1
PTH (pg/mL)	72 ± 9
TBS	1.24 ± 0.02
L1-L4 BMD (g/cm^2)	0.940 ± 0.039
T-score	-1.0 ± 0.4
Total hip BMD (g/cm^2)	0.808 ± 0.035
T-score	-1.1 ± 0.3
Femoral neck BMD (g/cm^2)	0.693 ± 0.030
T-score	-1.4 ± 0.3
1/3 radius BMD (g/cm^2)	0.616 ± 0.022
T-score	-1.3 ± 0.4
UD radius BMD (g/cm^2)	0.361 ± 0.018
T-score	-1.4 ± 0.3

Table 2: Correlation between TBS and HRpQCT/mechanical parameters at the radius and tibia in subjects with PHPT:

	HRpQCT and mechanical parameters	TBS	
		r-value	*r-value* adjusted for weight
Radius	Total area	-0.153	-0.063
	Total vBMD	0.489*	0.536*
	Ct.vBMD	0.507*	0.512*
	Ct.Th	0.453*	0.480*
	Tb.vBMD	0.476*	0.562*
	BV/TV	0.473*	0.559*
	Tb.N	0.505*	0.620*
	Tb.Th	0.317	0.337
	Tb.Sp (LOG)	-0.492*	-0.580*
	Tb.Sp SD (LOG)	-0.441*	-0.533*
	Trab. Stiffness	0.332	0.326
	Stiffness	0.442*	0.530*
Tibia	Total area	-0.373	-0.259
	Total vBMD	0.619*	0.668*
	Ct.vBMD	0.471*	0.465*
	Ct.Th	0.515*	0.545*
	Tb.vBMD	0.528*	0.606*
	BV/TV	0.530*	0.608*
	Tb.N	0.297	0.573*
	Tb.Th	0.056	-0.112
	Tb.Sp (LOG)	-0.365	-0.524*
	Tb.Sp SD (LOG)	-0.390	-0.483*
	Trab. Stiffness	0.262	0.403
	Stiffness	0.516*	0.609*

*$p<0.05$

TBS= trabecular bone score; Total vBMD= total volumetric bone mineral density; Ct.vBMD= cortical volumetric bone mineral density; Ct.Th= cortical thickness; Tb.vBMD= trabecular volumetric bone mineral density; BV/TV= trabecular bone volume; Tb.N= trabecular number; Tb.Th= trabecular thickness; Tb.Sp= trabecular separation; Tb.Sp.SD= trabecular distribution; Trab. Stiffness= trabecular stiffness; Stiffness= whole bone stiffness

Table 3: Univariate or multivariate linear regression analysis to predict the variability in HRpQCT indices and mechanical parameters:

	HRpQCT and mechanical parameters	TBS (R^2)	L1-L4 BMD (R^2)	TBS + L1-L4 BMD (R^2)
Radius	Total Area	0.023	0.004	0.039
	Total vBMD	0.239*	0.330*	0.420*
	Ct. vBMD	0.257*	0.209*	0.342*
	Ct.Th	0.205*	0.233*	0.321*
	Tb. vBMD	0.227*	0.479*	0.536*
	BV/TV	0.224*	0.479*	0.534*
	Tb.N	0.255*	0.460*	0.536*
	Tb.Th	0.100	0.269*	0.287*
	Tb.Sp	0.208*	0.345*	0.411*
	Tb.Sp SD	0.161	0.315*	0.359*
	Trab Stiffness	0.110	0.365*	0.379*
	Stiffness	0.195*	0.522*	0.558*
Tibia	Total Area	0.139	0.004	0.187
	Total vBMD	0.383*	0.369*	0.550*
	Ct. vBMD	0.222*	0.209*	0.315*
	Ct.Th	0.265*	0.276*	0.396*
	Tb. vBMD	0.278*	0.345*	0.458*
	BV/TV	0.280*	0.345*	0.459*
	Tb.N	0.088	0.642*	0.642*
	Tb.Th	0.003	0.184*	0.237
	Tb.Sp	0.127	0.343*	0.366*
	Tb.Sp SD	0.123	0.277*	0.306*
	Trab Stiffness	0.069	0.123	0.141
	Stiffness	0.266*	0.444*	0.518*

*$p<.05$

TBS= trabecular bone score; Total vBMD= total volumetric bone mineral density; Ct.vBMD= cortical volumetric bone mineral density; Ct.Th= cortical thickness; Tb.vBMD= trabecular volumetric bone mineral density; BV/TV= trabecular bone volume; Tb.N= trabecular number; Tb.Th= trabecular thickness; Tb.Sp= trabecular separation; Tb.Sp.SD= trabecular distribution; Trab. Stiffness= trabecular stiffness; Stiffness= whole bone stiffness

References:

1. **Cope O** 1966 The study of hyperparathyroidism at the Massachusetts General Hospital. N Engl J Med 274:1174-1182
2. **Rubin MR, Bilezikian JP, McMahon DJ, Jacobs T, Shane E, Siris E, Udesky J, Silverberg SJ** 2008 The natural history of primary hyperparathyroidism with or without parathyroid surgery after 15 years. J Clin Endocrinol Metab 93:3462-3470
3. **Silverberg SJ, Shane E, Jacobs TP, Siris E, Bilezikian JP** 1999 A 10-year prospective study of primary hyperparathyroidism with or without parathyroid surgery. N Engl J Med 341:1249-1255
4. **Bilezikian JP, Brandi ML, Rubin M, Silverberg SJ** 2005 Primary hyperparathyroidism: new concepts in clinical, densitometric and biochemical features. J Intern Med 257:6-17
5. **Silverberg SJ, Shane E, de la Cruz L, Dempster DW, Feldman F, Seldin D, Jacobs TP, Siris ES, Cafferty M, Parisien MV, et al.** 1989 Skeletal disease in primary hyperparathyroidism. Journal of bone and mineral research : the official journal of the American Society for Bone and Mineral Research 4:283-291
6. **Hansen S, Beck Jensen JE, Rasmussen L, Hauge EM, Brixen K** 2010 Effects on bone geometry, density, and microarchitecture in the distal radius but not the tibia in women with primary hyperparathyroidism: A case-control study using HR-pQCT. Journal of bone and mineral research : the official journal of the American Society for Bone and Mineral Research 25:1941-1947
7. **Stein EM, Silva BC, Boutroy S, Zhou B, Wang J, Udesky J, Zhang C, McMahon DJ, Romano M, Dworakowski E, Costa AG, Cusano N, Irani D, Cremers S, Shane E, Guo WE, Bilezikian JP** 2012 Primary Hyperparathyroidism is Associated with Abnormal Cortical and Trabecular Microstructure and Reduced Bone Stiffness in Postmenopausal Women. Journal of bone and mineral research : the official journal of the American Society for Bone and Mineral Research:submited
8. **Khosla S, Melton LJ, 3rd, Wermers RA, Crowson CS, O'Fallon W, Riggs B** 1999 Primary hyperparathyroidism and the risk of fracture: a population-based study. Journal of bone and mineral research : the official journal of the American Society for Bone and Mineral Research 14:1700-1707

9. **Vignali E, Viccica G, Diacinti D, Cetani F, Cianferotti L, Ambrogini E, Banti C, Del Fiacco R, Bilezikian JP, Pinchera A, Marcocci C** 2009 Morphometric vertebral fractures in postmenopausal women with primary hyperparathyroidism. J Clin Endocrinol Metab 94:2306-2312
10. **Yu N, Donnan PT, Flynn RW, Murphy MJ, Smith D, Rudman A, Leese GP** 2010 Increased mortality and morbidity in mild primary hyperparathyroid patients. The Parathyroid Epidemiology and Audit Research Study (PEARS). Clin Endocrinol (Oxf) 73:30-34
11. **Vestergaard P, Mosekilde L** 2003 Fractures in patients with primary hyperparathyroidism: nationwide follow-up study of 1201 patients. World journal of surgery 27:343-349
12. **Pothuaud L, Carceller P, Hans D** 2008 Correlations between grey-level variations in 2D projection images (TBS) and 3D microarchitecture: applications in the study of human trabecular bone microarchitecture. Bone 42:775-787
13. **Hans D, Barthe N, Boutroy S, Pothuaud L, Winzenrieth R, Krieg MA** 2011 Correlations between trabecular bone score, measured using anteroposterior dual-energy X-ray absorptiometry acquisition, and 3-dimensional parameters of bone microarchitecture: an experimental study on human cadaver vertebrae. Journal of clinical densitometry : the official journal of the International Society for Clinical Densitometry 14:302-312
14. **Pothuaud L, Barthe N, Krieg MA, Mehsen N, Carceller P, Hans D** 2009 Evaluation of the potential use of trabecular bone score to complement bone mineral density in the diagnosis of osteoporosis: a preliminary spine BMD-matched, case-control study. Journal of clinical densitometry : the official journal of the International Society for Clinical Densitometry 12:170-176
15. **Rabier B, Heraud A, Grand-Lenoir C, Winzenrieth R, Hans D** 2010 A multicentre, retrospective case-control study assessing the role of trabecular bone score (TBS) in menopausal Caucasian women with low areal bone mineral density (BMDa): Analysing the odds of vertebral fracture. Bone 46:176-181
16. **Winzenrieth R, Dufour R, Pothuaud L, Hans D** 2010 A retrospective case-control study assessing the role of trabecular bone score in postmenopausal Caucasian women with osteopenia: analyzing the odds of vertebral fracture. Calcified tissue international 86:104-109

17. **Del Rio LM, Winzenrieth R, Cormier C, Di Gregorio S** 2012 Is bone microarchitecture status of the lumbar spine assessed by TBS related to femoral neck fracture? A Spanish case-control study. Osteoporosis international : a journal established as result of cooperation between the European Foundation for Osteoporosis and the National Osteoporosis Foundation of the USA
18. **Popp A, Meer S, Krieg MA, Perrelet R, Hans D, Lippuner K** 2012 Bone Mineral Density (BMD) Combined with the Trabecular Bone Score (TBS) Significantly Improves the Identification of Women at High Risk of Fracture: The SEMOF Cohort Study. J Bone Miner Res 27 (Suppl 1):S303 (abstract)
19. **Hans D, Goertzen AL, Krieg MA, Leslie WD** 2011 Bone microarchitecture assessed by TBS predicts osteoporotic fractures independent of bone density: the Manitoba study. Journal of bone and mineral research : the official journal of the American Society for Bone and Mineral Research 26:2762-2769
20. **Boutroy S, Hans D, Sornay-Rendu E, Vilayphiou N, Winzenrieth R, Chapurlat R** 2012 Trabecular bone score improves fracture risk prediction in non-osteoporotic women: the OFELY study. Osteoporosis international : a journal established as result of cooperation between the European Foundation for Osteoporosis and the National Osteoporosis Foundation of the USA
21. **Bloch J, Hans D, Diebolt V, Kieffer D, Krieg M** 2008 Evaluation du risque fracturaire dans la zone d'ostéopénie: utilisation clinique d'un indice de la microarchitecture osseuse (TBS: trabéculométrie et trabéculographie). in SFR, Paris:abstract - avaivalbe at http://www.medimaps.fr/articles/cat/34
22. **Lamy O, Krieg MA, Stoll D, Aubry-Rozier B, Metzger M, Hans D** 2012 What Is the Performance in Vertebral Fracture Discrimination by Bone Mineral Density (BMD), Micro-architecture Estimation (TBS), Body Mass Index (BMI) and FRAX in Stand-alone or Combined Approaches: The OsteoLaus Study. J Bone Miner Res 27 (Suppl 1):S236 (abstract)
23. **Vasic J, Gojkovic F, Petranova T, Elez J, Culafic Vojinovic V, Winzenrieth R, Hans D, Rashkov R, Dimic A** 2012 Spine Micro-Architecture Estimation (TBS) Discriminates Major osteoporotic Fracture From Controls Equally Well Than Site Matched BMD And Independently: The Eastern Europe TBS Study. Osteoporos Int 23 (Suppl 2):S327 (abstract)

24. **Boutroy S, Bouxsein ML, Munoz F, Delmas PD** 2005 In vivo assessment of trabecular bone microarchitecture by high-resolution peripheral quantitative computed tomography. J Clin Endocrinol Metab 90:6508-6515

25. **Laib A, Hauselmann HJ, Ruegsegger P** 1998 In vivo high resolution 3D-QCT of the human forearm. Technology and health care : official journal of the European Society for Engineering and Medicine 6:329-337

26. **Boutroy S, Vilayphiou N, Roux JP, Delmas PD, Blain H, Chapurlat RD, Chavassieux P** 2011 Comparison of 2D and 3D bone microarchitecture evaluation at the femoral neck, among postmenopausal women with hip fracture or hip osteoarthritis. Bone 49:1055-1061

27. **Khosla S, Riggs BL, Atkinson EJ, Oberg AL, McDaniel LJ, Holets M, Peterson JM, Melton LJ, 3rd** 2006 Effects of sex and age on bone microstructure at the ultradistal radius: a population-based noninvasive in vivo assessment. Journal of bone and mineral research : the official journal of the American Society for Bone and Mineral Research 21:124-131

28. **Macneil JA, Boyd SK** 2008 Bone strength at the distal radius can be estimated from high-resolution peripheral quantitative computed tomography and the finite element method. Bone 42:1203-1213

29. **Christiansen P, Steiniche T, Vesterby A, Mosekilde L, Hessov I, Melsen F** 1992 Primary hyperparathyroidism: iliac crest trabecular bone volume, structure, remodeling, and balance evaluated by histomorphometric methods. Bone 13:41-49

30. **Dempster DW, Muller R, Zhou H, Kohler T, Shane E, Parisien M, Silverberg SJ, Bilezikian JP** 2007 Preserved three-dimensional cancellous bone structure in mild primary hyperparathyroidism. Bone 41:19-24

31. **Parisien M, Cosman F, Mellish RW, Schnitzer M, Nieves J, Silverberg SJ, Shane E, Kimmel D, Recker RR, Bilezikian JP, et al.** 1995 Bone structure in postmenopausal hyperparathyroid, osteoporotic, and normal women. Journal of bone and mineral research : the official journal of the American Society for Bone and Mineral Research 10:1393-1399

32. **Parisien M, Mellish RW, Silverberg SJ, Shane E, Lindsay R, Bilezikian JP, Dempster DW** 1992 Maintenance of cancellous bone connectivity in primary hyperparathyroidism: trabecular strut analysis. Journal of bone and mineral

research : the official journal of the American Society for Bone and Mineral Research 7:913-919

33. **Parisien M, Silverberg SJ, Shane E, de la Cruz L, Lindsay R, Bilezikian JP, Dempster DW** 1990 The histomorphometry of bone in primary hyperparathyroidism: preservation of cancellous bone structure. J Clin Endocrinol Metab 70:930-938

34. **Cohen A, Dempster DW, Muller R, Guo XE, Nickolas TL, Liu XS, Zhang XH, Wirth AJ, van Lenthe GH, Kohler T, McMahon DJ, Zhou H, Rubin MR, Bilezikian JP, Lappe JM, Recker RR, Shane E** 2010 Assessment of trabecular and cortical architecture and mechanical competence of bone by high-resolution peripheral computed tomography: comparison with transiliac bone biopsy. Osteoporosis international : a journal established as result of cooperation between the European Foundation for Osteoporosis and the National Osteoporosis Foundation of the USA 21:263-273

35. **MacNeil JA, Boyd SK** 2007 Accuracy of high-resolution peripheral quantitative computed tomography for measurement of bone quality. Medical engineering & physics 29:1096-1105

36. **Roux JP, Wegrzyn J, Boutroy S, Bouxsein M, Hans D** 2012 Association of Trabecular Bone Score (TBS) with Mechanical Behavior of Human Lumbar Vertebrae. J Bone Miner Res 27 (Suppl 1):S360 (abstract)

37. **Boutroy S, Van Rietbergen B, Sornay-Rendu E, Munoz F, Bouxsein ML, Delmas PD** 2008 Finite element analysis based on in vivo HR-pQCT images of the distal radius is associated with wrist fracture in postmenopausal women. Journal of bone and mineral research : the official journal of the American Society for Bone and Mineral Research 23:392-399

38. **Stein EM, Liu XS, Nickolas TL, Cohen A, Thomas V, McMahon DJ, Zhang C, Cosman F, Nieves J, Greisberg J, Guo XE, Shane E** 2011 Abnormal microarchitecture and stiffness in postmenopausal women with ankle fractures. J Clin Endocrinol Metab 96:2041-2048

39. **Stein EM, Liu XS, Nickolas TL, Cohen A, Thomas V, McMahon DJ, Zhang C, Yin PT, Cosman F, Nieves J, Guo XE, Shane E** 2010 Abnormal microarchitecture and reduced stiffness at the radius and tibia in postmenopausal women with fractures. Journal of bone and mineral research : the official journal of the American Society for Bone and Mineral Research 25:2572-2581

40. **Popp AW, Guler S, Lamy O, Senn C, Buffat H, Perrelet R, Hans D, Lippuner K** 2012 Effects of zoledronate versus placebo on spine bone mineral density (BMD) and microarchitecture assessed by the trabecular bone score (TBS) in postmenopausal women with osteoporosis. A 3-year study. Journal of bone and mineral research : the official journal of the American Society for Bone and Mineral Research

41. **Krieg MA, Aubry-Rozier B, Hans D, Leslie WD** 2012 Effects of anti-resorptive agents on trabecular bone score (TBS) in older women. Osteoporosis international : a journal established as result of cooperation between the European Foundation for Osteoporosis and the National Osteoporosis Foundation of the USA

42. **Romagnoli E, Cipriani C, Castro C, Carnevale V, Diacinti D, Pepe J, Ostuni L, Angelozzi M, Scarpiello A, Minisola S** 2012 Femur Strength Indices and Trabecular Bone Score (TBS) in Postmenopausal Patients With Primary Hyperparathyroidism. J Bone Miner Res 27 (Suppl 1):S141 (abstract)

43. **Mascarenhas MR, Barbosa AP, Simões V, Gonçalves A, Pinto DS, Bicho M, Hans D, do Carmo I** 2012 Bone Quality by TBS, BMD and Sex Steroids Levels in Normal Men. J Bone Miner Res 27 (Suppl 1):S361 (abstract)

4- CONSIDERAÇÕES FINAIS:

Resultados desse estudo reafirmam a necessidade de se reconsiderar o conceito de que, nas formas assintomáticas de PHPT, apenas o osso cortical é comprometido. Além disso, indicam que outras técnicas de avaliação óssea, combinadas à avaliação por DXA, podem fornecer informações adicionais sobre qualidade óssea nessa entidade. Uma vez que o achado de osteoporose em exames de densitometria óssea é uma das indicações para o tratamento cirúrgico das formas assintomáticas de PHPT (BILEZIKIAN *et al.*, 2009), é importante que a integridade óssea seja avaliada com precisão, evitando-se o subtratamento da doença.

Avaliação óssea por HRpQCT de 51 mulheres na pós menopausa com PHPT evidenciou que, mesmo na forma assintomática da doença, os compartimentos cortical e trabecular estão sujeitos a ações negativas do excesso crônico de PTH. Verificou-se redução da vBMD em ambos compartimentos esqueléticos do rádio distal e da tíbia. Esses achados são compatíveis com estudos prévios por pQCT (CHEN *et al.*, 2003; CHAROPOULOS *et al.*, 2006), mas tal técnica não permite avaliação da microestrutura óssea. Resultados do único estudo de HRpQCT em pacientes com PHPT (HANSEN *et al.*, 2010) confirmam nossos achados de redução generalizada da vBMD e deterioração da microarquitetura cortical e trabecular, mas, naquele estudo, as diferenças foram significativas apenas no rádio, talvez pelo número menor de pacientes avaliados (26, sendo 23 mulheres na pós menopausa).

Este projeto inaugura o uso de ITS para análise de imagens de HRpQCT no PHPT. Análise por ITS mostrou que, no PHPT, há redução maior de trabéculas em placa do que em haste, resultando em diminuição significativa da razão *P-R*. Uma vez que trabéculas em placa são as principais responsáveis pela resistência óssea (LIU *et al.*, 2008), essa alteração microestrutural do compartimento trabecular resultaria em aumento da fragilidade óssea nessa doença. Além disso, ITS revelou redução do aBV/TV, variável fortemente correlacionada com medidas de competência mecânica óssea (LIU *et al.*, 2008). Associadas a essas alterações estruturais, redução da rigidez óssea total e trabecular, bem como aumento da carga suportada pelo compartimento cortical,

estimados por FEA, confirmam os efeitos negativos do PTH sobre a qualidade óssea cortical e trabecular em pacientes com PHPT.

Confirmando achados de estudos anteriores, resultados deste trabalho demonstraram que aBMDs da coluna lombar foram semelhantes entre casos e controles. A inabilidade da densitometria óssea em detectar perda esquelética trabecular no PHPT poderia ser explicada por diferenças na geometria óssea. Nossos estudos de HRpQCT revelaram que pacientes com PHPT têm aumento da área óssea total. Uma vez que a medida da aBMD é influenciada pelo tamanho ósseo (CARTER *et al.*, 1992), o aumento da área óssea poderia superestimar a medida da aBMD nesses pacientes. Além disso, é possível que sítios ósseos diferentes respondam de maneira diversa ao excesso crônico de PTH. De fato, ausência de anormalidades no compartimento trabecular foi também observada por histomorfometria de biópsias ósseas de crista ilíaca, em estudos anteriores de pacientes com PHPT (PARISIEN *et al.*, 1990; CHRISTIANSEN *et al.*, 1992; PARISIEN *et al.*, 1992; PARISIEN *et al.*, 1995). Dado que medidas de microarquitetura trabecular por HRpQCT têm forte correlação com resultados de histomorfometria quando o mesmo sítio ósseo é avaliado (BOUTROY *et al.*, 2011), é possível que o fato de se ter avaliado sítios ósseos distintos explique os achados divergentes entre estudos de HRpQCT do rádio e tíbia e estudos histomorfométricos da crista ilíaca. Mesmo entre os dois sítios periféricos aqui avaliados, rádio e tíbia, há diferenças consideráveis. As ações deletérias do PTH sobre o osso trabecular foram menos evidentes na tíbia, possivelmente por tratar-se, diferente do rádio, de osso sujeito a sobrecarga mecânica.

Este trabalho não avaliou o risco de fratura em pacientes com PHPT. No entanto, estudos anteriores confirmam que redução da vBMD no rádio e tíbia por HRpQCT, bem como anormalidades na microarquitetura trabecular e cortical, estão relacionadas a risco aumentado de fratura osteoporótica vertebral e não vertebral em mulheres na pós menopausa (SORNAY-RENDU *et al.*, 2007; STEIN *et al.*, 2010; STEIN *et al.*, 2011; STEIN *et al.*, 2012). Da mesma forma, redução da rigidez óssea estimada por FEA, e redução do volume de trabéculas em placa, menor fração de volume trabecular alinhado no sentido axial e redução da conectividade entre placas, hastes e entre placas e hastes, avaliados por ITS, distinguiram mulheres com fratura por fragilidade de controles saudáveis (BOUTROY *et al.*, 2008; STEIN *et al.*, 2010; VILAYPHIOU *et al.*, 2010; STEIN *et al.*, 2011; LIU *et al.*, 2012). Dessa forma, as alterações estruturais e

biomecânicas evidenciadas em mulheres com PHPT neste estudo, similares às descritas em estudos que consideraram fratura como desfecho principal, são compatíveis com aumento do risco de fratura nessa doença.

Apesar de ter fornecido informações importantes sobre qualidade óssea em pacientes com PHPT e de ser um método não invasivo e de alta sensibilidade, a HRpQCT é um exame de alto custo e indisponível na maior parte dos centros médicos. Por isso, avaliamos se o TBS, novo método de análise de imagem, potencialmente disponível em qualquer centro médico que realize exames de densitometria óssea, poderia fornecer informações adicionais sobre a qualidade do esqueleto trabecular, constituindo uma alternativa para avaliação de pacientes com PHPT na prática clínica.

TBS foi desenvolvido para estimar a microarquitetura trabecular, podendo ser empregado a qualquer imagem de densitometria óssea de coluna lombar. Estudos clínicos envolvendo grande número de mulheres na pós menopausa confirmaram sua habilidade em predizer fratura por fragilidade (POTHUAUD *et al.*, 2009; RABIER *et al.*, 2010; WINZENRIETH *et al.*, 2010; HANS *et al.*, 2011b; DEL RIO *et al.*, 2012). Neste estudo, estimamos, pela primeira vez, a correlação entre TBS, parâmetros de HRpQCT e índices de rigidez óssea medidos por FEA em um subgrupo de 22 mulheres com PHPT.

TBS correlacionou-se com todos os índices determinados pela HRpQCT no rádio, exceto Tb.Th e rigidez trabecular. Na tíbia, correlações foram observadas entre TBS e densidades volumétricas, Ct.Th, BV/TV e rigidez de osso total. No entanto, correlações entre TBS e Tb.N, Tb.Sp e Tb.Sp.SD na tíbia foram evidentes apenas após ajuste para peso corporal. Da mesma forma, em modelos de análise de regressão linear, TBS foi incapaz de prever variações nos índices de microestrutura trabecular da tíbia. Acredita-se que essa falta de correlação entre TBS e estas medidas na tíbia seja explicada por diferenças na microestrutura trabecular inerentes a sítios ósseos distintos. Uma vez que coluna lombar e tíbia estão sujeitas a sobrecargas mecânicas diversas, sua estrutura trabecular adapta-se de modo próprio. O fato da correlação ter-se tornado significativa após ajuste para peso corporal, usado como substituto de sobrecarga mecânica, apoia essa teoria. Além disso, observou-se correlação significativa entre TBS e medidas de microestrutura trabecular por μCT quando ambos foram estimados no mesmo sítio ósseo (HANS *et al.*, 2011a). Por outro lado, a falta de correlação entre TBS e Tb.Th no rádio e

na tíbia, reflete, possivelmente, a falta de habilidade do TBS em estimar essa variável. De fato, quando TBS foi correlacionado com medidas de microarquitetura trabecular por μCT em estudo *ex vivo*, a correlação entre TBS e Tb.Th foi, inesperadamente, negativa (HANS *et al.*, 2011a). O motivo desse achado é desconhecido.

Apesar de não termos estudado risco de fratura, os achados de correlação positiva entre TBS e rigidez de osso total estimada por FEA sugerem que, a exemplo de estudos prévios em mulheres na pós menopausa, valores baixo de TBS podem estar relacionados a redução da resistência óssea e, consequentemente, maior risco de fratura também em pacientes com PHPT.

Confirmando estudos prévios (HANS *et al.*, 2011b; LAMY *et al.*, 2012; POPP *et al.*, 2012), não houve correlação significativa entre aBMD na coluna lombar e TBS, indicando que as duas medidas, apesar de calculadas a partir da mesma região de interesse, são, pelo menos, parcialmente independentes.

Baseado em estudos prévios, os seguintes pontos de corte foram sugeridos para classificação de TBS em mulheres na pós menopausa: TBS≤1,20= microarquitetura degradada; TBS entre 1,20 e 1,35= microarquitetura parcialmente degradada; TBS ≥1,35= microarquitetura normal. De acordo com essa classificação, TBS médio da nossa população de estudo foi indicativo de microarquitetura trabecular parcialmente degradada (TBS= 1,24). Enquanto 72% das pacientes com PHPT evidenciaram TBS compatível com microarquitetura degradada ou parcialmente degradada, apenas 46% delas foram classificadas como osteoporóticas ou osteopênicas pela avaliação do T-score da coluna lombar. De maneira similar, estudo recente demonstrou que TBS foi significativamente menor em grupo de pacientes com PHPT do em um grupo controle, apesar de valores semelhantes de aBMD da coluna lombar entre os dois grupos (ROMAGNOLI *et al.*, 2012). Dessa forma, é possível que TBS ajude a identificar anormalidades no osso trabecular em pacientes com PHPT com aparente preservação da aBMD em coluna lombar por densitometria óssea.

Esses resultados demonstraram que TBS, além de poder ser calculado a partir de qualquer imagem de densitometria óssea da coluna lombar, correlaciona-se significativamente com

índices de densidade volumétrica, microestrutura e rigidez de osso total estimados por HRpQCT em pacientes com PHPT. Apesar do número pequeno de pacientes estudados, é possível que, se avaliado em combinação com a medida de aBMD, TBS identifique maior número de pacientes com deterioração óssea trabecular do que a avaliação da aBMD isoladamente.

Viu-se, portanto, que o estudo por HRpQCT de 51 mulheres na pós menopausa com diagnóstico de PHPT revelou anormalidades importantes dos compartimentos trabecular e cortical do rádio e da tíbia. FEA e avaliação adicional por ITS confirmaram microestrutura trabecular susceptível a fratura e redução da competência biomecânica óssea nessa doença. Finalmente, correlações significativas entre TBS e achados da HRpQCT, exame de alta sensibilidade mas difícil acesso, indicam que TBS tem potencial para estimar a microarquitetura trabecular em pacientes com PHPT.

5- CONCLUSÕES:

A partir do estudo por HRpQCT de 51 mulheres na pós menopausa com PHPT, comparadas a 120 controles da mesma faixa etária e estado menopausal, conclui-se que:

1. mesmo na forma assintomática de PHPT, há redução generalizada da vBMD, bem como deterioração da microestrutura cortical e trabecular no rádio e na tíbia;
2. quando realizada ITS das imagens de HRpQCT, observa-se redução preferencial de trabéculas em placa, com redução da razão P-R, diminuição do volume trabecular em sentido axial e redução da conectividade entre trabéculas, revelando microestrutura trabecular mais susceptível a fraturas;
3. FEA das imagens de HRpQCT confirma redução da rigidez de osso total e trabecular, fornecendo explicação biomecânica para o achado clínico de aumento do risco de fratura nessa condição.

A partir do estudo por TBS de 22 mulheres na pós menopausa com PHPT, conclui-se que:

1. correlações significativas entre TBS e índices de densidade volumétrica, microestrutura e rigidez de osso total estimados por HRpQCT indicam que essa nova técnica de análise pode tornar-se útil para avaliação de pacientes com PHPT na prática clínica.

6- REFERÊNCIAS BIBLIOGRÁFICAS:

ADAMI, S.*, et al.* Epidemiology of primary hyperparathyroidism in Europe. **J Bone Miner Res,** v.17 Suppl 2, p.N18-23, Nov. 2002.

ALBRIGHT, F. A page out of the history of hyperparathyroidism. **J Clin Endocrinol Metab,** v.8 n.8, p.637-657, Aug. 1948.

ARNOLD, A.*, et al.* Molecular pathogenesis of primary hyperparathyroidism. **J Bone Miner Res,** v.17 Suppl 2, p.N30-36, Nov. 2002.

ARNOLD, A.*, et al.* Monoclonality and abnormal parathyroid hormone genes in parathyroid adenomas. **N Engl J Med,** v.318 n.11, p.658-662, Mar 17. 1988.

BANDEIRA, F.*, et al.* From mild to severe primary hyperparathyroidism: The Brazilian experience. **Arq Bras Endocrinol Metabol,** v.50 n.4, p.657-663, Aug. 2006.

BERSON, S. A.*, et al.* Immunoassay of Bovine and Human Parathyroid Hormone. **Proc Natl Acad Sci U S A,** v.49 n.5, p.613-617, May. 1963.

BILEZIKIAN, J. P. Primary hyperparathyroidism. **Endocr Pract,** v.18 n.5, p.781-790, Sep 1. 2012.

BILEZIKIAN, J. P.*, et al.* Guidelines for the Management of Asymptomatic Primary Hyperparathyroidism: Summary Statement from the Third International Workshop. **J Clin Endocrinol Metab,** v.94 n.2, p.335-339, Feb. 2009.

BILEZIKIAN, J. P.*, et al.* Primary hyperparathyroidism: new concepts in clinical, densitometric and biochemical features. **J Intern Med,** v.257 n.1, p.6-17, Jan. 2005.

BILEZIKIAN, J. P.*, et al.* Primary Hyperparathyroidism. In. ARINOVICHE, R. and ARRIAGADA, M. **Temas de Osteoporosis y otras Enfermedades Óseas.** 1st ed. Santiago, Chile: Fundación Chilena de Osteoporosis, 2012. cap.28. p**.**403-424.

BOLLERSLEV, J.*, et al.* Medical observation, compared with parathyroidectomy, for asymptomatic primary hyperparathyroidism: a prospective, randomized trial. **J Clin Endocrinol Metab,** v.92 n.5, p.1687-1692, May. 2007.

BOUTROY, S.*, et al.* In vivo assessment of trabecular bone microarchitecture by high-resolution peripheral quantitative computed tomography. **J Clin Endocrinol Metab,** v.90 n.12, p.6508-6515, Dec. 2005.

BOUTROY, S.*, et al.* Trabecular bone score improves fracture risk prediction in non-osteoporotic women: the OFELY study. **Osteoporos Int**, Oct 16. 2012.

BOUTROY, S.*, et al.* Finite element analysis based on in vivo HR-pQCT images of the distal radius is associated with wrist fracture in postmenopausal women. **J Bone Miner Res,** v.23 n.3, p.392-399, Mar. 2008.

BOUTROY, S.*, et al.* Comparison of 2D and 3D bone microarchitecture evaluation at the femoral neck, among postmenopausal women with hip fracture or hip osteoarthritis. **Bone,** v.49 n.5, p.1055-1061, Nov. 2011.

BRANDI, M. L.*, et al.* Guidelines for diagnosis and therapy of MEN type 1 and type 2. **J Clin Endocrinol Metab,** v.86 n.12, p.5658-5671, Dec. 2001.

BRINGHURST, F. R.*, et al.* Hormones and Disorders of Mineral Metabolism In. KRONENBERG, H. M., MELMED, S., POLONSKY, K. S. and LARSEN, P. R. **Williams Textbook of Endocrinology.** 11th ed. Philadelphia: Saunders Elsevier, 2008. cap.27. p**.**1203-1268.

BURGHARDT, A. J.*, et al.* High-resolution computed tomography for clinical imaging of bone microarchitecture. **Clin Orthop Relat Res,** v.469 n.8, p.2179-2193, Aug. 2011.

CARRELLI, A.*, et al.* Endothelial Function in Mild Primary Hyperparathyroidism. **Clin Endocrinol (Oxf)**, Jul 3. 2012.

CARTER, D. R.*, et al.* New approaches for interpreting projected bone densitometry data. **J Bone Miner Res,** v.7 n.2, p.137-145, Feb. 1992.

CHAROPOULOS, I.*, et al.* Effect of primary hyperparathyroidism on volumetric bone mineral density and bone geometry assessed by peripheral quantitative computed tomography in postmenopausal women. **J Clin Endocrinol Metab,** v.91 n.5, p.1748-1753, May. 2006.

CHEN, Q.*, et al.* Effects of an excess and a deficiency of endogenous parathyroid hormone on volumetric bone mineral density and bone geometry determined by peripheral quantitative computed tomography in female subjects. **J Clin Endocrinol Metab,** v.88 n.10, p.4655-4658, Oct. 2003.

CHRISTIANSEN, P.*, et al.* Primary hyperparathyroidism: iliac crest trabecular bone volume, structure, remodeling, and balance evaluated by histomorphometric methods. **Bone,** v.13 n.1, p.41-49, 1992.

COHEN A., *et al.* Assessment of trabecular and cortical architecture and mechanical competence of bone by high-resolution peripheral computed tomography: comparison with transiliac bone biopsy. **Osteoporos Int,** v.21 n.2, p.263-273, 2010.

COPE, O. The study of hyperparathyroidism at the Massachusetts General Hospital. **N Engl J Med,** v.274 n.21, p.1174-1182, May 26. 1966.

DAMILAKIS, J.*, et al.* Radiation exposure in X-ray-based imaging techniques used in osteoporosis. **Eur Radiol,** v.20 n.11, p.2707-2714, Nov. 2010.

DEL RIO, L. M.*, et al.* Is bone microarchitecture status of the lumbar spine assessed by TBS related to femoral neck fracture? A Spanish case-control study. **Osteoporos Int**, May 12. 2012.

DEMPSTER, D. W.*, et al.* Preserved three-dimensional cancellous bone structure in mild primary hyperparathyroidism. **Bone,** v.41 n.1, p.19-24, Jul. 2007.

HANS, D.*, et al.* Correlations between trabecular bone score, measured using anteroposterior dual-energy X-ray absorptiometry acquisition, and 3-dimensional parameters of bone microarchitecture: an experimental study on human cadaver vertebrae. **J Clin Densitom,** v.14 n.3, p.302-312, Jul-Sep. 2011a.

HANS, D.*, et al.* Bone microarchitecture assessed by TBS predicts osteoporotic fractures independent of bone density: the Manitoba study. **J Bone Miner Res,** v.26 n.11, p.2762-2769, Nov. 2011b.

HANSEN, S.*, et al.* Effects on bone geometry, density, and microarchitecture in the distal radius but not the tibia in women with primary hyperparathyroidism: A case-control study using HR-pQCT. **J Bone Miner Res,** v.25 n.9, p.1941-1947, Sep. 2010.

HOLICK, M. F. Vitamin D deficiency. **N Engl J Med,** v.357 n.3, p.266-281, Jul 19. 2007.

IWATA, S.*, et al.* Aortic valve calcification in mild primary hyperparathyroidism. **J Clin Endocrinol Metab,** v.97 n.1, p.132-137, Jan. 2012.

KEATING, F. R., JR. Diagnosis of primary hyperparathyroidism. Clinical and laboratory aspects. **JAMA,** v.178, p.547-555, Nov 11. 1961.

KHOSLA, S.*, et al.* Primary hyperparathyroidism and the risk of fracture: a population-based study. **J Bone Miner Res,** v.14 n.10, p.1700-1707, Oct. 1999.

KHOSLA, S.*, et al.* Effects of sex and age on bone microstructure at the ultradistal radius: a population-based noninvasive in vivo assessment. **J Bone Miner Res,** v.21 n.1, p.124-131, Jan. 2006.

KOCHERSBERGER, G.*, et al.* What is the clinical significance of bone loss in primary hyperparathyroidism? **Arch Intern Med,** v.147 n.11, p.1951-1953, Nov. 1987.

KULAK, C.A.M.*, et al.* Marked Improvement in Bone Mass after Parathyroidectomy in Osteitis Fibrosa Cystica. **J Clin Endocrinol Metab,** v.83 n.3, p.732-735, Mar. 1998.

LAMY, O.*, et al.* What Is the Performance in Vertebral Fracture Discrimination by Bone Mineral Density (BMD), Micro-architecture Estimation (TBS), Body Mass Index (BMI) and FRAX in Stand-alone or Combined Approaches: The OsteoLaus Study. **J Bone Miner Res 27 (Suppl 1)**, p.S236 (abstract) 2012.

LARSSON, K.*, et al.* The risk of hip fractures in patients with primary hyperparathyroidism: a population-based cohort study with a follow-up of 19 years. **J Intern Med,** v.234 n.6, p.585-593, Dec. 1993.

LIU, X. S.*, et al.* Individual trabeculae segmentation (ITS)-based morphological analysis of high-resolution peripheral quantitative computed tomography images detects abnormal trabecular plate and rod microarchitecture in premenopausal women with idiopathic osteoporosis. **J Bone Miner Res,** v.25 n.7, p.1496-1505, Jul. 2010.

LIU, X. S.*, et al.* Complete volumetric decomposition of individual trabecular plates and rods and its morphological correlations with anisotropic elastic moduli in human trabecular bone. **J Bone Miner Res,** v.23 n.2, p.223-235, Feb. 2008.

LIU, X. S.*, et al.* Individual trabecula segmentation (ITS)-based morphological analysis of microscale images of human tibial trabecular bone at limited spatial resolution. **J Bone Miner Res,** v.26 n.9, p.2184-2193, Sep. 2011a.

LIU, X. S.*, et al.* Individual trabecula segmentation (ITS)-based morphological analyses and microfinite element analysis of HR-pQCT images discriminate postmenopausal fragility fractures independent of DXA measurements. **J Bone Miner Res,** v.27 n.2, p.263-272, Feb. 2012.

LIU, X. S.*, et al.* Better skeletal microstructure confers greater mechanical advantages in Chinese-American women versus white women. **J Bone Miner Res,** v.26 n.8, p.1783-1792, Aug. 2011b.

MACNEIL, J. A. and S. K. BOYD Accuracy of high-resolution peripheral quantitative computed tomography for measurement of bone quality. **Med Eng Phys,** v.29 n.10, p.1096-1105, Dec. 2007.

MACNEIL, J. A. and S. K. BOYD Bone strength at the distal radius can be estimated from high-resolution peripheral quantitative computed tomography and the finite element method. **Bone,** v.42 n.6, p.1203-1213, Jun. 2008.

MALLETTE, L. E.*, et al.* Primary hyperparathyroidism: clinical and biochemical features. **Medicine (Baltimore),** v.53 n.2, p.127-146, Mar. 1974.

MARCOCCI, C.*, et al.* Parathyroid carcinoma. **J Bone Miner Res,** v.23 n.12, p.1869-1880, Dec. 2008.

MARX, S. J.*, et al.* Hyperparathyroidism in hereditary syndromes: special expressions and special managements. **J Bone Miner Res,** v.17 Suppl 2, p.N37-43, Nov. 2002.

MOLLERUP, C. L.*, et al.* Risk of renal stone events in primary hyperparathyroidism before and after parathyroid surgery: controlled retrospective follow up study. **BMJ,** v.325 n.7368, p.807, Oct 12. 2002.

NEVES, M. C.*, et al.* A 10-year experience in intraoperative parathyroid hormone measurements for primary hyperparathyroidism: a prospective study of 91 previous unexplored patients. **J Osteoporos,** v.2012, p.914214, 2012.

OHE, M. N.*, et al.* Changes in clinical and laboratory findings at the time of diagnosis of primary hyperparathyroidism in a University Hospital in Sao Paulo from 1985 to 2002. **Braz J Med Biol Res,** v.38 n.9, p.1383-1387, Sep. 2005.

PARISIEN, M.*, et al.* Bone structure in postmenopausal hyperparathyroid, osteoporotic, and normal women. **J Bone Miner Res,** v.10 n.9, p.1393-1399, Sep. 1995.

PARISIEN, M.*, et al.* Maintenance of cancellous bone connectivity in primary hyperparathyroidism: trabecular strut analysis. **J Bone Miner Res,** v.7 n.8, p.913-919, Aug. 1992.

PARISIEN, M.*, et al.* The histomorphometry of bone in primary hyperparathyroidism: preservation of cancellous bone structure. **J Clin Endocrinol Metab,** v.70 n.4, p.930-938, Apr. 1990.

PASIEKA, J. L.*, et al.* Patient-based surgical outcome tool demonstrating alleviation of symptoms following parathyroidectomy in patients with primary hyperparathyroidism. **World J Surg,** v.26 n.8, p.942-949, Aug. 2002.

PATTEN, B. M.*, et al.* Neuromuscular disease in primary hyperparathyroidism. **Ann Intern Med,** v.80 n.2, p.182-193, Feb. 1974.

PISTOIA, W.*, et al.* Estimation of distal radius failure load with micro-finite element analysis models based on three-dimensional peripheral quantitative computed tomography images. **Bone,** v.30 n.6, p.842-848, Jun. 2002.

POPP, A.*, et al.* Bone Mineral Density (BMD) Combined with the Trabecular Bone Score (TBS) Significantly Improves the Identification of Women at High Risk of

Fracture: The SEMOF Cohort Study. **J Bone Miner Res 27 (Suppl 1)**, p.S303 (abstract), 2012.

POTHUAUD, L.*, et al.* Evaluation of the potential use of trabecular bone score to complement bone mineral density in the diagnosis of osteoporosis: a preliminary spine BMD-matched, case-control study. **J Clin Densitom,** v.12 n.2, p.170-176, Apr-Jun. 2009.

POTHUAUD, L.*, et al.* Correlations between grey-level variations in 2D projection images (TBS) and 3D microarchitecture: applications in the study of human trabecular bone microarchitecture. **Bone,** v.42 n.4, p.775-787, Apr. 2008.

POTTS, J. T. Parathyroid hormone: past and present. **J Endocrinol,** v.187 n.3, p.311-325, Dec. 2005.

QUIROS, R. M.*, et al.* Health-related quality of life in hyperparathyroidism measurably improves after parathyroidectomy. **Surgery,** v.134 n.4, p.675-681; discussion 681-673, Oct. 2003.

RABIER, B.*, et al.* A multicentre, retrospective case-control study assessing the role of trabecular bone score (TBS) in menopausal Caucasian women with low areal bone mineral density (BMDa): Analysing the odds of vertebral fracture. **Bone,** v.46 n.1, p.176-181, Jan. 2010.

ROMAGNOLI, E.*, et al.* Femur Strength Indices and Trabecular Bone Score (TBS) in Postmenopausal Patients With Primary Hyperparathyroidism. **J Bone Miner Res 27 (Suppl 1)**, p.S141 (abstract), 2012.

RUBIN, M. R.*, et al.* The natural history of primary hyperparathyroidism with or without parathyroid surgery after 15 years. **J Clin Endocrinol Metab,** v.93 n.9, p.3462-3470, Sep. 2008.

SARQUIS, M. S.*, et al.* Familial hyperparathyroidism: surgical outcome after 30 years of follow-up in three families with germline HRPT2 mutations. **Surgery,** v.143 n.5, p.630-640, May. 2008.

SILVERBERG, S. J.*, et al.* Presentation of asymptomatic primary hyperparathyroidism: proceedings of the third international workshop. **J Clin Endocrinol Metab,** v.94 n.2, p.351-365, Feb. 2009.

SILVERBERG, S. J.*, et al.* Skeletal disease in primary hyperparathyroidism. **J Bone Miner Res,** v.4 n.3, p.283-291, Jun. 1989.

SILVERBERG, S. J.*, et al.* A 10-year prospective study of primary hyperparathyroidism with or without parathyroid surgery. **N Engl J Med,** v.341 n.17, p.1249-1255, Oct 21. 1999.

SIMONDS, W. F.*, et al.* Familial isolated hyperparathyroidism: clinical and genetic characteristics of 36 kindreds. **Medicine (Baltimore),** v.81 n.1, p.1-26, Jan. 2002.

SORNAY-RENDU, E.*, et al.* Alterations of cortical and trabecular architecture are associated with fractures in postmenopausal women, partially independent of decreased BMD measured by DXA: the OFELY study. **J Bone Miner Res,** v.22 n.3, p.425-433, Mar. 2007.

STEIN, E. M.*, et al.* Microarchitectural Abnormalities Are More Severe in Postmenopausal Women with Vertebral Compared to Nonvertebral Fractures. **J Clin Endocrinol Metab**, Jul 20. 2012.

STEIN, E. M.*, et al.* Abnormal microarchitecture and stiffness in postmenopausal women with ankle fractures. **J Clin Endocrinol Metab,** v.96 n.7, p.2041-2048, Jul. 2011.

STEIN, E. M.*, et al.* Abnormal microarchitecture and reduced stiffness at the radius and tibia in postmenopausal women with fractures. **J Bone Miner Res,** v.25 n.12, p.2572-2581, Dec. 2010.

VASIC, J.*, et al.* Spine Micro-Architecture Estimation (TBS) Discriminates Major osteoporotic Fracture From Controls Equally Well Than Site Matched BMD And Independently: The Eastern Europe TBS Study. **Osteoporos Int 23 (Suppl 2)**, p.S327 (abstract), 2012.

VESTERGAARD, P. and L. MOSEKILDE Fractures in patients with primary hyperparathyroidism: nationwide follow-up study of 1201 patients. **World J Surg,** v.27 n.3, p.343-349, Mar. 2003.

VICO, L.*, et al.* High-resolution pQCT analysis at the distal radius and tibia discriminates patients with recent wrist and femoral neck fractures. **J Bone Miner Res,** v.23 n.11, p.1741-1750, Nov. 2008.

VIEIRA, J. G. H. Hiperparatireoidismo Primário. In. SAAD, M. J. A., MACIEL, R. M. B. and MENDONÇA, B. B. **Endocrinologia.** 1ª ed. São Paulo, Rio de Janeiro, Ribeirão Preto, and Belo Horizonte: Atheneu, 2007. cap.27. p**.**509-513.

VIGNALI, E.*, et al.* Morphometric vertebral fractures in postmenopausal women with primary hyperparathyroidism. **J Clin Endocrinol Metab,** v.94 n.7, p.2306-2312, Jul. 2009.

VILAYPHIOU, N., *et al.* Finite element analysis performed on radius and tibia HR-pQCT images and fragility fractures at all sites in postmenopausal women. **Bone,** v.46 n.4, p.1030-1037, Apr. 2010.

VILAYPHIOU, N., *et al.* Finite element analysis performed on radius and tibia HR-pQCT images and fragility fractures at all sites in men. **J Bone Miner Res,** v.26 n.5, p.965-973, May. 2011.

WALKER, M. D., *et al.* Cardiac structure and diastolic function in mild primary hyperparathyroidism. **J Clin Endocrinol Metab,** v.95 n.5, p.2172-2179, May. 2010.

WALKER, M. D., *et al.* Neuropsychological features in primary hyperparathyroidism: a prospective study. **J Clin Endocrinol Metab,** v.94 n.6, p.1951-1958, Jun. 2009.

WILSON, R. E., *et al.* Hyperparathyroidism: The Problem of Acute Parathyroid Intoxication. **Ann Surg,** v.159, p.79-93, Jan. 1964.

WILSON, R. J., *et al.* Mild asymptomatic primary hyperparathyroidism is not a risk factor for vertebral fractures. **Ann Intern Med,** v.109 n.12, p.959-962, Dec 15. 1988.

WINZENRIETH, R., *et al.* A retrospective case-control study assessing the role of trabecular bone score in postmenopausal Caucasian women with osteopenia: analyzing the odds of vertebral fracture. **Calcif Tissue Int,** v.86 n.2, p.104-109, Feb. 2010.

YU, N., *et al.* Increased mortality and morbidity in mild primary hyperparathyroid patients. The Parathyroid Epidemiology and Audit Research Study (PEARS). **Clin Endocrinol (Oxf),** v.73 n.1, p.30-34, Jul. 2010.

7- ANEXOS:

Artigo de revisão publicado sobre o tema:

Catabolic and anabolic actions of parathyroid hormone on the skeleton

J. Endocrinol. Invest 2011; 34: 801-810

REVIEW ARTICLE

Catabolic and anabolic actions of parathyroid hormone on the skeleton

B.C. Silva, A.G. Costa, N.E. Cusano, S. Kousteni, and J.P. Bilezikian

Metabolic Bone Diseases Unit, Division of Endocrinology, Department of Medicine, College of Physicians and Surgeons, Columbia University, USA

ABSTRACT. PTH, an 84-amino acid peptide hormone synthesized by the parathyroid glands, is essential for the maintenance of calcium homeostasis. While in its traditional metabolic role, PTH helps to maintain the serum calcium concentration within narrow, normal limits and participates as a determinant of bone remodeling, more specific actions, described as catabolic and anabolic are also well known. Clinically, the catabolic effect of PTH is best represented by primary hyperparathyroidism (PHPT), while the osteoanabolic effect of PTH is best seen when PTH or its biological amino-terminal fragment [PTH(1-34)] is used as a therapy for osteoporosis. These dual functions of PTH are unmasked under very specific pathological (PHPT) or therapeutic conditions. At the cellular level, PTH favors bone resorption, mostly by affecting the receptor activator of nuclear factor κ-B (RANK) ligand (RANKL)-osteoprotegerin-RANK system, leading to an increase in osteoclast formation and activity. Increased bone formation due to PTH therapy is explained best by its ability to enhance osteoblastogenesis and/or osteoblast survival. The PTH-induced bone formation is mediated, in part, by a decrease in SOST/sclerostin expression in osteocytes. This review focuses on the dual anabolic and catabolic actions of PTH on bone, situations where one is enhanced over the other, and the cellular and molecular mechanisms by which these actions are mediated.

(J. Endocrinol. Invest. 34: ??-??, 2011)

INTRODUCTION

PTH, an 84-amino acid peptide hormone, is synthesized in the cells of the parathyroid glands. Release of PTH occurs both with circadian dynamics and in pulsatile fashion stochastically. Through its direct actions on bone and kidney, the principle target organs, and indirectly on the gastrointestinal tract (by facilitating the activation of vitamin D), PTH helps to maintain the serum calcium within narrow, normal limits. At the level of bone, it promotes calcium release; at the level of the kidney, it promotes tubular calcium reabsorption. The indirect effect on the gastrointestinal tract promotes calcium absorption (1). A hypocalcemic signal will lead to greater PTH release (and synthesis), thus leading to these organ-specific events and restoring the serum calcium to normal.

The direct actions of PTH are initiated by an interaction with its receptor (PTH1R), a G-protein-coupled receptor expressed in target cells, such as osteoblasts in bone and tubular cells in the kidney (2). Events following the binding of PTH to the PTH1R include stimulation of $G\alpha_s$-mediated activation of adenyl cyclase, which in turn promotes cAMP production and subsequent activation of protein kinase A (PKA). The PTH1R is also linked to $G\alpha_q$-mediated activation of phospholipase and protein kinase C (PKC) (3, 4). Regulation of these activation events occurs, in part, at the level of the PTH1R when it is internalized (5). Recently, PTH has been shown to downregulate sclerostin, an important regulator of bone formation. This effect is also mediated by cAMP signaling in osteocytes (6).

The catabolic effect of PTH is best represented by the classic disorder of PTH excess, primary hyperparathyroidism (PHPT). In this setting, in which patients are exposed to continuously high amounts of circulating PTH, bone loss is common. When PHPT was invariably a symptomatic disease, bone loss was often accompanied by fractures. With the more modern clinical profile of PHPT emerging at around the time that dual energy X-ray absorptiometry (DXA) became available in the 1980's, discovery of PHPT was likely to be in asymptomatic individuals whose bone loss could be gleaned only by DXA. Insights into this phenotype revealed clues to the anabolic proclivity of this hormone (7), namely that cancellous bone microstructure is preserved in comparison to postmenopausal women without PHPT (8-10).

Further insight that exploited the idea that PTH could be primarily anabolic under certain circumstances came in the 1990's when studies by Dobnig et al. (11) showed that the way in which PTH is administered dictates whether it will serve primarily an anabolic or catabolic role. In rats treated once daily (i.e., intermittently) with low doses of PTH, marked anabolic effects on the skeleton were observed while continuous, 24-h exposure was associated with the catabolic effects. This key observation was developed further as the foreshortened amino terminal fragment of PTH, teriparatide [PTH(1-34)] and, later, the full-length hormone [PTH(1-84)] were shown to be anabolic when administered once daily in low doses (12, 13).

At the cellular level, gene expression profiling of inter-

Key-words: Hyperparathyroidism, osteoblastogenesis, osteoclastogenesis, PTH, PTH(1-84), teriparatide.

Correspondence: J.P. Bilezikian, MD, 630 W, 168th Street, New York, NY 10032, USA.

E-mail: jpb2@columbia.edu

Accepted August 24, 2011.

First published online September 23, 2011.

mittent *vs* continuous PTH administration *in vivo* and *in vitro* suggests that the two modes of administration of PTH can regulate different set of genes, one favoring bone formation and the other favoring bone resorption (14, 15).
This review focuses on both the anabolic and catabolic skeletal effects of PTH, and discusses the cellular basis by which PTH exerts these effects.

PHPT

Historically, symptomatic PHPT is associated with a devastating, catabolic destruction of the skeleton with bone loss, brown tumors, bone cysts, and subperiosteal bone resorption of the phalanges (16, 17). *Osteitis fibrosa cystica*, the term given to this severe bone disease, is still seen in the developing world, but in most regions where biochemical screening is routine, asymptomatic PHPT predominates. Asymptomatic PHPT rarely is accompanied by these specific skeletal features (18-20). Rather, bone densitometry technology has permitted a different kind of insight into the skeleton of subjects with PHPT.

Bone density and skeletal microarchitecture

Silverberg et al. (7) evaluated the presence and extent of bone disease in patients with asymptomatic PHPT, by DXA and by histomorphometry of bone biopsies. The greatest reduction in bone mineral density (BMD) was found at the distal 1/3 radius, a site of predominantly cortical bone. The ability to perform 3-site DXA gave further information at the other 2 sites, the lumbar spine, a site primarily comprised of cancellous bone, and the hip, a site that is an even admixture of cortical and cancellous bone. BMD of the lumbar spine was within 5% of expected for non-hyperparathyroid, post-menopausal women. The hip regions showed values that were intermediate between the preferentially reduced cortical bone of the distal radius and the maintained BMD of the lumbar spine (Fig. 1).
The findings by DXA were followed up by an extensive series of histomorphometric studies by Dempster et al. (7, 9, 10, 21). Preferential involvement of cortical bone with preservation of cancellous areas was confirmed by histomorphometric analysis. The vast majority of patients with PHPT showed reductions in cortical width. In contrast, the cancellous compartment of the bone biopsy specimen showed greater than average values for trabecular bone volume. Other features of trabecular bone such as trabecular number, connectivity and separation indicated preservation of this compartment of bone in most patients with PHPT. Analysis of bone biopsy specimens by microcomputed tomography (μCT) also demonstrated in mild PHPT preserved cancellous bone architecture (Fig. 2) (8). Histomorphometric studies of bone biopsies in PHPT have confirmed that while the trabecular compartment is preserved, the cortical compartment is at risk with cortical thinning and increased cortical porosity commonly seen (9, 10, 21, 22).
The 10- and 15-yr natural history studies of Silverberg et al. (18, 20) showed that lumbar spine bone density remains stable for as long as subjects were followed, while the sites with more cortical bone, namely the distal 1/3 radius and the femoral neck, began to experience substantial declines after 10 yr of observation.
The characteristic densitometric and histomorphometric pattern described above, with preferential reduction of the cortical compartment, is not always seen in PHPT. The descriptions provided are the most common ones. Obviously, these features will vary with the extent of the disease, and predisposing factors that could favor losses in other skeletal compartments and thus other patterns. For example, Silverberg et al. described a minority of patients with PHPT whose lumbar spine bone density was preferentially reduced (23). This could reflect preferential loss of cancellous bone due to the menopause *per se*, prior to the development of PHPT. Other studies have demonstrated more universal loss of BMD in PHPT (24-26), a finding that would not be unexpected in patients with more severe disease. Recently, Hansen et al. (24), using a newer non-invasive technology, high-resolution peripheral CT (HR-pQCT), showed decreased bone mass in the radius in both the cortical and trabecular compartments, in 27 women with mild PHPT, as compared to a normal control group. In this study, subjects with PHPT had reduced BMD at the lumbar spine by DXA. It is not surprising, therefore, that the cancellous compartment would be abnormal by HR-pQCT in this cohort. It is likely that when more typical phenotype of PHPT is examined by HR-pQCT, microstructural analysis by HR-pQCT will be consistent with preserved cancellous bone.

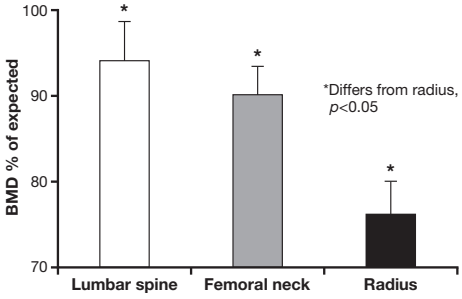

Fig. 1 - *The densitometric signature of primary hyperparathyroidism (PHPT) in the modern era. Bone densitometry at lumbar spine, femoral neck and radius in PHPT. Bone mineral density (BMD) is presented in comparison to expected values for normal controls. [Adapted from (7)].*

Fracture risk

Given the catabolic skeletal actions of continuously elevated PTH levels, typically at cortical sites, one would expect increased non-vertebral fracture risk in patients with PHPT. The preserved cancellous skeleton would be expected to be associated with reduced fracture risk in the spine. Some studies, though, have reported an increase in overall fracture risk (27, 28), including vertebral (17, 28, 29), forearm, rib, and pelvic fractures (28) in PHPT. Increased risk of vertebral and hip fractures has not, how-

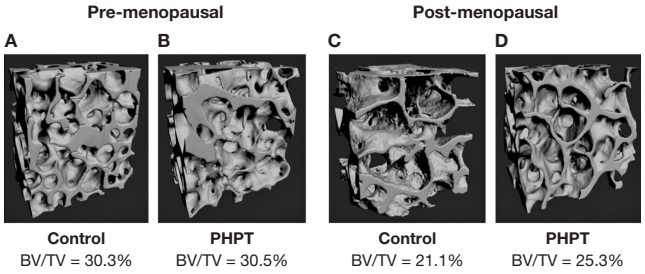

Fig. 2 - *Microarchitectural features in pre- and post-menopausal women with primary hyperparathyroidism (PHPT). 3D micorcomputed tomography reconstructions of cancellous bone in pre- and post-menopausal women with PHPT (B and D), and normal controls (A and C). [Adapted from (8)].*

ever, been uniformly observed (30-32). These controversial findings may reflect reports that vary in the severity of the PHPT. Vignali et al. (29) assessed vertebral fracture risk in 150 subjects with PHPT according to the severity of the disease. Patients with symptomatic PHPT had a higher rate of vertebral fracture than patients with asymptomatic PHPT. When subjects with asymptomatic PHPT were classified according to whether they did or did not meet the criteria for surgery, established by the 2002 Workshop on asymptomatic PHPT, the rate of fracture was significant in those who met surgical guidelines but not in those who did not meet surgical guidelines.

It is hard to draw any conclusions from these studies because many of them are observational and cross-sectional. Some studies suffer by a surveillance bias in which the known PHPT state may have been more likely to be associated with x-rays for complaints of back pain, for example. It is still not clear, then, whether or not patients with mild, asymptomatic PHPT have increased fracture risk.

There are structural issues that may confound the simple expectations by BMD of increased fracture risk at cortical sites and reduced fracture risk at cancellous sites in PHPT. PTH is known, for example, to have other effects on bone qualities beside BMD. As reported in many series, preserved cancellous microarchitecture in mild PHPT might counteract the cortical thinning at cortical sites. Moreover, PTH may increase periosteal apposition, leading to an increase in cross sectional diameter of the bone, favorably altering bone geometry (33, 34). The increase in the outer diameter of bone will increase bone strength independent of BMD (35). Thus, a number of other factors have to be taken into account that altogether defines fracture risk in PHPT.

PTH AS AN ANABOLIC SKELETAL THERAPY

The clues described earlier to the anabolic potential of PTH led to its successful development and that of its biologically active but foreshortened fragment, PTH(1-34) as a therapy for osteoporosis. PTH represents the only osteoanabolic class available at this time for the treatment of osteoporosis. These PTH forms have been shown to increase BMD, improve microarchitecture of the bone, and reduce vertebral fractures. For teriparatide [PTH(1-34)], a reduction in non-vertebral fractures has also been demonstrated (12, 13, 36-41).

Mode of action

Treatment with PTH leads to an increase in bone turnover, with an interesting bitemporal characteristic, in which there is an early stimulation of bone formation followed later by a stimulation of bone turnover (bone resorption and bone formation). The dichomatous kinetics between early effects on bone formation (a bone modeling effect) and a general increase in bone turnover (a bone remodeling effect) has led to the concept of an "anabolic window", the period of time when PTH is maximally anabolic (Fig. 3) (13, 42-45). Even when bone remodeling is stimulated, for at least a limited period of time, bone formation exceeds bone resorption, continuing the anabolic property of PTH albeit perhaps less marked.

The concept of the anabolic window is supported not only by studies of the kinetics of bone markers in the circulation but also by histomorphometric analysis of iliac crest bone biopsies. Using techniques of standard double-labeling and novel quadruple labeling techniques, it has been demonstrated by Dempster et al. (46) that PTH initially stimulates bone formation without prior resorption. This suggests that the process of bone accrual is occur-

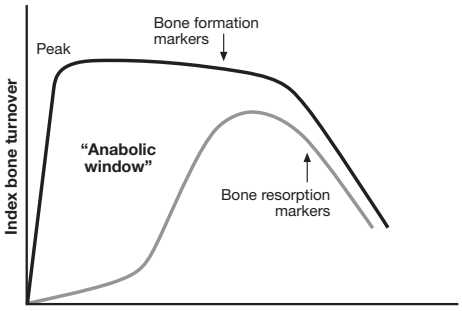

Fig. 3 - *PTH as an anabolic agent for bone: a kinetic model. Treatment with PTH leads to increased bone turnover, with an early stimulation of bone formation followed later by a stimulation of bone resorption. It is thus formed an "anabolic window", the period of time when PTH is maximally anabolic. When bone formation and resorption are stimulated, bone formation exceeds bone resorption, continuing the anabolic property of PTH. [Adapted from (45)]*

ring on quiescent bone surfaces, which is classically a modeling-based event. Modeling is not usually observed in normal, adult human bone, but would appear to occur in this special situation of early PTH exposure (47). Lindsay et al. (46) evaluated bone biopsies of 10 post-menopausal women treated with teriparatide for 4 weeks and compared them to a matched control group. The authors relied on the appearance of the bone surface underneath the newly formed bone to classify the bone formation as modeling or remodeling-based. In the case of modeling-based bone formation, the surface underneath newly formed bone is smooth, and the collagen fibers have similar orientation to the adjacent bone tissue. In remodeling-based bone formation, that surface is irregular, with interrupted collagen fibers, indicating that bone resorption has occurred (47). In the analysis, modeling-based bone formation with teriparatide accounted for approximately 30% and 22% of the bone formation in cancellous and endocortical bone respectively. In control subjects, formation was exclusively remodeling-based (46). In agreement with the concept of the anabolic window, the ability of PTH to increase bone formation in the absence of prior resorption appears to be more pronounced in the early stages of the therapy, since the proportion of modeling-based bone formation decreases over the course of the treatment. When biopsies are carried out after 12-24 months after treatment with 20 or 40 µg daily of teriparatide treatment, only 2.8% and 7.7%, respectively, of bone formation in cancellous bone was a modeling process (38). The modeling-based bone formation induced by PTH can occur not only on quiescent bone surfaces, but also in areas of remodeling in which there is overfilling of bone resorption pits with extension of bone formation beyond the margins of the resorption cavity (46-48). Anabolic action also is appreciated when remodeling becomes the dominant profile of PTH action because there is more bone formation occurring than bone resorption (47).

Bone density and microarchitecture

Densitometric findings in men and women who are treated with PTH(1-84) or teriparatide demonstrate major increments in BMD at the lumbar spine (12, 13, 40, 44). By histomorphometry and µCT of paired iliac crest biopsy specimens from women treated with teriparatide for 11-24 months, improvements in cancellous bone volume, connectivity, and cancellous bone morphology with conversion from a more rod-like to a more normal plate-like appearance have been appreciated (39). Similar effects on cancellous bone were seen upon administration of PTH(1-84) for 18 or 24 months (Fig. 4) (37, 41).
Smaller increases in BMD are appreciated at the hip sites (total hip and femoral neck). The 1/3 radial site typically is not increased and may actually show a small reduction in BMD (12, 13, 40, 44). The small or even negative effects of PTH on BMD at sites containing predominantly cortical bone were not confirmed when bone microarchitecture was assessed. Dempster et al. (36) have shown maintenance or an increase in cortical width in men and women treated with teriparatide for 18 and 36 months, respectively, without increases in cortical porosity. Images obtained during µCT analysis suggest that the increase in cortical thickness seen with teriparatide results from increased bone formation at both the periosteal and endosteal surfaces (39). The increase in cortical thickness, however, is not always seen (37, 41).

Bone geometry and fracture risk

Iliac crest bone biopsies from post-menopausal women treated with teriparatide for 1 month confirm a 4- to 5-fold increase in bone formation rate on the cancellous, endocortical, and periosteal surfaces when compared to a control a group. The increase in bone formation rate on the periosteal surface suggests that PTH has also the potential to increase bone diameter (48).
Bone geometry was assessed by peripheral quantitative CT (pQCT) in a subgroup of 101 women enrolled in the teriparatide fracture prevention trial, at the forearm, the site at which cortical bone predominates (49). There were significant increases in cortical bone area, total bone mineral content and total bone area in teriparatide-treated subjects (20 or 40 µg daily) as compared to patients receiving placebo. Cortical thickness was not changed. Periosteal circumference was significantly higher in both teriparatide groups, as well as the polar cross-sectional moment of inertia. These changes in bone geometry are known to be associated with increased bone strength and improved resistance to fracture (49).
Although PTH can increase cortical porosity and bone resorption at the inner endocortical surface of the bone, it can stimulate periosteal bone apposition, and conse-

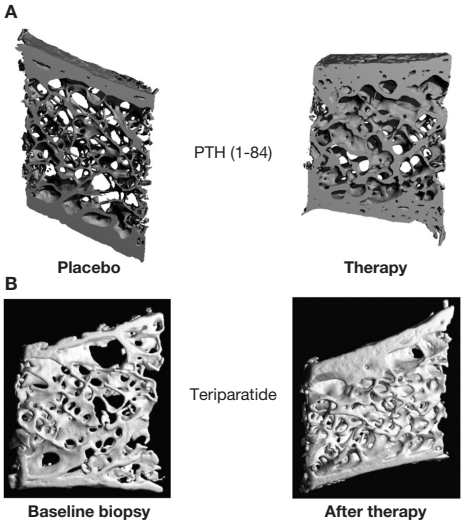

Fig. 4 - *Microcomputed tomography images of iliac crest biopsies of postmenopausal women treated with either PTH(1-84) or teriparatide. A) Osteoporotic postmenopausal women treated with placebo or PTH(1-84) for 18 months. B) Paired biopsy specimens from a 64-yr-old woman before and after treatment with teriparatide for 36 months. [Adapted from (36, 37)].*

quently, increase the outer diameter of the bone. The periosteal apposition partly offsets the loss of compressive and bending strength produced by cortical thinning and porosity, and the resultant change in the ratio of the outer to inner diameter of bone, leads, ultimately, to increased bone strength (45, 50). This favorable change in bone geometry observed with PTH could well account for the reduction in non-vertebral fracture risk (12), even though BMD is not changed or somewhat reduced at cortical sites. The paradox of reduced cortical BMD and reduced fracture risk at sites of cortical bone is thus explained by these affects of PTH on bone size and microstructure.

CELLULAR ACTIONS OF PTH ON THE SKELETON

Cellular actions of PTH contributing to increased bone resorption: Catabolic

Increased bone resorption is the most recognized catabolic action of PTH. It is one of the essential mechanisms by which PTH maintains calcium homeostasis, particularly in the face of a hypocalcemic stimulus. *In vivo*, PTH enhances bone resorption by increasing osteoclastic activity. However, *in vitro* studies demonstrate that osteoclast-like cells in culture do not show increased activity in response to PTH, unless osteoclasts are co-cultured with stromal or osteoblast-like cells or conditioned medium from osteoblasts previously treated with PTH (51-53). It is likely therefore, that PTH induces bone resorption by activating osteoclasts indirectly, through its actions on osteoblasts.

In osteoblasts, PTH regulates the expression of the receptor activator of nuclear factor-κB (RANK) ligand (RANKL), and its soluble decoy receptor osteoprotegerin (OPG), which both play a dominant role in osteoclastogenesis (54-56). RANKL, a tumor necrosis factor (TNF) family member, binds to the RANK on the surface of hematopoietic precursors of osteoclast, promoting their differentiation and survival. RANKL also stimulates fully formed osteoclasts. The catabolic effects of RANKL are inhibited by OPG, a TNF receptor family member that binds to RANKL and thereby prevents access of RANKL to its receptor RANK. The balance between amounts of RANKL and OPG is a determinant of osteoclastogenesis (57). Continuous infusion of PTH increases *RANKL* and inhibits *OPG* mRNA expression in primary murine osteoblasts and in bone from rats (54, 55, 58). *In vitro* studies conducted by Fu et al. (59) showed that PTH directly increases *RANKL* expression by activation of cAMP/PKA-CREB pathway, and inhibits OPG expression *via* a PKA-CREB-AP-1 pathway. These PTH actions lead to an increase in the *RANKL/OPG* ratio, which is believed to be the main mechanism by which PTH influences osteoclastogenesis and bone resorption (Fig. 5).

Clinical studies also argue for RANKL as a key intermediate in the catabolic actions of PTH. Circulating levels of RANKL were elevated in 29 patients with mild PHPT, correlating positively with bone resorption markers and with rates of bone loss at the total femur (60). The *RANKL/OPG* ratio, as determined by mRNA analysis of bone biopsies, significantly declines after parathyroid surgery (61). The pre-operative RANKL/OPG ratio correlated positively with 1-yr post-operative increases in bone mass.

In addition to the RANKL/OPG system, it has been reported that the monocyte chemoattractant protein-1 (MCP-1) can mediate the action of PTH on osteoclastogenesis. PTH increases the expression of MCP-1 in rat osteoblastic cells and in the femur of rats treated with intermittent or continuous infusion of PTH *via* the PKA pathway (62). MCP-1 promotes chemoattraction of pre-osteoclasts, and enhances RANKL-induced osteoclastogenesis and fusion, contributing to the increase in bone

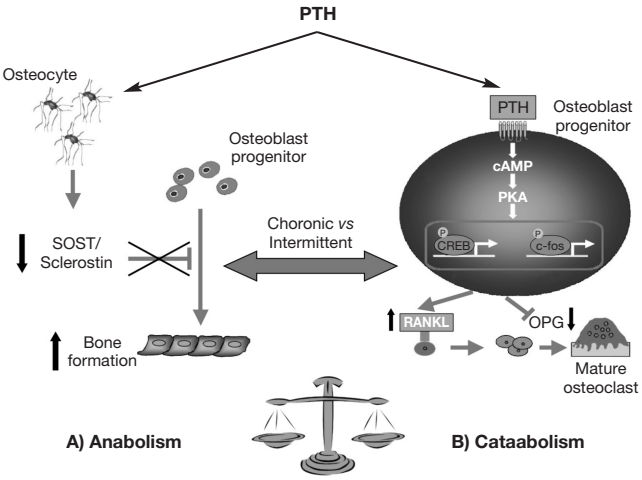

Fig. 5 - *Anabolic and catabolic pathways of PTH on the skeleton. A) PTH decreases* SOST/*sclerostin expression in osteocytes. Sclerostin functions as a negative regulator of bone formation, and its downregulation by PTH contributes for the PTH-induced osteoanabolism. B) PTH favors bone resorption, mostly by increasing receptor activator of nuclear factor kappa-B ligand (RANKL) and decreasing osteoprotegerin (OPG) expression in osteoblasts, which ultimately leads to an increase in osteoclast formation and activity.*

resorption (62). Although the increase in MCP-1 expression was more pronounced in rats treated with intermittent doses of PTH than in rats treated with continuous infusion of this hormone, the latter mode of administration led to moderated but sustained up-regulation of MCP-1 mRNA levels, explaining the catabolic action of PTH observed upon continuous infusion of PTH.
Although many studies have failed to demonstrate consistently a direct effect of PTH on osteoclasts, Langub et al. (63) showed that the PTH receptor PTH1R is expressed in osteoclasts from patients with the secondary hyperparathyroidism of chronic kidney disease. More recently, Dempster et al. (64), have also demonstrated that the PTH1R is expressed in human osteoclasts derived from peripheral blood mononuclear cells at the mRNA and protein level. It is still unclear, though, if PTH can directly activate osteoclasts independent of its actions on osteoblasts.

Cellular actions of PTH contributing to increased bone formation: Osteoanabolic

Pre-clinical and clinical studies have demonstrated that intermittent administration of PTH promotes bone formation (12, 13, 65-67). The anabolic actions of PTH on bone mass depend on its direct action on cells of osteoblastic lineage. Following the interaction PTH-PTH1R (6), $G\alpha_s$ and $G\alpha_q$ are activated, with subsequent activation of PKA and PKC. It has been demonstrated that cAMP/PKA signaling is a dominant mechanism by which PTH increases bone anabolism, and that PKC is not required for the osteoanabolic action of PTH (68). In fact, a recent study showed that the $G\alpha_q$-PKC signal in osteoblasts is inhibitory to the anabolic actions of PTH on bone mass (69).
The osteoanabolic action of PTH is due to its ability to increase osteoblast number, which can be achieved by an increase in osteoblastogenesis, decrease in osteoblast apoptosis or a combination of the two events (70, 71). The increase in osteoblastogenesis is explained mostly by an increase in osteoblast differentiation rather than increased proliferation. It is generally accepted that differentiation requires exit from the cell cycle and, as a result, proliferation is attenuated as differentiation proceeds (71). Thus, it has been suggested that one of the mechanisms by which PTH promotes its anabolic actions is to arrest the cell cycle progression of osteoblasts, enhancing their commitment to a differentiated osteogenic fate (72). Indeed, anti-proliferative effects have been reported in osteoblastic cell lines, cultures of primary cells, and in rodents treated with PTH, which is explained by both an attenuation of the expression of cyclin D1, a protein required for cell cycle progression, and an increase in the expression of the cell cycle inhibitors $p27^{Kip1}$ and $p21^{Cip1}$ (73-75). However, the effect of PTH on osteoblast proliferation may be specific to the differentiation/developmental stage of the osteoblastic cell. Although PTH suppresses proliferation of committed osteoprogenitor cells, there is evidence that suggests that it does not affect or increase the replication of uncommitted osteoblast progenitors (71, 73, 75, 76). In agreement with these data, *in vitro* and *in vivo* studies in rodents conducted by Ogita et al. (77), showed that cyclic PTH treatment promotes osteoblast differentiation from periosteum-derived mesenchymal progenitors, and has a biphasic effect to enhance, then suppress proliferation of periosteal osteoblast progenitors.
Beyond the effects on the cell cycle itself, PTH enhances osteoblast differentiation. It stimulates osteoblast differentiation and osteoblastic lineage commitment in primary calvarial cells, bone marrow-derived, and in periosteal cells (15, 77, 78). Evidence from *in vitro* and *in vivo* studies suggests that PTH increases the expression of genes that typically signal bone formation, such as the osteoblast-specific transcription factor Runx2, as well as alkaline phosphatase (79), collagen type I alpha 1 (COL1A1), and osteocalcin (14, 15, 78, 80). Recently, a novel bone formation-related factor, Tmem119, was shown to be rapidly stimulated in mouse osteoblastic cell lines by PTH (81). Consistent with a PTH-induced increase in the number of differentiating osteoblasts, intermittent PTH enhances ossicle development from bone marrow derived stromal cells implanted into immunocompromised mice (82).
Alternatively, PTH can increase osteoblast number by decreasing osteoblast apoptosis. Daily injections of PTH to adult mice showed an anti-apoptotic effect of PTH on osteoblasts in femoral and vertebral sections (83). The prevalence of osteoblast apoptosis was inversely correlated with serum osteocalcin, bone formation rate, and osteoblast number, suggesting that the prosurvival effect of PTH on osteoblasts accounts, at least in part, for its anabolic effect on bone (83). *In vitro*, PTH treatment also inhibits pro-apoptotic effects of dexamethasone, etoposide, hydrogen peroxide induced oxidative stress, UV irradiation, serum withdrawal and nutrient deprivation in a variety of osteoblastic cells (79, 83, 84). Mechanistically, PTH phosphorylates and inactivates the pro-apoptotic protein Bad, and increases the expression of survival genes like Bcl-2. These actions are mediated by activation of PKA (83). The increased expression of Runx2 is also required for the anti-apoptotic effect of intermittent PTH (83). Moreover, it was recently shown that PTH treatment of cultured osteoblasts augments DNA repair, and enhances cell survival under extreme metabolic stress and direct DNA damage, which was proposed as another mechanism by which PTH can suppress osteoblast apoptosis (84).

MEDIATORS OF PTH ACTIONS ON BONE FORMATION

Sclerostin

Sclerostin, a product of the *SOST* gene expressed primarily by osteocytes, is a secreted glycoprotein that functions as a key negative regulator of bone formation (85). In the human genetic diseases van Buchem's disease and sclerosteosis, reduced sclerostin concentration and/or activity are translated into generalized and progressive overgrowth of bone and sclerosis of the skeleton (86-88). Likewise, *Sost* knockout mice have high bone mass. Preclinical studies show that an antisclerostin antibody has osteoanabolic effects in rodents (89, 90). Early studies in human subjects are also confirming the anabolic effects of an antisclerostin antibody (91).

The finding that osteocytes secrete sclerostin, and express the PTH1R (92) raised the hypothesis that the osteocyte-derived sclerostin could be a mediator of the anabolic action of PTH on the skeleton. Indeed, downregulation of *SOST*/sclerostin by PTH has been demonstrated *in vitro*, in animals, and in humans, and the regulation of SOST by this hormone is currently recognized as having a key role in PTH-induced bone formation (Fig. 5) (93-98). PTH decreases *Sost* mRNA levels *in vitro*, and in rodents treated with either continuous or intermittent administration of PTH (93, 96). Similarly, transgenic mice overexpressing a constitutively active PTH1R specifically in osteocytes, have increased bone mass, and decreased Sost expression (94). In these mice, concomitant overexpression of *Sost*, also in osteocytes, abolishes the increase in cortical bone area, periosteal bone formation rate, and cancellous bone volume, supporting the hypothesis that the anabolic effect of PTH requires downregulation of sclerostin in osteocytes (94). In human subjects, serum sclerostin levels are reported to be lower in patients with PHPT than in controls, and a negative correlation between circulating sclerostin and PTH is observed (97-99). Moreover, intermittent PTH therapy in post-menopausal women decreases circulating sclerostin levels, which sustains the idea that the downregulation of sclerostin accounts for the osteoanabolic action of PTH also in humans (95).

The mechanism by which sclerostin inhibits bone formation is not completely understood. Until recently, it was assumed that sclerostin would pass through the osteocytic canaliculi to access the bone surface, where it would bind to the LDL-receptor related protein (LRP) 5 and 6, inhibiting the osteoblastic canonical Wnt/β-catenin signaling (6, 100, 101). In this way, sclerostin would antagonize the pro-differentiating and survival actions of Wnts on osteoblasts. However, an effect through LRP5 in the Wnt signaling pathway has recently been questioned by studies suggesting that LRP5 does not function as a Wnt coreceptor (102). Thus, the definition mechanism(s) by which sclerostin inhibits bone formation is still unknown.

IGF

IGF-I is a regulator of cell growth and function, and, in osteoblasts, acts as a prodifferentiating and a prosurvival factor. PTH can induce skeletal expression of IGF-I, which would act as an autocrine/paracrine factor to mediate the PTH effects on osteoblasts (103, 104). Indeed, animal studies have shown that *IGF-I* plays a key role in the osteoanabolic effects of PTH. IGF-I-deficient mice had an attenuated effect of the anabolic actions of PTH on cortical bone (105), and deletion of the insulin receptor substrate adapting molecule-1 (which transmits IGF-I receptor signaling) blunted the anabolic response to intermittent PTH administration (106). The anabolic actions of PTH on bone were also altered in mice with deletion of the IGF-I receptor specifically in mature osteoblasts (103). Increased cancellous bone volume at the primary spongiosa, and enhanced bone formation, mineralization, and cortical thickness at the cortical bone observed upon PTH administration to the control mice were blunted in the IGF-I receptor knockout mice (103). At the cellular level, IGF-I receptor deletion decreased the ability of PTH to stimulate osteoprogenitor cell proliferation and differentiation, as measured by the number of ALP-expressing colonies and mineralized nodules in cultures of bone marrow-derived stromal cells treated with PTH.

The role of T cells

T cells that express PTH receptors may be involved in both the anabolic and catabolic actions of PTH through CD40 Ligand, a surface molecule of activated T cells that induces CD40 signaling in stromal cells (107, 108). The work of Pacifici et al. has shown that deletion of T cells or T cell-expressed CD40 Ligand blunts the catabolic activity of PTH in bone by decreasing bone marrow stromal cell number, RANK/OPG production and osteoclastogenic activity (109). Silencing of the PTH receptor in T cells also blocks the bone loss and the osteoclastic expansion induced by continuous PTH, thus demonstrating that PTH signaling in T cells may also be central to PTH-induced bone loss. T cells also play a permissive role in the anabolic effect of intermittent PTH, which is reduced in T cell-deficient mice. The mechanism involves activation of Wnt signaling by T cells in pre-osteoblasts.

CONCLUSION

The human skeleton is being renewed constantly by the dynamic process of bone remodeling, which consists of two normally balanced phases of bone resorption and bone formation. When these two processes are balanced, bone is neither gained nor lost. An imbalance between these two, favoring bone resorption, results in a catabolic net effect on bone mass, while an anabolic net effect ensues if bone formation exceeds bone resorption. Although the increase in bone resorption was the most recognized action of PTH in the skeleton, this hormone can, indeed, increase bone formation, and its final effect on bone mass, either catabolic or anabolic, will depend on which process or processes are being favored.

Continuous exposure to high levels of PTH is associated with catabolic effects on bone, while intermittent exposure to low doses of PTH has anabolic actions. The former is exemplified by the chronic disorder of PTH excess, PHPT, and the second is best represented by the use of PTH to treat osteoporosis. However, it is now recognized that PTH can have anabolic effects even in states of continuously elevated PTH, as evidenced by a preserved cancellous bone and a normal or greater trabecular connectivity observed in patients with PHPT. Similarly, decrease in BMD at cortical sites can be appreciated in subjects being treated with PTH, which, however, does not lead to negative effects on bone strength. In fact, decrease in facture risk at vertebral and non-vertebral sites was demonstrated in patients treated with PTH.

Mechanistically, although PTH can regulate different sets of genes when it is administered intermittently or continuously, favoring bone formation or resorption, respectively, some genes are regulated in the same way upon continuous or intermittent endogenous exposure to PTH. Decreased circulating sclerostin levels, for example, are observed in patients with PHPT, as well as in patients treated with recombinant PTH. In the same way, *Sost* mRNA levels decrease in rodents treated with either continuous or intermittent administration of PTH.

Despite advances in elucidating the mechanism of action of PTH on bone, the different skeletal responses to PTH are still incompletely understood. Although the response to PTH can be clearly catabolic or anabolic depending on the mode of exposure to this hormone, increases and decreases in bone mass at different skeletal sites can actually coexist in the same subject or condition. Future studies may elucidate a means to perturb molecular pathways that are regulated by PTH so that the anabolic response to this hormone is primarily expressed. Then these new insights could be applied into a medical therapy for PHPT.

REFERENCES

1. Hanley DA, Watson PH, Hodsman AB, Dempster DW. Pharmacological Mechanisms of Therapeutics: Parathyroid Hormone. In: Bilezikian J, Raisz LG, Martin TJ (eds). Principles of Bone Biology. Amsterdam: Elsevier. 2008, 1661-95.
2. Datta NS, Abou-Samra AB. PTH and PTHrP signaling in osteoblasts. Cell Signal 2009, 21: 1245-54.
3. Kousteni S, Bilezikian JP. The cell biology of parathyroid hormone in osteoblasts. Curr Osteoporos Rep 2008, 6: 72-6.
4. Potts JT. Parathyroid hormone: past and present. J Endocrinol 2005, 187: 311-25.
5. Datta NS, Samra TA, Mahalingam CD, Datta T, Abou-Samra AB. Role of PTH1R internalization in osteoblasts and bone mass using a phosphorylation-deficient knock-in mouse model. J Endocrinol 2010, 207: 355-65.
6. Kramer I, Keller H, Leupin O, Kneissel M. Does osteocytic SOST suppression mediate PTH bone anabolism? Trends Endocrinol Metab 2010, 21: 237-44.
7. Silverberg SJ, Shane E, de la Cruz L, et al. Skeletal disease in primary hyperparathyroidism. J Bone Miner Res 1989, 4: 283-91.
8. Dempster DW, Muller R, Zhou H, et al. Preserved three-dimensional cancellous bone structure in mild primary hyperparathyroidism. Bone 2007, 41: 19-24.
9. Parisien M, Mellish RW, Silverberg SJ, et al. Maintenance of cancellous bone connectivity in primary hyperparathyroidism: trabecular strut analysis. J Bone Miner Res 1992, 7: 913-9.
10. Parisien M, Silverberg SJ, Shane E, et al. The histomorphometry of bone in primary hyperparathyroidism: preservation of cancellous bone structure. J Clin Endocrinol Metab 1990, 70: 930-8.
11. Dobnig H, Turner RT. The effects of programmed administration of human parathyroid hormone fragment (1-34) on bone histomorphometry and serum chemistry in rats. Endocrinology 1997, 138: 4607-12.
12. Neer RM, Arnaud CD, Zanchetta JR, et al. Effect of parathyroid hormone (1-34) on fractures and bone mineral density in postmenopausal women with osteoporosis. N Engl J Med 2001, 344: 1434-41.
13. Greenspan SL, Bone HG, Ettinger MP, et al; Treatment of Osteoporosis with Parathyroid Hormone Study Group. Effect of recombinant human parathyroid hormone (1-84) on vertebral fracture and bone mineral density in postmenopausal women with osteoporosis: a randomized trial. Ann Intern Med 2007, 146: 326-39.
14. Onyia JE, Helvering LM, Gelbert L, et al. Molecular profile of catabolic versus anabolic treatment regimens of parathyroid hormone (PTH) in rat bone: an analysis by DNA microarray. J Cell Biochem 2005, 95: 403-18.
15. Locklin RM, Khosla S, Turner RT, Riggs BL. Mediators of the biphasic responses of bone to intermittent and continuously administered parathyroid hormone. J Cell Biochem 2003, 89: 180-90.
16. Cope O. The study of hyperparathyroidism at the Massachusetts General Hospital. N Engl J Med 1966, 274: 1174-82.
17. Dauphine RT, Riggs BL, Scholz DA. Back pain and vertebral crush fractures: an unemphasized mode of presentation for primary hyperparathyroidism. Ann Intern Med 1975, 83: 365-7.
18. Rubin MR, Bilezikian JP, McMahon DJ, et al. The natural history of primary hyperparathyroidism with or without parathyroid surgery after 15 years. J Clin Endocrinol Metab 2008, 93: 3462-70.
19. Heath H 3rd, Hodgson SF, Kennedy MA. Primary hyperparathyroidism. Incidence, morbidity, and potential economic impact in a community. N Engl J Med 1980, 302: 189-93.
20. Silverberg SJ, Shane E, Jacobs TP, Siris E, Bilezikian JP. A 10-year prospective study of primary hyperparathyroidism with or without parathyroid surgery. N Engl J Med 1999, 341: 1249-55.
21. Parisien M, Cosman F, Mellish RW, et al. Bone structure in postmenopausal hyperparathyroid, osteoporotic, and normal women. J Bone Miner Res 1995, 10: 1393-9.
22. Uchiyama T, Tanizawa T, Ito A, Endo N, Takahashi HE. Microstructure of the trabecula and cortex of iliac bone in primary hyperparathyroidism patients determined using histomorphometry and node-strut analysis. J Bone Miner Metab 1999, 17: 283-8.
23. Silverberg SJ, Locker FG, Bilezikian JP. Vertebral osteopenia: a new indication for surgery in primary hyperparathyroidism. J Clin Endocrinol Metab 1996, 81: 4007-12.
24. Hansen S, Beck Jensen JE, Rasmussen L, Hauge EM, Brixen K. Effects on bone geometry, density, and microarchitecture in the distal radius but not the tibia in women with primary hyperparathyroidism: A case-control study using HR-pQCT. J Bone Miner Res 2010, 25: 1941-7.
25. Bilezikian JP, Brandi ML, Rubin M, Silverberg SJ. Primary hyperparathyroidism: new concepts in clinical, densitometric and biochemical features. J Intern Med 2005, 257: 6-17.
26. Kulak CA, Bandeira C, Voss D, et al. Marked improvement in bone mass after parathyroidectomy in osteitis fibrosa cystica. J Clin Endocrinol Metab 1998, 83: 732-5.
27. Yu N, Donnan PT, Flynn RW, et al. Increased mortality and morbidity in mild primary hyperparathyroid patients. The Parathyroid Epidemiology and Audit Research Study (PEARS). Clin Endocrinol (Oxf) 2010, 73: 30-4.
28. Khosla S, Melton LJ 3rd, Wermers RA, Crowson CS, O'Fallon W, Riggs B. Primary hyperparathyroidism and the risk of fracture: a population-based study. J Bone Miner Res 1999, 14: 1700-7.
29. Vignali E, Viccica G, Diacinti D, et al. Morphometric vertebral fractures in postmenopausal women with primary hyperparathyroidism. J Clin Endocrinol Metab 2009, 94: 2306-12.
30. Wilson RJ, Rao S, Ellis B, Kleerekoper M, Parfitt AM. Mild asymptomatic primary hyperparathyroidism is not a risk factor for vertebral fractures. Ann Intern Med 1988, 109: 959-62.
31. Melton LJ 3rd, Atkinson EJ, O'Fallon WM, Heath H 3rd. Risk of age-related fractures in patients with primary hyperparathyroidism. Arch Intern Med 1992, 152: 2269-73.
32. Larsson K, Ljunghall S, Krusemo UB, Naessén T, Lindh E, Persson I. The risk of hip fractures in patients with primary hyperparathyroidism: a population-based cohort study with a follow-up of 19 years. J Intern Med 1993, 234: 585-93.
33. Parfitt AM. Parathyroid hormone and periosteal bone expansion. J Bone Miner Res 2002, 17: 1741-3.
34. Bilezikian JP. Bone strength in primary hyperparathyroidism. Osteoporos Int 2003, 14 (Suppl 5): S113-5.
35. Burr DB, Hirano T, Turner CH, Hotchkiss C, Brommage R, Hock JM. Intermittently administered human parathyroid hormone(1-34) treatment increases intracortical bone turnover and porosity without reducing bone strength in the humerus of ovariectomized cynomolgus monkeys. J Bone Miner Res 2001, 16: 157-65.
36. Dempster DW, Cosman F, Kurland ES, et al. Effects of daily treatment with parathyroid hormone on bone microarchitecture and turnover in patients with osteoporosis: a paired biopsy study. J Bone Miner Res 2001, 16: 1846-53.
37. Recker RR, Bare SP, Smith SY, et al. Cancellous and cortical bone architecture and turnover at the iliac crest of postmenopausal osteoporotic women treated with parathyroid hormone 1-84. Bone 2009, 44: 113-9.
38. Ma YL, Zeng Q, Donley DW, et al. Teriparatide increases bone formation in modeling and remodeling osteons and enhances IGF-II immunoreactivity in postmenopausal women with osteoporosis. J Bone Miner Res 2006, 21: 855-64.
39. Jiang Y, Zhao JJ, Mitlak BH, Wang O, Genant HK, Eriksen EF. Recombinant human parathyroid hormone (1-34) [teriparatide] im-

proves both cortical and cancellous bone structure. J Bone Miner Res 2003, 18: 1932-41.

40. Orwoll ES, Scheele WH, Paul S, et al. The effect of teriparatide [human parathyroid hormone (1-34)] therapy on bone density in men with osteoporosis. J Bone Miner Res 2003, 18: 9-17.
41. Fox J, Miller MA, Recker RR, Bare SP, Smith SY, Moreau I. Treatment of postmenopausal osteoporotic women with parathyroid hormone 1-84 for 18 months increases cancellous bone formation and improves cancellous architecture: a study of iliac crest biopsies using histomorphometry and micro computed tomography. J Musculoskelet Neuronal Interact 2005, 5: 356-7.
42. Dobnig H, Sipos A, Jiang Y, et al. Early changes in biochemical markers of bone formation correlate with improvements in bone structure during teriparatide therapy. J Clin Endocrinol Metab 2005, 90: 3970-7.
43. Lane NE, Sanchez S, Genant HK, Jenkins DK, Arnaud CD. Short-term increases in bone turnover markers predict parathyroid hormone-induced spinal bone mineral density gains in postmenopausal women with glucocorticoid-induced osteoporosis. Osteoporos Int 2000, 11: 434-42.
44. Kurland ES, Cosman F, McMahon DJ, Rosen CJ, Lindsay R, Bilezikian JP. Parathyroid hormone as a therapy for idiopathic osteoporosis in men: effects on bone mineral density and bone markers. J Clin Endocrinol Metab 2000, 85: 3069-76.
45. Rubin MR, Bilezikian JP. Parathyroid hormone as an anabolic skeletal therapy. Drugs 2005, 65: 2481-98.
46. Lindsay R, Cosman F, Zhou H, et al. A novel tetracycline labeling schedule for longitudinal evaluation of the short-term effects of anabolic therapy with a single iliac crest bone biopsy: early actions of teriparatide. J Bone Miner Res 2006, 21: 366-73.
47. Compston JE. Skeletal actions of intermittent parathyroid hormone: effects on bone remodelling and structure. Bone 2007, 40: 1447-52.
48. Lindsay R, Zhou H, Cosman F, Nieves J, Dempster DW, Hodsman AB. Effects of a one-month treatment with PTH(1-34) on bone formation on cancellous, endocortical, and periosteal surfaces of the human ilium. J Bone Miner Res 2007, 22: 495-502.
49. Zanchetta JR, Bogado CE, Ferretti JL, et al. Effects of teriparatide [recombinant human parathyroid hormone (1-34)] on cortical bone in postmenopausal women with osteoporosis. J Bone Miner Res 2003, 18: 539-43.
50. Seeman E, Delmas PD. Bone quality--the material and structural basis of bone strength and fragility. N Engl J Med 2006, 354: 2250-61.
51. Chambers TJ, Fuller K, McSheehy PM, Pringle JA. The effects of calcium regulating hormones on bone resorption by isolated human osteoclastoma cells. J Pathol 1985, 145: 297-305.
52. McSheehy PM, Chambers TJ. Osteoblastic cells mediate osteoclastic responsiveness to parathyroid hormone. Endocrinology 1986, 118: 824-8.
53. Kaji H, Sugimoto T, Kanatani M, Fukase M, Chihara K. Involvement of dual signal transduction systems in the stimulation of osteoclast-like cell formation by parathyroid hormone and parathyroid hormone-related peptide. Biochem Biophys Res Commun 1993, 194: 157-62.
54. Lee SK, Lorenzo JA. Parathyroid hormone stimulates TRANCE and inhibits osteoprotegerin messenger ribonucleic acid expression in murine bone marrow cultures: correlation with osteoclast-like cell formation. Endocrinology 1999, 140: 3552-61.
55. Ma YL, Cain RL, Halladay DL, et al. Catabolic effects of continuous human PTH (1--38) in vivo is associated with sustained stimulation of RANKL and inhibition of osteoprotegerin and gene-associated bone formation. Endocrinology 2001, 142: 4047-54.
56. Kanzawa M, Sugimoto T, Kanatani M, Chihara K. Involvement of osteoprotegerin/osteoclastogenesis inhibitory factor in the stimulation of osteoclast formation by parathyroid hormone in mouse bone cells. Eur J Endocrinol 2000, 142: 661-4.
57. Kearns AE, Khosla S, Kostenuik PJ. Receptor activator of nuclear factor kappaB ligand and osteoprotegerin regulation of bone remodeling in health and disease. Endocr Rev 2008, 29: 155-92.
58. Huang JC, Sakata T, Pfleger LL, et al. PTH differentially regulates expression of RANKL and OPG. J Bone Miner Res 2004, 19: 235-44.
59. Fu Q, Jilka RL, Manolagas SC, O'Brien CA. Parathyroid hormone stimulates receptor activator of NFkappa B ligand and inhibits osteoprotegerin expression via protein kinase A activation of cAMP-response element-binding protein. J Biol Chem 2002, 277: 48868-75.
60. Nakchbandi IA, Lang R, Kinder B, Insogna KL. The role of the receptor activator of nuclear factor-kappaB ligand/osteoprotegerin cytokine system in primary hyperparathyroidism. J Clin Endocrinol Metab 2008, 93: 967-73.
61. Stilgren LS, Rettmer E, Eriksen EF, Hegedüs L, Beck-Nielsen H, Abrahamsen B. Skeletal changes in osteoprotegerin and receptor activator of nuclear factor-kappab ligand mRNA levels in primary hyperparathyroidism: effect of parathyroidectomy and association with bone metabolism. Bone 2004, 35: 256-65.
62. Li X, Qin L, Bergenstock M, Bevelock LM, Novack DV, Partridge NC. Parathyroid hormone stimulates osteoblastic expression of MCP-1 to recruit and increase the fusion of pre/osteoclasts. J Biol Chem 2007, 282: 33098-106.
63. Langub MC, Monier-Faugere MC, Qi Q, Geng Z, Koszewski NJ, Malluche HH. Parathyroid hormone/parathyroid hormone-related peptide type 1 receptor in human bone. J Bone Miner Res 2001, 16: 448-56.
64. Dempster DW, Hughes-Begos CE, Plavetic-Chee K, et al. Normal human osteoclasts formed from peripheral blood monocytes express PTH type 1 receptors and are stimulated by PTH in the absence of osteoblasts. J Cell Biochem 2005, 95: 139-48.
65. Shen V, Dempster DW, Birchman R, Xu R, Lindsay R. Loss of cancellous bone mass and connectivity in ovariectomized rats can be restored by combined treatment with parathyroid hormone and estradiol. J Clin Invest 1993, 91: 2479-87.
66. Wronski TJ, Yen CF, Qi H, Dann LM. Parathyroid hormone is more effective than estrogen or bisphosphonates for restoration of lost bone mass in ovariectomized rats. Endocrinology 1993, 132: 823-31.
67. Iwaniec UT, Moore K, Rivera MF, Myers SE, Vanegas SM, Wronski TJ. A comparative study of the bone-restorative efficacy of anabolic agents in aged ovariectomized rats. Osteoporos Int 2007, 18: 351-62.
68. Yang D, Singh R, Divieti P, Guo J, Bouxsein ML, Bringhurst FR. Contributions of parathyroid hormone (PTH)/PTH-related peptide receptor signaling pathways to the anabolic effect of PTH on bone. Bone 2007, 40: 1453-61.
69. Ogata N, Shinoda Y, Wettschureck N, et al. G alpha(q) signal in osteoblasts is inhibitory to the osteoanabolic action of parathyroid hormone. J Biol Chem 2011, 286: 13733-40.
70. Jilka RL. Molecular and cellular mechanisms of the anabolic effect of intermittent PTH. Bone 2007, 40: 1434-46.
71. Kousteni S, Bilezikian J. Cellular Actions of Parathyroid Hormone. In: Bilezikian J, Raisz LG, Martin TJ (eds). Principles of Bone Biology. Amsterdam: Elsevier. 2008, 639-56.
72. Wang YH, Liu Y, Rowe DW. Effects of transient PTH on early proliferation, apoptosis, and subsequent differentiation of osteoblast in primary osteoblast cultures. Am J Physiol Endocrinol Metab 2007, 292: E594-603.
73. Qin L, Li X, Ko JK, Partridge NC. Parathyroid hormone uses multiple mechanisms to arrest the cell cycle progression of osteoblastic cells from G1 to S phase. J Biol Chem 2005, 280: 3104-11.
74. Onishi T, Hruska K. Expression of p27Kip1 in osteoblast-like cells during differentiation with parathyroid hormone. Endocrinology 1997, 138: 1995-2004.
75. Datta NS, Kolailat R, Fite A, Pettway G, Abou-Samra AB. Distinct roles for mitogen-activated protein kinase phosphatase-1 (MKP-1) and ERK-MAPK in PTH1R signaling during osteoblast proliferation and differentiation. Cell Signal 2010, 22: 457-66.
76. Datta NS, Pettway GJ, Chen C, Koh AJ, McCauley LK. Cyclin D1 as a target for the proliferative effects of PTH and PTHrP in early osteoblastic cells. J Bone Miner Res 2007, 22: 951-64.
77. Ogita M, Rached MT, Dworakowski E, Bilezikian JP, Kousteni S. Differentiation and proliferation of periosteal osteoblast progenitors are differentially regulated by estrogens and intermittent parathyroid hormone administration. Endocrinology 2008, 149: 5713-23.
78. Ishizuya T, Yokose S, Hori M, et al. Parathyroid hormone exerts disparate effects on osteoblast differentiation depending on exposure time in rat osteoblastic cells. J Clin Invest 1997, 99: 2961-70.

79. Chen HL, Demiralp B, Schneider A, et al. Parathyroid hormone and parathyroid hormone-related protein exert both pro- and anti-apoptotic effects in mesenchymal cells. J Biol Chem 2002, 277: 19374-81.
80. Krishnan V, Moore TL, Ma YL, et al. Parathyroid hormone bone anabolic action requires Cbfa1/Runx2-dependent signaling. Mol Endocrinol 2003, 17: 423-35.
81. Hisa I, Inoue Y, Hendy GN, et al. Parathyroid hormone-responsive Smad3-related factor, Tmem119, promotes osteoblast differentiation and interacts with the bone morphogenetic protein-Runx2 pathway. J Biol Chem 2011, 286: 9787-96.
82. Pettway GJ, Schneider A, Koh AJ, et al. Anabolic actions of PTH (1-34): use of a novel tissue engineering model to investigate temporal effects on bone. Bone 2005, 36: 959-70.
83. Bellido T, Ali AA, Plotkin LI, et al. Proteasomal degradation of Runx2 shortens parathyroid hormone-induced anti-apoptotic signaling in osteoblasts. A putative explanation for why intermittent administration is needed for bone anabolism. J Biol Chem 2003, 278: 50259-72.
84. Schnoke M, Midura SB, Midura RJ. Parathyroid hormone suppresses osteoblast apoptosis by augmenting DNA repair. Bone 2009, 45: 590-602.
85. Poole KE, van Bezooijen RL, Loveridge N, et al. Sclerostin is a delayed secreted product of osteocytes that inhibits bone formation. FASEB J 2005, 19: 1842-4.
86. Balemans W, Ebeling M, Patel N, et al. Increased bone density in sclerosteosis is due to the deficiency of a novel secreted protein (SOST). Hum Mol Genet 2001, 10: 537-43.
87. Balemans W, Patel N, Ebeling M, et al. Identification of a 52 kb deletion downstream of the SOST gene in patients with van Buchem disease. J Med Genet 2002, 39: 91-7.
88. Loots GG, Kneissel M, Keller H, et al. Genomic deletion of a long-range bone enhancer misregulates sclerostin in Van Buchem disease. Genome Res 2005, 15: 928-35.
89. Li X, Ominsky MS, Niu QT, et al. Targeted deletion of the sclerostin gene in mice results in increased bone formation and bone strength. J Bone Miner Res 2008, 23: 860-9.
90. Li X, Ominsky MS, Warmington KS, et al. Sclerostin antibody treatment increases bone formation, bone mass, and bone strength in a rat model of postmenopausal osteoporosis. J Bone Miner Res 2009, 24: 578-88.
91. Padhi D, Jang G, Stouch B, Fang L, Posvar E. Single-dose, placebo-controlled, randomized study of AMG 785, a sclerostin monoclonal antibody. J Bone Miner Res 2011, 26: 19-26.
92. Fermor B, Skerry TM. PTH/PTHrP receptor expression on osteoblasts and osteocytes but not resorbing bone surfaces in growing rats. J Bone Miner Res 1995, 10: 1935-43.
93. Bellido T, Ali AA, Gubrij I, et al. Chronic elevation of parathyroid hormone in mice reduces expression of sclerostin by osteocytes: a novel mechanism for hormonal control of osteoblastogenesis. Endocrinology 2005, 146: 4577-83.
94. Rhee Y, Allen MR, Condon K, et al. PTH receptor signaling in osteocytes governs periosteal bone formation and intracortical remodeling. J Bone Miner Res 2011, 26: 1035-46.
95. Drake MT, Srinivasan B, Mödder UI, et al. Effects of parathyroid hormone treatment on circulating sclerostin levels in postmenopausal women. J Clin Endocrinol Metab 2010, 95: 5056-62.
96. Keller H, Kneissel M. SOST is a target gene for PTH in bone. Bone 2005, 37: 148-58.
97. Mirza FS, Padhi ID, Raisz LG, Lorenzo JA. Serum sclerostin levels negatively correlate with parathyroid hormone levels and free estrogen index in postmenopausal women. J Clin Endocrinol Metab 2010, 95: 1991-7.
98. van Lierop AH, Witteveen JE, Hamdy NA, Papapoulos SE. Patients with primary hyperparathyroidism have lower circulating sclerostin levels than euparathyroid controls. Eur J Endocrinol 2010, 163: 833-7.
99. Costa A, Cremers S, Rubin M, et al. Circulating Sclerostin Levels in Disorders of Parathyroid Function: Primary Hyperparathyroidism (PHPT) and Hypoparathyroidism (HypoPT). ASBMR 2010 Annual Meeting 2010: S158 (abstract).
100. Semënov M, Tamai K, He X. SOST is a ligand for LRP5/LRP6 and a Wnt signaling inhibitor. J Biol Chem 2005, 280: 26770-5.
101. Li X, Zhang Y, Kang H, et al. Sclerostin binds to LRP5/6 and antagonizes canonical Wnt signaling. J Biol Chem 2005, 280: 19883-7.
102. Yadav VK, Ryu JH, Suda N, et al. Lrp5 controls bone formation by inhibiting serotonin synthesis in the duodenum. Cell 2008, 135: 825-37.
103. Wang Y, Nishida S, Boudignon BM, et al. IGF-I receptor is required for the anabolic actions of parathyroid hormone on bone. J Bone Miner Res 2007, 22: 1329-37.
104. Lombardi G, Di Somma C, Vuolo L, Guerra E, Scarano E, Colao A. Role of IGF-I on PTH effects on bone. J Endocrinol Invest 2010, 33 (7 Suppl): 22-6.
105. Yakar S, Bouxsein ML, Canalis E, et al. The ternary IGF complex influences postnatal bone acquisition and the skeletal response to intermittent parathyroid hormone. J Endocrinol 2006, 189: 289-99.
106. Yamaguchi M, Ogata N, Shinoda Y, et al. Insulin receptor substrate-1 is required for bone anabolic function of parathyroid hormone in mice. Endocrinology 2005, 146: 2620-8.
107. Pacifici R. T cells: critical bone regulators in health and disease. Bone 2010, 47: 461-71.
108. Gao Y, Wu X, Terauchi M, et al. T cells potentiate PTH-induced cortical bone loss through CD40L signaling. Cell Metab 2008, 8: 132-45.
109. Tawfeek H, Bedi B, Li JY, et al. Disruption of PTH receptor 1 in T cells protects against PTH-induced bone loss. PLoS One 2010, 5: e12290.

FACULDADE DE MEDICINA
CENTRO DE PÓS-GRADUAÇÃO
Av. Prof. Alfredo Balena 190 / sala 533
Belo Horizonte - MG - CEP 30.130-100
Fone: (031) 3409.9641 FAX: (31) 3409.9640

UFMG

DECLARAÇÃO

A Comissão Examinadora abaixo assinada, composta pelos Professores: Maria Marta Sarquis Soares/ orientadora, Luiz Armando Cunha de Marco, Carolina Aguiar Moreira Kulak, Marise Lazaretti Castro, John P. Bilezikian, Beatriz Santana Soares, aprovou a defesa da dissertação intitulada: **"HIPERPARATIREOIDISMO PRIMÁRIO – AVALIAÇÃO ÓSSEA POR TOMOGRAFIA COMPUTADORIZADA QUANTITATIVA PERIFÉRICA DE ALTA RESOLUÇÃO E ESCORE DE OSSO TRABECULAR."**, de **BÁRBARA CAMPOLINA CARVALHO SILVA** estando a mesma apta à obtenção do título de Doutorado em Medicina Molecular, pelo Programa de Pós-Graduação em Medicina Molecular, da Faculdade de Medicina da Universidade Federal de Minas Gerais.

Belo Horizonte, 14 de Dezembro de 2012.

Prof.ª Maria Marta Sarquis Soares/ orientadora

Prof. Luiz Armando Cunha de Marco

Prof.ª Carolina Aguiar Moreira Kulak

Prof.ª Marise Lazaretti Castro

Prof. John P. Bilezikian

Prof.ª Beatriz Santana Soares

CONFERE COM ORIGINAL
Centro de Pós-Graduação
Faculdade de Medicina - UFMG